Endothelial Progenitor Cell Recruitment for Therapeutic Neovascularization using Alginate Hydrogels for VEGF and SDF Delivery

Endothelial Progenitor Cell Recruitment for Therapeutic Neovascularization using Alginate Hydrogels for VEGF and SDF Delivery

A dissertation presented

by

Erin Michelle Anderson

to

The School of Engineering and Applied Sciences

in partial fulfillment of the requirements

for the degree of

Doctor of Philosophy

in the subject of

Engineering Sciences

Harvard University

Cambridge, Massachusetts

February 2014

Dissertation Advisor : Dr. David J. Mooney Erin Michelle Anderson

Endothelial Progenitor Cell Recruitment for Therapeutic Neovascularization using Alginate Hydrogels for VEGF and SDF Delivery

ABSTRACT

Endothelial progenitor cells are potentially useful as a cell therapy for the treatment of ischemic cardiovascular diseases, but clinical outcomes have been limited likely because very few systemically delivered cells reach the target tissue. Biomaterials may improve outcomes of endothelial progenitor-based therapies because they can generate well-defined microenvironments capable of directing cell behavior. The hypothesis guiding this thesis is that local, sustained delivery of exogenous Vascular Endothelial Growth Factor (VEGF) and Stromal Cell-Derived Factor (SDF) from alginate hydrogels can enhance recruitment of endothelial progenitors to ischemic sites and also promote their contribution to new blood vessel growth.

In vitro and *in vivo* model systems were used to investigate the effects of VEGF and SDF on endothelial progenitor recruitment and regenerative potential. All studies were performed with both Outgrowth Endothelial Cells (OECs) and Circulating Angiogenic Cells (CACs), two populations of 'endothelial progenitors.' Exposing OECs and CACs to SDF promoted adhesion to mature endothelial cells, and VEGF and SDF increased migration of these cells, two key steps in the homing process. Alginate hydrogels that release VEGF and SDF enhanced *in vivo* recruitment of systemically delivered OECs and CACs to both ischemic and non-ischemic muscle tissue. Three-dimensional *in vitro* assays modeling the initial stages of angiogenesis showed that OECs formed sprouts, while CACs did not. The combination of VEGF and SDF enhanced OEC sprout formation by reducing sprout initiation time and

improving sprout maintenance. CACs alternatively contributed to sprout formation by mature endothelial cells in a paracrine manner by secreting angiogenesis-promoting growth factors and cytokines, which were more potent than the factors secreted by OECs on a per cell basis. *In vivo* experiments testing the functional contribution of both endothelial progenitor cell types revealed that CACs, which accumulated in the ischemic hind-limb with local delivery of VEGF and SDF from an alginate hydrogel, promoted perfusion recovery better than accumulated OECs or gels alone. These studies demonstrate the therapeutic potential of biomaterials for enhancing endothelial progenitor cell recruitment and participation in neovascularization.

Table of Contents

Chapter 1: Introduction **1**
1.1 Motivation / Problem Statement 1
1.2 Background 2
1.3 Hypothesis and Specific Aims 14
1.4 General Strategy and Thesis Outline 14
1.5 Significance 16
1.6 References 17

Chapter 2: Effects of VEGF and SDF on Recruitment of Endothelial Progenitor Cells **26**
2.1 Purpose of Chapter 26
2.2 Introduction 26
2.3 Materials and Methods 29
2.4 Results 38
2.5 Discussion 61
2.6 References 68

Chapter 3: Endothelial Progenitor Cell Contribution to New Blood Vessel Growth and the Effects of VEGF and SDF **74**
3.1 Purpose of Chapter 74
3.2 Introduction 74
3.3 Materials and Methods 76
3.4 Results 82
3.5 Discussion 95
3.6 References 101

Chapter 4: Major Conclusions, Implications and Future Directions **104**
4.1 Major Conclusions 104
4.2 Implications and Future Directions 106
4.3 References 112

APPENDICES **114**
Appendix A: Chapter 2 Supplemental Figures and Tables 114
Appendix B: Chapter 3 Supplemental Figures 119

Appendix C: Dual Compartment Microfluidic Device for Studying Endothelial Progenitor Adhesion and Migration 121
Appendix D: Systems to Study Cell Migration in Response to Chemotactic Gradients 127
Appendix E: Recruitment of Bone Marrow Cells to SDF-releasing PLG Scaffolds 131
Appendix F: Expanded Flow Cytometry Characterization of Circulating Angiogenic Cells 134
Appendix G: Comparison of OEC vs. HUVEC Network Formation in Fibrin-PLGA Scaffolds 137
Appendix H: Auto-fluorescence Characterization of Ischemic Hind-limbs Imaged with the In Vivo Imaging System (IVIS) 140
Appendix I: Protocol for Adhesion of OECs/CACs to Endothelial Cells 144
Appendix J: Protocol for ICAM Adhesion Assay 145
Appendix K: Protocol for Adhesion Assay in PDMS-based Wide Flow Channel 147
Appendix L: Protocol for Muscle Cell Isolation and Staining for Flow Cytometry 150

List of Figures and Tables

Figures

Figure 1.1 Endothelial Progenitor Cell Trafficking Processes and Key Molecules 9

Figure 2.1 Flow cytometry characterization of OECs and CACs 39

Figure 2.2 Adhesion of OECs and CACs to endothelial cells, and role of B2 integrins 42

Figure 2.3 SDF effects on OEC and CAC adhesion 46

Figure 2.4 OEC and CAC migration toward SDF and VEGF 47

Figure 2.5 Characterization of cytokine and growth factor release from injectable alginate hydrogels ... 48

Figure 2.6 OEC and CAC recruitment to non-ischemic mouse hind-limbs with VEGF and SDF delivery 50

Figure 2.7 Recruitment of progenitors to hind-limb muscle tissue after ischemia surgery 55

Figure 2.8 Characterization of inflammatory cell infiltration due to ischemia 58

Figure 2.9 OEC and CAC recruitment, and inflammatory cell infiltration, into ischemic and non-ischemic limbs with VEGF+SDF delivery via alginate gels..... 60

Figure 3.1 Phase contrast images of OECs and CACs after cell seeding procedure on 200μm diameter, collagen-coated dextran beads and OEC sprout examples 83

Figure 3.2 Endothelial sprouting behavior in response to SDF, VEGF and the combination at 72 hours 85

Figure 3.3 Kinetics of initial OEC sprout formation 87

Figure 3.4 Effect of VEGF and SDF on sprouting at 24, 48, and 72 hours 88

Figure 3.5 Direct comparison of OEC sprouting with HUVECs and HMVECs 89

Figure 3.6 Paracrine effects of factors secreted by OECs and CACs 91

Figure 3.7 Blood vessel perfusion recovery and capillary density after hind-limb ischemia surgery with VEGF and SDF treatment, with and without OEC or CAC delivery 94

Supplemental Figure 2.1 Photomicrographs of OECs, CACs and Lymphocytes adhered to HMVECs 114

Supplemental Figure 2.2 Relative integrin expression of OECs and CACs 114

Supplemental Figure 2.3 OEC adhesion to HMVECs with recombinant human soluble ICAM protein added 115

Supplemental Figure 2.4 ICAM surface coating method verification 115

Supplemental Figure 2.5 Parallel flow channel design and characterization 116

Supplemental Figure 2.6 Accumulation of fluorescent OECs in the lungs for different routes of systemic administration 117

Supplemental Figure 2.7 Detection of OECs by immunohistochemistry on mouse muscle sections ... 117

Supplemental Figure 3.1 Effect of temporal presentation of SDF in combination with a decreasing VEGF profile 119

Supplemental Figure 3.2 Changes in secretion of factors from OECs and CACs with VEGF+SDF exposure 120

Figure C1 Fabrication of dual-compartment microfluidic device 122

Figure C2 Microfluidic device with endothelial cell monolayers 123

Figure C3 Changes in the concentration gradient of SDF down the length of the 2cm channel 124

Figure C4 OEC adhesion to endothelial cells in the microfluidic device 125

Figure D1 Experimental setup and OEC monitoring in 2D migration microfluidic devices 128

Figure D2 Three-dimensional device used to track endothelial progenitor migration in response to chemokines 129

Figure E1 Experimental timeline for GFP bone marrow cell recruitment to PLG scaffolds 131

Figure E2 Cumulative release of SDF from porous PLG scaffolds 132

Figure E3 Bone marrow cell expression of CXCR4 and recruitment to SDF scaffolds 132

Figure F1 Flow cytometry characterization of CACs 135

Figure G1 Fluorescent images of vessel-like network formation by OECs and HUVECs on days 5 and 8 138

Figure H1 Auto-fluorescence characterization in ischemic hind-limbs on day 3 following surgery 141

Figure H2 Persistence of increased auto-fluorescence following ischemia surgery at excitation and emission wavelengths of 640nm and 680nm, respectively 142

Figure H3 Luminescent images taken with the IVIS 3 days following surgery 143

Figure K1 Tubing components necessary for cell culture in the flow device..... 149

Figure K2 PDMS channel bonded to a glass slide..... 149

Figure L1 Example images of cell suspension after completing the muscle digestion procedure..... 151

Tables

Supplemental Table 2.1. 3-way ANOVA table for main effect analysis of Ischemia, Cell type, and VEGF+SDF treatment 118

Acknowledgements

First and foremost I would like to thank my advisor, Dr. Dave Mooney. He has always impressed me with his extensive depth and breadth of knowledge in many engineering and biological areas. Dave exhibited a great deal of patience with me, as he does with all of his students, allowing us to make new discoveries and develop as individual scientists. His unwavering emphasis on structured, hypothesis-based research makes him an incredible scientist, and is the foundation for all of his well-deserved recognition. I truly appreciate the experience I have had here at Harvard, and I look forward to applying the many lessons I've learned, in lab and in life, to the rest of my career. I would also like to thank my committee members, Dr. Don Ingber and Dr. Uli von Andrian, for their time and guidance. Their constructive criticism truly made me a better scientist. Dr. Buddy Ratner, Professor of Bioengineering and Chemical Engineering at the University of Washington, also deserves my appreciation. He provided me with tremendous opportunities and support as an undergraduate, from advising my senior research project, to providing advice on graduate school applications, and allowing me to attend conferences where I had the opportunity to meet and learn from amazing professors in the Biomaterials field.

During my years as a graduate student, I have had the privilege to work with numerous intelligent, hard-working, and very generous colleagues. I would specifically like to thank Eduardo Silva for his mentorship in my early years as a graduate student, and Brian Kwee for his hours of hands on help with complicated, time-consuming animal experiments. Other colleagues from the Mooney lab that I would like to recognize include Omar Ali, Praveen Arany, Sidi Bencherif, Yaron Blinder, Christina Borselli, Kamal Bouhadir, Cristiana Branco da Cunha, Thomas Braschler, Yevgeny Brudno, Lan Cao, Christine Cezar, Gail Chan, Ovi Chaudhuri, Alex Cheung, Max Darnell, Rajiv Desai, Luo Gu, Cathal Kearney, Steve Kennedy, Jaeyun Kim, Darinka Klumpers, Anu Kod, Sandeep Koshy, Kangwon Lee, Aileen Li, Evi Lippens, Beverly Lu, Angelo Mao, Manav Mehta, Theresa Raimondo, Ellen Roche, Warren Sands, Ting-Yu Shih, Jae-Won Shin, Hadas Skaat, Hannah Storie, Dima Svartsman, Prakriti Tayalia, Catia Verbeke, Simon Young, and Will Yuen. Also, the support staff who are so dedicated to keep the lab

running deserve a huge thanks; this includes Kurt Schellenburg, Katie Parodi, Nora McDonald, Jill Larson, and Arlene Stevens. The high standards of all of these individuals created a work environment that encourages the dedication and resilience required to develop into a great scientist. Many of these people have become my best friends, not only from their support during work hours, but also thanks to the fun times we had outside the lab.

In addition to being a member in the Mooney lab, I conducted a large portion of my research at the Wyss Institute in the Longwood Medical Area, and had numerous colleagues and friends that I interacted with on a regular basis. I would first like to thanks Sarah Lewin for her time helping with animal experiments. Other close Wyss colleagues include Ahmed Bayoumi, Ed Doherty, Jake Fraser, Basma Hashmi, Bryan Hassel, Dan Huh, Mohammed Khan, Hyun Jung Kim, Dan Leslie, Katie Martinick, Ali Poyan Mehr, Bobak Mosadegh, Steve Perrault, Dan Shea, Sasha Stafford, and Des White. The Wyss also has a tremendous support staff, including Garry Cuneo, Tom Ferrante, Jean Lai, Susan Kelly, Jeanie Nisbet, and Martín Montoya. These individuals played tremendous roles in getting the Wyss off the ground, keeping the entire institute running smoothly, and have also individually provided me with resources or training numerous times over the years.

Finally, I would like to thank my family and friends for their generous love and support over the years. My friends in Boston were my outlet from the challenges I faced in the lab. It has been a long six and a half years living far from most of my family in Oregon, but everyone has recognized that this was a great opportunity for me and provided nothing but encouragement. To my brothers and sister, you are the best. And to my mom, who has dedicated her life to making sure her kids are happy, healthy and successful, you are my rock.

Last but not least, I would like to thank the Wyss Institute and the NIH for funding this research project.

Erin Anderson

February 2014

Be true to yourself and you will never fall.

– Beastie Boys

CHAPTER 1: Introduction

1.1 Motivation / Problem Statement

Cardiovascular disease is the primary cause of mortality in the developed world, leading to extensive research into multiple possible treatment modalities[1]. Cell therapies are increasingly attractive as researchers uncover the vast regenerative potential of various kinds of stem and progenitor cells[2–4]. Endothelial progenitor cells have been heavily investigated for their therapeutic potential in the treatment of ischemic cardiovascular diseases, such as peripheral vascular disease and myocardial infarction, with many clinical trials stemming from successful pre-clinical studies[5–8]. Unfortunately, therapeutic outcomes have been limited following systemic delivery of these cells, likely because too few cells reach the target tissue and those that do are not integrated into a tissue environment that promotes regeneration[9,10]. Improving the targeting capacity of systemically delivered endothelial progenitors, and enhancing their contribution to neovascularization are two strategies to enhance the therapeutic efficacy of these cells.

Biomaterials can be designed to create a well-defined microenvironment in the tissue which can specifically direct cell behavior and regenerative potential, and may be useful for improving outcomes of endothelial progenitor-based therapies[11,12]. In particular, biomaterials can control the release of growth factors and cytokines in a spatiotemporally regulated manner to mimic endogenous signals that cells use for specific processes, and the concentration can be tuned to levels effective for promoting the desired behavior[13]. This thesis investigates the potential of using a biomaterial, designed to replicate a pro-recruitment and pro-regenerative tissue environment, to increase endothelial progenitor targeting to ischemic tissue and to enhance endothelial progenitor contribution to new blood vessel formation in a model of peripheral vascular disease.

1.2 Background

The background information presented here reviews the types of endothelial progenitors, previous work to utilize the cells therapeutically, and strategies, including the use of biomaterials, to enhance the therapeutic effect of these cells.

Categorizing Endothelial Progenitors

Putative endothelial progenitor cells were initially discovered in 1997 by Asahara and colleagues[14]. The hypothesis driving their research was that a common precursor may give rise to the hematopoietic cells and angioblasts that condense to form blood islands during the initial phase of vascular development[15], and that it may be possible to identify an adult progenitor cell using the shared markers between the hematopoietic cells and angioblasts, namely CD34 and Flk-1 (or VEGFR2). CD34+ blood cells were magnetically sorted to a purity of 15.7%, and VEGFR2 cells were sorted to a purity of 20.0%. When CD34+ cells were plated on fibronectin, they adhered and proliferated for 4 weeks, whereas the CD34- cells did not. Plating the positive and negative populations together increased cell proliferation, cluster formation and also formation of tube-like structures. Further, these plated CD34+ cells took up acetylated-LDL and expressed higher levels of endothelial cell markers compared to freshly sorted CD34+ cells. Most importantly, the plated CD34+ cells were found co-localized with CD31+ cells at sites of new blood vessel growth in a rodent model of hindlimb ischemia. Together, these results demonstrated an endothelial phenotype, behavior, and apparent contribution to new blood vessel growth by the isolated CD34+ cells. Further, this was the first evidence of the existence of a circulating endothelial progenitor which could possibly participate in the growth of new vasculature. These findings motivated many researchers to equivalently search for and prove the existence of an endothelial progenitor cell.

In the following years, many papers were published about these putative endothelial progenitor cells, but as findings varied widely, it became clear that different cell types were all being referred to as ‘endothelial progenitors.’ There is still no single, agreed upon definition of an endothelial progenitor by

surface markers or gene expression, but the differing characteristics of the various cell types all previously called 'endothelial progenitors' have become more clear in recent years[16–20]. The different cell populations generally fall into three categories: 1) CD34+ cells and subsets, 2) Circulating Angiogenic Cells, and 3) Outgrowth Endothelial Cells. This nomenclature has been adopted here after careful review of the most current literature in the field. The cells in each of these categories exhibit very different roles in terms of how they contribute to the formation of new vasculature, and hence may differ in how they should be used therapeutically.

CD34+ cells and Subsets

Since the initially discovered EPCs were defined based on expression of CD34, many researchers began isolating these cells, and subsets of these cells, to gain further clarity on their role in postnatal vasculogenesis. In early reports, the endothelial phenotype of isolated CD34+ cells was repeatedly demonstrated and compared to Human Umbilical Vein Endothelial Cells (HUVECs), and *in vivo* CD34+ cells showed the ability to colonize matrigel plugs, to coat vascular grafts, and augment ischemic neovascularization[21–24]. CD34+ cells were also divided into various subsets, of which CD34+ VEGFR2+ CD133+ cells were heavily investigated. The combination that included CD133, an early hematopoietic marker, was thought to identify a less mature progenitor[25,26]. These cells had endothelial-like characteristics and lost CD133 expression as they matured[26–28]. *In vivo*, CD34+ VEGFR2+ CD133+ cells were found at sites of neovascularization and engrafted on left ventricular assist devices[24,26–29]. Alternatively, subjecting these cells to clonal assays revealed that CD34+ VEGFR2+ CD133+ cells also expressed CD45, another hematopoietic marker, and that these cells could form hematopoietic colonies, but not endothelial colonies[30]. Only the CD34+ CD45- population could form endothelial colonies with any proliferative potential[30,31], ending the search for an endothelial progenitor within this subpopulation of cells. Other subpopulations of CD34+ cells have also been isolated by flow cytometry, using markers such as CD14 and combinations of cKit, Sca-1, and Lin, to investigate both functionality and origin[32–34]. While EPCs still cannot be identified by a single surface marker or any combination, it has become clear

that CD34+ cells represent a heterogeneous population, mostly of hematopoietic lineage. Even though CD34+ cells may not directly participate in blood vessel regeneration, mounting evidence does suggest they may act as an accessory cell in contributing to neovascularization[35].

Circulating Angiogenic Cells (CACs)

Rather than using surface molecule expression to isolate endothelial progenitors, the culture protocols employed by Asahara and colleagues have been used to yield the Circulating Angiogenic Cell (CAC) population[14,17,36]. CACs are isolated from the mononuclear cell fraction of cord or adult blood by plating on fibronectin coated dishes in endothelial cell growth media for approximately 4 days. The adherent cells are termed CACs, and express endothelial surface markers, such as CD31, VEGFR2 and vWF, and these phenotypic similarities were used as evidence of differentiation into endothelial cells. It was quickly learned that CACs were not actually endothelial cells, but rather monocytes that in some ways mimic endothelial cell expression of surface markers when cultured in these specific conditions[37–41]. CACs express CD14, a marker for monocytes, maintain monocyte function in culture, and do not incorporate into new blood vessels[36,42–46]. But, CACs have been shown to form cord-like structures in a two-dimensional assay for angiogenic behavior, and helped promote perfusion recovery after ischemic injury[42,47,48]. Interestingly, only CD14+ cells cultured to obtain CACs exhibited this blood vessel growth promoting behavior, whereas freshly isolated monocytes did not[47]. Other researchers have attempted to reduce the monocyte contribution to the CAC population by modifying the culture process. Specifically, the population of cells that initially adheres to fibronectin contains monocytes, which can be eliminated by collecting and re-plating the non-adherent population. This was first done by Ito and colleagues at 24 hours, and later by Hill and colleagues at 48 hours[49,50], and resulted in colony formation, with round centrally located cells surrounded by spindle-shaped cells at the periphery. This method has been commercialized into a kit containing specific media and is known as the CFU-Hill assay, in which reduced colony formation is used as an indicator of cardiovascular risk[50]. While quantitatively useful as a diagnostic, too few cells are obtained with this culture method to substantiate their use therapeutically.

Furthermore, the colonies do not contain a true endothelial progenitor, but instead still contain monocytes, and also T cells which are necessary for colony formation[36,51–54]. Even though the CAC population was mistakenly identified initially as an endothelial progenitor population, these cells have demonstrated their angiogenic promoting ability via paracrine signaling, and are thus still valuable to investigate for therapeutic purposes[38,46–48,55,56].

Outgrowth Endothelial Cells (OECs)

The last population of 'endothelial progenitors' that has been widely investigated does contain cells that exhibit true progenitor behavior, and are called Outgrowth Endothelial Cells (OECs), or sometimes Endothelial Colony Forming Cells[57]. These cells were named because of their late-outgrowth behavior, with colonies appearing 10-14 days after isolation from cord blood or bone marrow, as opposed to the early outgrowth by CACs[58]. In contrast to the low or absent proliferative potential of the CAC population, OECs exhibited a high-proliferative potential and formed colonies in single cell re-plating assays, as would be expected of a true progenitor[36,57–59]. These cells were shown to originate in the bone marrow, but not from a CD133+ or CD45+ population, nor did they express CD14[31,58–60]. OECs demonstrated close similarities to endothelial cells in their surface marker expression and genetic profile, and directly participated in blood vessel formation[57,58,61–63]. OECs formed networks of blood vessels *ex vivo* through the process of vasculogenesis in three-dimensional matrices, and demonstrated superior survival upon implantation in comparison to mature endothelial cells[64–68]. *Ex vivo* engineered OEC vascular networks anastomosed with host vessels upon implantation into a mouse, and were robust enough to undergo serial transplantion[66,69]. OECs have also been directed to migrate out of three-dimensional scaffolds, where they contributed to the formation of new vessels and helped restore perfusion in a mouse model of hindlimb ischemia[63,70]. Together, these data demonstrate the progenitor cell properties of OECs and their therapeutic potential.

Therapeutic Use of Endothelial Progenitors

All three types of 'endothelial progenitors,' CD34+ cells, CACs and OECs, have demonstrated a capacity to improve outcomes when used therapeutically for the treatment of ischemia in animal models. Systemic delivery of CD34+ cells, CACs and OECs showed increased perfusion recovery in some mouse models of hind-limb ischemia, and mixed transplantation of OECs and CACs appeared to have a synergistic benefit[34,48,59,71]. Similar trends were obtained with a biomaterial system designed to release cells locally into ischemic hind-limbs; CACs and OECs alone demonstrated a therapeutic benefit, while the best perfusion recovery was achieved with co-delivery of both cell types[63]. Further, cell delivery from within the biomaterial lead to enhanced recovery, as compared to local injections of either cell type, likely because the material protects the transplanted cells and acts as a depot from which cells can slowly migrate out. In addition to the use of endothelial progenitors therapeutically in models of peripheral vascular disease, delivery of these cells has also shown benefit in models of myocardial infaction[72–76]. The positive results of these studies motivated clinical investigations of the therapeutic utility of these cells.

Endothelial progenitors have transitioned from pre-clinical animal studies into clinical trials for the treatment of both peripheral vascular disease and myocardial infarction (See References [6, 7, 77-79] for extensive review). In clinical trials, the ease with which a cell population is obtained becomes a primary concern, and in the case of endothelial progenitors, this has inhibited the use of CACs or OECs, as both cell types require days of cell culture for isolation. The most common cell sources used for clinical treatment of ischemia have been bone marrow mononuclear cells, Granulocyte Macrophage-Colony Stimulating Factor (GM-CSF)-mobilized peripheral blood mononuclear cells, and more recently CD34+ cells[77–79]. These cell populations likely contain some endothelial progenitors (e.g. approximately 1% of the total cells delivered are CD34+ cells), but are dominated by various other cell types, necessitating the delivery of a large number of cells (10^7-10^9)[7,77]. The first clinical trial in this area (TOPCARE-AMI) delivered bone marrow mononuclear cells into the coronary artery after myocardial infarction[80]. Results of this study showed improvements in left ventricular ejection fraction, regional wall motion and left

ventricular end systolic volume, in addition to establishing the safety and feasibility of using these cells therapeutically. One year and five year follow-up reports indicated that early positive results matched long term outcomes[81,82]. Alternatively, other clinical trials for the treatment of myocardial infarction, including the BOOST trial, demonstrated mixed results, where short and long term outcomes did not always match[83–91].Combining the results of multiple clinical trials through meta-analysis has shown that bone marrow and mobilized peripheral blood mononuclear cells improved left ventricular ejection fraction by an average of 2.55% and 3.31%, respectively, which are small but significant differences[92,93]. There have been over 20 clinical trials completed using these same cell populations for the treatment of peripheral vascular disease[7]. While nearly all trials had an absence of adverse events, which confirmed the safety of using these cells therapeutically, efficacy results were mixed. Some trials were able to demonstrate improvements in ankle-brachial index, leg/rest pain, and walking distance, while others did not show any significant differences between treated groups and placebo when cells were either delivered intra-arterially or intra-muscularly. Even large trials comparing bone marrow versus mobilized peripheral blood mononuclear cells had differing results, although these specific trials all demonstrated improvements in various measures with cell delivery[94–97]. Two trials explored the use of intramuscularly injected CD34+ cells for the treatment of critical limb ischemia. Kawamoto and colleagues showed a significant improvement in efficacy score, which is a combination of toe-brachial pressure index, pain scale, and total walking distance, and Losordo and colleagues showed a trend toward decreased amputation rate with an increasing number of cells delivered[78,79]. Overall, while variable results and small effects in clinical trials have been a challenge to interpret, outcomes have generally been positive and support continued investigation of these cells for therapeutic use. Progress also continues outside of the clinic, with a continuing search for surface markers that allow a true endothelial progenitor to be prospectively isolated from the circulation.

Potential Strategies to Improve Therapeutic Outcomes

Improving the therapeutic effect of endothelial progenitor cells may be achieved by enhancing the targeting capability of delivered cells to ensure they accumulate in the tissue of interest, and increasing the potency of delivered cells by protecting them and promoting their contribution to new vessel formation. Biomaterials are of potential utility for both of these strategies, because they can be designed to exert exquisite control on the local tissue microenvironment, and they may allow creation of an optimal cell recruitment or cell delivery platform.

First, an understanding of the molecules and cell-cell interactions that influence the ability of circulating endothelial progenitors to home to a tissue is necessary in order to develop therapies that can actively recruit these cells. The process of endothelial progenitor homing consists of mobilization from the bone marrow into the blood stream, followed by recruitment to the target tissue (Figure 1.1). The recruitment process includes responding to chemokines, adhering to the endothelium, and migrating into the local tissue site where the cells can then participate in blood vessel regeneration[98]. Each of these steps is intricately coordinated, and can potentially be targeted to enhance endothelial progenitor homing.

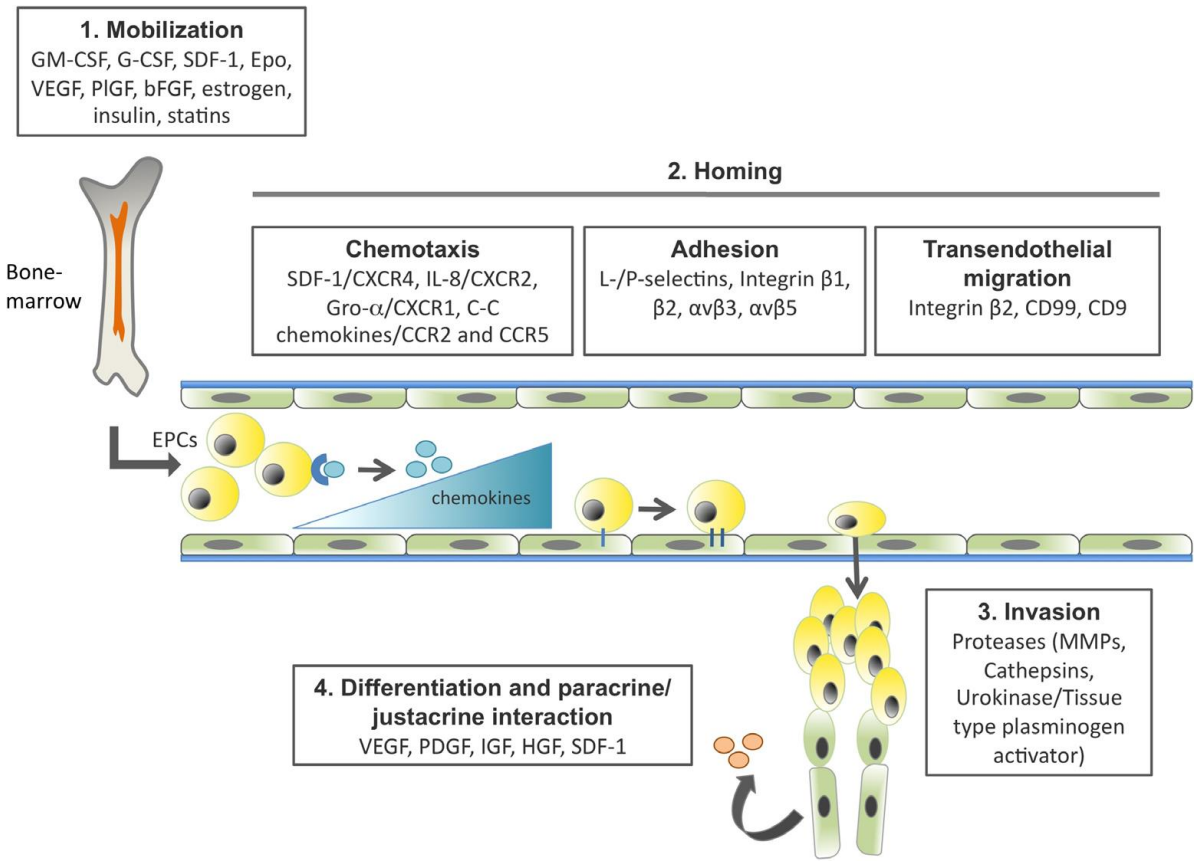

Figure 1.1 Endothelial Progenitor Cell Trafficking Processes and Key Molecules. Adapted from [100].

Role of Cytokines in Mobilization

Endothelial progenitor cells are held in the bone marrow by gradients of Stromal Cell- Derived Factor (SDF), and mobilize to the blood stream when this gradient is disrupted. Systemic delivery of Granulocyte-Colony Stimulating Factor (G-CSF) or cyclophosphamide was shown to cause the release of neutrophil elastase and cathepsin G in the bone marrow, which degraded both bone marrow SDF and CXCR4, the receptor for SDF, and resulted in CD34+ cell mobilization from the bone marrow into the blood stream[99,100]. GM-CSF and Vascular Endothelial Growth Factor (VEGF) were also shown to stimulate mobilization of endothelial progenitors, which was further enhanced with co-delivery of a CXCR4-antagonist[101–103]. Alternatively, instead of disrupting the bone marrow SDF levels, increasing the concentration of SDF in the blood and effectively reversing the direction of the SDF gradient caused

progenitor mobilization[104]. Delivery of thrombopoietin and soluble kit ligand also increased the plasma SDF concentration by stimulating release from platelets[105]. Lastly, induction of ischemia in a mouse hind-limb model resulted in elevated plasma SDF concentration and subsequent mobilization of progenitors[102,105,106]. These *in vivo* data illustrate the strong chemoattractive effect of SDF on progenitors, in addition to repeated demonstrations of this effect in transwell assays[99,100,107–109].

Role of Cytokines in Recruitment

Once endothelial progenitors are in the circulation, they must then be recruited to a target tissue in order to exert a therapeutic effect. Not only does SDF regulate progenitor cell mobilization, but it was shown to be expressed in ischemic tissue and exerted a chemoattractive effect on circulating progenitors, helping to recruit these cells to the tissue[106]. Ischemia also caused local upregulation of IL-8 and Gro-α, two cytokines that demonstrated a chemoattractive effect on CD34+ cells[110]. VEGF was similarly shown to induce recruitment of progenitor cells[111,112]. Exposure to chemoattractants is followed by adhesion of the circulating progenitors to the endothelium and extravasation from the blood vessel into the tissue of interest. Similar to circulating lymphocytes, endothelial progenitors use integrin – adhesion molecule interactions for adhesion and migration. CD34+ cells were shown to use both α4β1 and αLβ2 integrins for adhesion, but transendothelial migration was only dependent on αLβ2, which was followed by α5β1-dependent migration on the extracellular matrix protein, fibronectin[113,114]. SDF exposure enhanced CD34+ cell adhesion, likely by a similar mechanism to that used by lymphocytes[107,113–116]. These studies together demonstrated that SDF exposure and concentration gradients significantly impact multiple processes involved in endothelial progenitor cell trafficking, which subsequently encouraged investigation of the possible uses of SDF for enhancing the homing of circulating cells to tissues of interest.

Multiple modes of exposure to SDF have been investigated for their utility in controlling endothelial progenitor homing, including simple methods such as pre-treatment of cells or local tissue injections, as well as cell transfection procedures and the use controlled-release biomaterials for more prolonged

exposure. CD34+ cells that have be pre-stimulated with SDF before systemic injection increased capillary density in a mouse model of hind-limb ischemia, and similarly, an intramuscular injection of SDF in ischemic hind-limbs increased recruitment of systemically delivered cells[108,114]. Since the effects of SDF are limited in these cases due to short exposure time, researchers alternatively injected cells that were transfected to express SDF in order to increase the concentration locally and further affect endogenous cell recruitment. Both mesenchymal stem cells and skeletal myoblasts transfected to express SDF and delivered into the ischemic myocardium reduced infarct size, increased blood vessel density and improved overall left ventricular contractile function[117,118]. Genetic modification of cells may upregulate cytokine expression and secretion in a well-defined *in vitro* environment, but once implanted *in vivo*, the effective concentration of SDF secreted by the cells is left uncontrolled.

Potential Roles for Biomaterials

Biomaterials can be designed to spatiotemporally control the release of cytokines and growth factors that direct cell behavior in a local tissue area and/or effect cell trafficking at a distance, and could be used to increase the targeting capability of systemically delivered endothelial progenitors[11]. For example, delivery of VEGF followed by slower release of PDGF from a poly-lactide-co-glycolide scaffold enhanced local blood vessel regeneration and maturation in a mouse model of hind-limb ischemia[119]. Similarly, co-delivery of VEGF and an anti-VEGF antibody in a layered scaffold created a spatially regulated angiogenic zone, where blood vessel growth was locally promoted[120]. SDF has also been delivered from various materials for local and circulating cell recruitment purposes. Heparinized-collagen and poly(lactide-co-glycolide) scaffolds that were loaded with SDF promoted hematopoietic cell infiltration[121,122]. SDF-releasing polycaprolactone and poly(lactide ethylene oxide fumarate) scaffolds recruited mesenchymal stem cells and bone marrow stromal cells, respectively[123,124]. Subcutaneous implantation of an SDF-releasing poly(ethylene glycol)-heparin hydrogel was shown to recruit systemically delivered CACs, and SDF-releasing gelatin hydrogels lead to enhanced angiogenesis within the gel[125,126]. These studies demonstrate the robust cell recruitment capabilities of SDF-releasing

biomaterials, likely due to the steep concentration gradient created between the scaffolds and surrounding tissue. Since endothelial progenitors are strongly attracted to gradients of SDF, as previously discussed, biomaterials could be designed to increase homing of systemically delivered cells to the scaffold implantation site.

Biomaterials can also potentially increase the potency of delivered endothelial progenitors by protecting them and promoting their contribution to new blood vessel formation. For endothelial progenitors to effectively contribute to new vasculature following localization to ischemic tissue, it is likely they must be in an environment where the surrounding cells are working together to support vessel growth. VEGF is one of the strongest promoters of angiogenesis, and is essential for the formation of new blood vessels and recovery from ischemia[127,128]. VEGF is also necessary for survival of cultured endothelial progenitors, and promotes proliferation of OECs. OECs that were delivered to ischemic tissue in scaffolds containing VEGF demonstrated increased blood vessel density compared to OECs delivered without VEGF[63]. Here, the VEGF likely was acting both on the OECs and on the endogenous endothelial cells, as well as other cells participating in regeneration, since delivery of VEGF alone from polymer scaffolds enhances neovascularization in mouse models of hind-limb ischemia[129–131]. Still, the OECs alone could not compensate for the lack of VEGF, likely because prolonged exposure to VEGF is crucial for the creation of a pro-angiogenic environment[63]. Hence, establishing this angiogenic environment using biomaterials to deliver VEGF, or possibly other factors, may be required to enhance endothelial progenitor participation in neovascularization.

Even with establishment of a pro-angiogenic environment, it is still possible that too few cells are recruited to ischemic tissue to effectively enhance regeneration, in which case biomaterials can be used to deliver endothelial progenitors, in addition to growth factors. Delivery of OECs and CACs within an alginate hydrogel that was designed to deploy the cells into the surrounding tissue resulted in superior perfusion recovery compared to delivery of either cell type alone within the hydrogel or local injection of both cell types into the tissue without the protective alginate hydrogel[63]. Lastly, rather than encourage

participation of endothelial progenitors with controlled recruitment or delivery from biomaterials, the vasculature could be grown *ex vivo* on a biomaterial and then implanted. OECs have been pre-formed into networks of blood vessels within three-dimensional scaffolds, and anastomosed with host vasculature upon implantation[66–69]. Extensive research has been performed on the growth and engineering of these vascular networks, most often to support specific tissue engineering applications, but their use could easily be adapted for therapeutic delivery of endothelial progenitors for the treatment of ischemic diseases[132–134].

Summary

In summary, endothelial progenitors have demonstrated significant therapeutic potential since their discovery, despite years of confusion over the types of 'progenitors' and the lack of a surface marker-defined true progenitor cell. CD34+ cells, CACs and OECs each exhibit unique properties that encourage continued investigation of their individual roles in contributing to neovascularization, and exploration of the best delivery methods for each cell type. Mononuclear cell fractions containing CD34+ cells have been used in clinical trials for the treatment of peripheral vascular disease and myocardial infarction, but with limited success. Enhancing the targeting capability of systemically delivered cells should improve therapeutic outcomes by increasing the number of cells that reach the diseased tissue and subsequently participate in regeneration. Finally, the use of biomaterials to improve cell recruitment and tissue regeneration is promising, because they can be designed to control the release of cytokines and growth factors that influence endothelial progenitor homing and survival, such as SDF and VEGF.

1.3 Hypothesis and Specific Aims

The hypothesis guiding this research is that local, sustained delivery of exogenous VEGF and SDF from alginate hydrogels can enhance recruitment of endothelial progenitors to ischemic sites and also promote progenitor cell contribution to new blood vessel growth.

Aim 1: Evaluate effects of VEGF and SDF *in vitro* on the adhesion and migration of OECs and CACs, and determine if this combination of factors increases *in vivo* recruitment of OECs and CACs to ischemic tissue.

Aim 2: Use *in vitro* sprouting assays to model the potential contributions to new blood vessel formation by OECs and CACs recruited to ischemic hind-limbs by VEGF and SDF-releasing scaffolds, and determine the functional ability to restore perfusion *in vivo*.

1.4 General Strategy and Thesis Outline

To investigate the guiding hypothesis for this thesis, two aims were developed to focus on 1) endothelial progenitor cell recruitment and 2) contribution to new blood vessel formation. Within each of these aims, the effects of VEGF and SDF were investigated in order to determine if exposure to these factors can increase recruitment and enhance regeneration in a therapeutically effective manner. An injectable alginate hydrogel system previously developed in the lab was used to provide the local, sustained release of VEGF and SDF during *in vivo* experiments[131]. Further, as discussed in the background section, there are three types of 'endothelial progenitors.' Previous studies have explored the recruitment potential of CD34+ cells, as the use of this cell type has already transitioned into the clinic[79,108,114]. Few, if any,

publications have examined methods to improve recruitment and therapeutic efficacy of systemically delivered OECs or CACs. In this thesis, the therapeutic utility OECs and CACs was examined and compared.

Chapter 2 is dedicated to investigating Aim 1, using both *in vitro* and *in vivo* model systems. Specifically, the mechanisms that OECs and CACs use for adhesion were compared to the well-understood integrin – adhesion molecule interactions used by lymphocytes, and the effect of SDF on endothelial progenitor adhesion was uncovered. VEGF was not expected to affect adhesion, and was not tested in these studies. The effect of VEGF and SDF on OEC and CAC migration was tested in transwell assays. *In vivo*, VEGF and SDF-releasing alginate hydrogels were tested for their ability to increase recruitment of both OECs and CACs to ischemic and non-ischemic tissue.

Chapter 3 is focused on Aim 2, modeling and uncovering the contributions to blood vessel formation by OECs and CACs, both *in vitro* and *in vivo*. Three-dimensional sprouting assays were used to model direct participation in blood vessel formation and also indirect contribution in a paracrine manner. The effect of VEGF and SDF on each of these processes was examined. Last, OECs and CACs, which were systemically delivered and subsequently recruited to ischemic hind-limbs by VEGF and SDF-releasing alginate hydrogels, were tested for their ability to restore functional perfusion *in vivo*.

Chapter 4 discusses the major conclusions, implications and future directions of this work. The appendices address additional projects related to this work, which did not otherwise fit into this thesis or require further investigation or analysis. Supplemental figures for Chapters 2 and 3 are included in the appendices, as well as detailed protocols.

1.5 Significance

The use of various types of stem and progenitor cells as therapies is continuously expanding as the regenerative potential of these cells is uncovered. Often though, the results of pre-clinical studies and clinical trials using cell therapies are mixed, and demonstrate only small effects. These poor outcomes are most likely due to too few cells reaching the target tissue, and those that do are not being incorporated into an environment that allows their contribution to regeneration. Enhancing the targeting of systemically delivered cells and creating microenvironments that promote recovery are two strategies to improve the therapeutic efficacy and outcomes. This thesis investigates the potential of a biomaterial system to improve endothelial progenitor cell accumulation and participation in blood vessel regeneration *in vivo* in ischemic tissue, by releasing factors that are shown to increase adhesion, migration and sprout formation in *in vitro* assays. The use of biomaterials for cell recruitment purposes is basically non-existent in the clinic, and therefore every demonstration of efficacy with these systems may impact their clinical development and future use. Even incremental improvements in cell targeting may have significant effects on the overall outcome.

Scientifically, researchers who study 'endothelial progenitors' have largely focused on defining the cell type and discovering the correct identification markers. While this is reasonable considering the age of the field and the early discrepancies discussed previously, the studies presented here demonstrate the specific roles of OECs and CACs in contributing to neovascularization. These results confirm that only OECs can directly participate in blood vessel growth by forming new sprouts. The potential to contribute in a paracrine manner is investigated, and a panel of angiogenic factors secreted by each cell type is presented. Further, as all of these studies are completed with both OECs and CACs in direct comparison, the therapeutic potential of each cell type is elucidated, offering useful information as to how each cell type may possibly be used in the clinic.

1.6 References

1. Morbididty and Mortality: 2012 Chartbook on Cardiovascular, Lung and Blood Diseases. (2012). at <http://www.nhlbi.nih.gov/resources/docs/cht-book.htm>

2. Laird, D. J., von Andrian, U. H. & Wagers, A. J. Stem cell trafficking in tissue development, growth, and disease. *Cell* **132,** 612–30 (2008).

3. Segers, V. F. M. & Lee, R. T. Stem-cell therapy for cardiac disease. *Nature* **451,** 937–942 (2008).

4. Haraguchi, Y., Shimizu, T., Yamato, M. & Okano, T. Concise review: cell therapy and tissue engineering for cardiovascular disease. *Stem Cells Transl. Med.* **1,** 136–41 (2012).

5. Kawamoto, A. & Losordo, D. W. Endothelial progenitor cells for cardiovascular regeneration. *Trends Cardiovasc. Med.* **18,** 33–7 (2008).

6. Möbius-Winkler, S., Höllriegel, R., Schuler, G. & Adams, V. Endothelial progenitor cells: implications for cardiovascular disease. *Cytom. Part A J. Int. Soc. Anal. Cytol.* **75,** 25–37 (2009).

7. Raval, Z. & Losordo, D. W. Cell therapy of peripheral arterial disease: from experimental findings to clinical trials. *Circ. Res.* **112,** 1288–302 (2013).

8. ClinicalTrials.gov. (2013).

9. Krenning, G., van Luyn, M. J. a & Harmsen, M. C. Endothelial progenitor cell-based neovascularization: implications for therapy. *Trends Mol. Med.* **15,** 180–9 (2009).

10. Chavakis, E., Urbich, C. & Dimmeler, S. Homing and engraftment of progenitor cells: a prerequisite for cell therapy. *J. Mol. Cell. Cardiol.* **45,** 514–22 (2008).

11. Huebsch, N. & Mooney, D. J. Inspiration and application in the evolution of biomaterials. *Nature* **462,** 426–32 (2009).

12. Augst, A. D., Kong, H. J. & Mooney, D. J. Alginate hydrogels as biomaterials. *Macromol. Biosci.* **6,** 623–633 (2006).

13. Fischbach, C. & Mooney, D. J. Polymers for pro- and anti-angiogenic therapy. *Biomaterials* **28,** 2069–2076 (2007).

14. Asahara, T. *et al.* Isolation of Putative Progenitor Endothelial Cells for Angiogenesis. *Science.* **275,** 964–966 (1997).

15. Risau, W. & Flamme, I. Vasculogenesis. *Annu. Rev. Cell Dev. Biol.* **11,** 73–91 (1995).

16. Ingram, D. a, Caplice, N. M. & Yoder, M. C. Unresolved questions, changing definitions, and novel paradigms for defining endothelial progenitor cells. *Blood* **106,** 1525–1531 (2005).

17. Fadini, G. P., Losordo, D. & Dimmeler, S. Critical reevaluation of endothelial progenitor cell phenotypes for therapeutic and diagnostic use. *Circ. Res.* **110,** 624–37 (2012).

18. Losordo, D. W. & Dimmeler, S. Therapeutic angiogenesis and vasculogenesis for ischemic disease: part II: cell-based therapies. *Circulation* **109,** 2692–7 (2004).

19. Urbich, C. & Dimmeler, S. Endothelial progenitor cells: characterization and role in vascular biology. *Circ. Res.* **95,** 343–53 (2004).

20. Yoder, M. C. Human endothelial progenitor cells. *Cold Spring Harb. Perspect. Med.* **2,** a006692 (2012).

21. Shi, Q. *et al.* Evidence for circulating bone marrow-derived endothelial cells. *Blood* **92,** 362–7 (1998).

22. Bompais, H. *et al.* Human endothelial cells derived from circulating progenitors display specific functional properties compared with mature vessel wall endothelial cells. *Blood* **103,** 2577–84 (2004).

23. Murohara, T. *et al.* Transplanted cord blood-derived endothelial precursor cells augment postnatal neovascularization. *J. Clin. Invest.* **105,** 1527–36 (2000).

24. Popa, E. R. *et al.* Circulating CD34+ progenitor cells modulate host angiogenesis and inflammation in vivo. *J. Mol. Cell. Cardiol.* **41,** 86–96 (2006).

25. Yin, a H. *et al.* AC133, a novel marker for human hematopoietic stem and progenitor cells. *Blood* **90,** 5002–12 (1997).

26. Peichev, M. *et al.* Expression of VEGFR-2 and AC133 by circulating human CD34(+) cells identifies a population of functional endothelial precursors. *Blood* **95,** 952–958 (2000).

27. Quirici, N. *et al.* Differentiation and expansion of endothelial cells from human bone marrow CD133(+) cells. *Br. J. Haematol.* **115,** 186–194 (2001).

28. Reyes, M. *et al.* Origin of endothelial progenitors in human postnatal bone marrow. **109,** 313–315 (2002).

29. Gehling, U. M. *et al.* In vitro differentiation of endothelial cells from AC133-positive progenitor cells. *Blood* **95,** 3106–3112 (2000).

30. Case, J. *et al.* Human CD34+AC133+VEGFR-2+ cells are not endothelial progenitor cells but distinct, primitive hematopoietic progenitors. *Exp. Hematol.* **35,** 1109–18 (2007).

31. Timmermans, F. *et al.* Endothelial outgrowth cells are not derived from CD133+ cells or CD45+ hematopoietic precursors. *Arterioscler. Thromb. Vasc. Biol.* **27,** 1572–9 (2007).

32. Harraz, M., Jiao, C., Hanlon, H. D., Hartley, R. S. & Schatteman, G. C. CD34- blood-derived human endothelial cell progenitors. *Stem Cells* **19,** 304–12 (2001).

33. Estes, M. L. *et al.* Application of polychromatic flow cytometry to identify novel subsets of circulating cells with angiogenic potential. *Cytometry. A* **77,** 831–9 (2010).

34. Yang, J. *et al.* CD34+ cells represent highly functional endothelial progenitor cells in murine bone marrow. *PLoS One* **6,** e20219 (2011).

35. Kawamoto, A. & Asahara, T. Role of progenitor endothelial cells in cardiovascular disease and upcoming therapies. *Catheter. Cardiovasc. Interv. Off. J. Soc. Card. Angiogr. Interv.* **70,** 477–484 (2007).

36. Prater, D. N., Case, J., Ingram, D. a & Yoder, M. C. Working hypothesis to redefine endothelial progenitor cells. *Leukemia* **21,** 1141–1149 (2007).

37. Fernandez Pujol, B. *et al.* Endothelial-like cells derived from human CD14 positive monocytes. *Differentiation.* **65,** 287–300 (2000).

38. Rehman, J. Peripheral Blood "Endothelial Progenitor Cells" Are Derived From Monocyte/Macrophages and Secrete Angiogenic Growth Factors. *Circulation* **107,** 1164–1169 (2003).

39. Rohde, E. *et al.* Blood monocytes mimic endothelial progenitor cells. *Stem Cells* **24,** 357–67 (2006).

40. Hassan, N. F., Campbell, D. E. & Douglas, S. D. Purification of human monocytes on gelatin-coated surfaces. *J. Immunol. Methods* **95,** 273–6 (1986).

41. Miyamoto, Y., Suyama, T., Yashita, T., Akimaru, H. & Kurata, H. Bone marrow subpopulations contain distinct types of endothelial progenitor cells and angiogenic cytokine-producing cells. *J. Mol. Cell. Cardiol.* **43,** 627–635 (2007).

42. Schmeisser, a *et al.* Monocytes coexpress endothelial and macrophagocytic lineage markers and form cord-like structures in Matrigel under angiogenic conditions. *Cardiovasc. Res.* **49,** 671–80 (2001).

43. Schmeisser, A., Graffy, C., Daniel, W. G. & Strasser, R. H. Phenotypic overlap between monocytes and vascular endothelial cells. *Adv. Exp. Med. Biol.* **522,** 59–74 (2003).

44. Ziegelhoeffer, T. *et al.* Bone marrow-derived cells do not incorporate into the adult growing vasculature. *Circ. Res.* **94,** 230–8 (2004).

45. Zhang, S. J. *et al.* Adult endothelial progenitor cells from human peripheral blood maintain monocyte/macrophage function throughout in vitro culture. *Cell Res.* **16,** 577–84 (2006).

46. Okuno, Y., Nakamura-Ishizu, A., Kishi, K., Suda, T. & Kubota, Y. Bone marrow-derived cells serve as proangiogenic macrophages but not endothelial cells in wound healing. *Blood* **117,** 5264–72 (2011).

47. Urbich, C. *et al.* Relevance of monocytic features for neovascularization capacity of circulating endothelial progenitor cells. *Circulation* **108,** 2511–2516 (2003).

48. Kalka, C. *et al.* Transplantation of ex vivo expanded endothelial progenitor cells for therapeutic neovascularization. *PNAS* **97,** 3422–7 (2000).

49. Ito, H. *et al.* Endothelial Progenitor Cells as Putative Targets for Angiostatin Advances in Brief Endothelial Progenitor Cells as Putative Targets for Angiostatin. 5875–5877 (1999).

50. Hill, J. M. *et al.* Circulating endothelial progenitor cells, vascular function, and cardiovascular risk. *N. Engl. J. Med.* **348,** 593–600 (2003).

51. Hur, J. *et al.* Identification of a novel role of T cells in postnatal vasculogenesis: characterization of endothelial progenitor cell colonies. *Circulation* **116,** 1671–82 (2007).

52. Rohde, E. *et al.* Immune cells mimic the morphology of endothelial progenitor colonies in vitro. *Stem Cells* **25,** 1746–52 (2007).

53. Van Beem, R. T. *et al.* The presence of activated CD4(+) T cells is essential for the formation of colony-forming unit-endothelial cells by CD14(+) cells. *J. Immunol.* **180,** 5141–8 (2008).

54. Desai, A. *et al.* Microarray-based characterization of a colony assay used to investigate endothelial progenitor cells and relevance to endothelial function in humans. *Arterioscler. Thromb. Vasc. Biol.* **29,** 121–7 (2009).

55. Laurent, J., Touvrey, C., Botta, F., Kuonen, F. & Ruegg, C. Emerging paradigms and questions on pro-angiogenic bone marrow-derived myelomonocytic cells. *Int. J. Dev. Biol.* **55,** 527–34 (2011).

56. Favre, J., Terborg, N. & Horrevoets, A. J. G. The diverse identity of angiogenic monocytes. *Eur. J. Clin. Invest.* **43,** 100–7 (2013).

57. Ingram, D. a *et al.* Identification of a novel hierarchy of endothelial progenitor cells using human peripheral and umbilical cord blood. *Blood* **104,** 2752–2760 (2004).

58. Yoder, M. C. *et al.* Redefining endothelial progenitor cells via clonal analysis and hematopoietic stem/progenitor cell principals. *Blood* **109,** 1801–1809 (2007).

59. Hur, J. *et al.* Characterization of two types of endothelial progenitor cells and their different contributions to neovasculogenesis. *Arterioscler. Thromb. Vasc. Biol.* **24,** 288–93 (2004).

60. Lin, Y., Weisdorf, D. J., Solovey, a & Hebbel, R. P. Origins of circulating endothelial cells and endothelial outgrowth from blood. *J. Clin. Invest.* **105,** 71–7 (2000).

61. Medina, R. J. *et al.* Molecular analysis of endothelial progenitor cell (EPC) subtypes reveals two distinct cell populations with different identities. *BMC Med. Genomics* **3,** 18 (2010).

62. Mund, J. a, Estes, M. L., Yoder, M. C., Ingram, D. a & Case, J. Flow cytometric identification and functional characterization of immature and mature circulating endothelial cells. *Arterioscler. Thromb. Vasc. Biol.* **32,** 1045–53 (2012).

63. Silva, E. a, Kim, E.-S., Kong, H. J. & Mooney, D. J. Material-based deployment enhances efficacy of endothelial progenitor cells. *PNAS* **105,** 14347–14352 (2008).

64. Finkenzeller, G., Torio-Padron, N., Momeni, A., Mehlhorn, A. T. & Stark, G. B. In vitro angiogenesis properties of endothelial progenitor cells: a promising tool for vascularization of ex vivo engineered tissues. *Tissue Eng.* **13,** 1413–1420 (2007).

65. Au, P. *et al.* Differential in vivo potential of endothelial progenitor cells from human umbilical cord blood and adult peripheral blood to form functional long-lasting vessels. *Blood* **111,** 1302–5 (2008).

66. Melero-Martin, J. M. *et al.* Engineering robust and functional vascular networks in vivo with human adult and cord blood-derived progenitor cells. *Circ. Res.* **103,** 194–202 (2008).

67. Melero-Martin, J. M. *et al.* In vivo vasculogenic potential of human blood-derived endothelial progenitor cells. *Blood* **109,** 4761–8 (2007).

68. Wu, X. *et al.* Tissue-engineered microvessels on three-dimensional biodegradable scaffolds using human endothelial progenitor cells. *Am. J. Physiol. Heart Circ. Physiol.* **287,** H480–7 (2004).

69. Kang, K.-T., Allen, P. & Bischoff, J. Bioengineered human vascular networks transplanted into secondary mice reconnect with the host vasculature and re-establish perfusion. *Blood* **118,** 6718–21 (2011).

70. Vacharathit, V., Silva, E. a & Mooney, D. J. Viability and functionality of cells delivered from peptide conjugated scaffolds. *Biomaterials* **32,** 3721–8 (2011).

71. Yoon, C.-H. *et al.* Synergistic neovascularization by mixed transplantation of early endothelial progenitor cells and late outgrowth endothelial cells: the role of angiogenic cytokines and matrix metalloproteinases. *Circulation* **112,** 1618–27 (2005).

72. Kocher, A. A. *et al.* Neovascularization of ischemic myocardium by human bone-marrow-derived angioblasts prevents cardiomyocyte apoptosis, reduces remodeling and improves cardiac function. *Nat. Med.* **7,** 430–436 (2001).

73. Schuster, M. D. *et al.* Myocardial neovascularization by bone marrow angioblasts results in cardiomyocyte regeneration. *Am. J. Physiol. Heart Circ. Physiol.* **287,** H525–H532 (2004).

74. Kawamoto, A. *et al.* Therapeutic Potential of Ex Vivo Expanded Endothelial Progenitor Cells for Myocardial Ischemia. *Circulation* **103,** 634–637 (2001).

75. Kawamoto, A. *et al.* CD34-positive cells exhibit increased potency and safety for therapeutic neovascularization after myocardial infarction compared with total mononuclear cells. *Circulation* **114,** 2163–9 (2006).

76. Kawamoto, A. *et al.* Intramyocardial Transplantation of Autologous Endothelial Progenitor Cells for Therapeutic Neovascularization of Myocardial Ischemia. *Circulation* **107,** 461–468 (2002).

77. Kumar, A. H. S. & Caplice, N. M. Clinical potential of adult vascular progenitor cells. *Arterioscler. Thromb. Vasc. Biol.* **30,** 1080–7 (2010).

78. Kawamoto, A. *et al.* Intramuscular transplantation of G-CSF-mobilized CD34+ cells in patients with critical limb ischemia: a phase I/IIa, multicenter, single-blinded, dose-escalation clinical trial. *Stem Cells* **27,** 2857–64 (2009).

79. Losordo, D. W. *et al.* A randomized, controlled pilot study of autologous CD34+ cell therapy for critical limb ischemia. *Circ. Cardiovasc. Interv.* **5,** 821–30 (2012).

80. Assmus, B. *et al.* Transplantation of Progenitor Cells and Regeneration Enhancement in Acute Myocardial Infarction (TOPCARE-AMI). *Circulation* **106,** 3009–3017 (2002).

81. Schächinger, V. *et al.* Transplantation of progenitor cells and regeneration enhancement in acute myocardial infarction: final one-year results of the TOPCARE-AMI Trial. *J. Am. Coll. Cardiol.* **44,** 1690–9 (2004).

82. Leistner, D. M. *et al.* Transplantation of progenitor cells and regeneration enhancement in acute myocardial infarction (TOPCARE-AMI): final 5-year results suggest long-term safety and efficacy. *Clin. Res. Cardiol.* **100,** 925–34 (2011).

83. Stamm, C. *et al.* Autologous bone-marrow stem-cell transplantation for myocardial regeneration. *Lancet* **361,** 45–6 (2003).

84. Assmus, B. *et al.* Transcoronary transplantation of progenitor cells after myocardial infarction. *N. Engl. J. Med.* **355,** 1222–32 (2006).

85. Erbs, S. *et al.* Restoration of microvascular function in the infarct-related artery by intracoronary transplantation of bone marrow progenitor cells in patients with acute myocardial infarction: the Doppler Substudy of the Reinfusion of Enriched Progenitor Cells and Infa. *Circulation* **116,** 366–74 (2007).

86. Li, Z. *et al.* The clinical study of autologous peripheral blood stem cell transplantation by intracoronary infusion in patients with acute myocardial infarction (AMI). *Int. J. Cardiol.* **115,** 52–6 (2007).

87. Ahmadi, H. *et al. Safety analysis and improved cardiac function following local autologous transplantation of CD133(+) enriched bone marrow cells after myocardial infarction. Curr. Neurovasc. Res.* **4,** 153–160 (2007).

88. Tatsumi, T. *et al.* Intracoronary transplantation of non-expanded peripheral blood-derived mononuclear cells promotes improvement of cardiac function in patients with acute myocardial infarction. *Circ. J.* **71,** 1199–207 (2007).

89. Boyle, A. J. *et al.* Intra-coronary high-dose CD34+ stem cells in patients with chronic ischemic heart disease: a 12-month follow-up. *Int. J. Cardiol.* **109,** 21–7 (2006).

90. Losordo, D. W. *et al.* Intramyocardial transplantation of autologous CD34+ stem cells for intractable angina: a phase I/IIa double-blind, randomized controlled trial. *Circulation* **115,** 3165–72 (2007).

91. Meyer, G. P. *et al.* Intracoronary bone marrow cell transfer after myocardial infarction: 5-year follow-up from the randomized-controlled BOOST trial. *Eur. Heart J.* **30,** 2978–2984 (2009).

92. Delewi, R. *et al.* Impact of intracoronary bone marrow cell therapy on left ventricular function in the setting of ST-segment elevation myocardial infarction: a collaborative meta-analysis. *Eur. Heart J.* 1–10 (2013). doi:10.1093/eurheartj/eht372

93. Zimmet, H. *et al.* Short- and long-term outcomes of intracoronary and endogenously mobilized bone marrow stem cells in the treatment of ST-segment elevation myocardial infarction: a meta-analysis of randomized control trials. *Eur. J. Heart Fail.* **14,** 91–105 (2012).

94. Tateishi-Yuyama, E. *et al.* Therapeutic angiogenesis for patients with limb ischaemia by autologous transplantation of bone-marrow cells: a pilot study and a randomised controlled trial. *Lancet* **360,** 427–35 (2002).

95. Matoba, S. *et al.* Long-term clinical outcome after intramuscular implantation of bone marrow mononuclear cells (Therapeutic Angiogenesis by Cell Transplantation [TACT] trial) in patients with chronic limb ischemia. *Am. Heart J.* **156,** 1010–8 (2008).

96. Huang, P. P. *et al.* Randomised comparison of G-CSF-mobilized peripheral blood mononuclear cells versus bone marrow-mononuclear cells for the treatment of patients with lower limb arteriosclerosis obliterans. 1335–1342 (2007). doi:10.1160/TH07

97. Kamata, Y. *et al.* Local implantation of autologous mononuclear cells from bone marrow and peripheral blood for treatment of ischaemic digits in patients with connective tissue diseases. *Rheumatology (Oxford).* **46,** 882–4 (2007).

98. Caiado, F. & Dias, S. Endothelial progenitor cells and integrins: adhesive needs. *Fibrogenesis Tissue Repair* **5,** 4 (2012).

99. Lévesque, J.-P., Hendy, J., Takamatsu, Y., Simmons, P. J. & Bendall, L. J. Disruption of the CXCR4/CXCL12 chemotactic interaction during hematopoietic stem cell mobilization induced by GCSF or cyclophosphamide. *J. Clin. Invest.* **111,** 187–196 (2003).

100. Petit, I. *et al.* G-CSF induces stem cell mobilization by decreasing bone marrow SDF-1 and up-regulating CXCR4. *Nat. Immunol.* **3,** 687–694 (2002).

101. Pitchford, S. C., Furze, R. C., Jones, C. P., Wengner, A. M. & Rankin, S. M. Differential mobilization of subsets of progenitor cells from the bone marrow. *Cell Stem Cell* **4,** 62–72 (2009).

102. Takahashi, T. *et al.* Ischemia- and cytokine-induced mobilization of bone marrow-derived endothelial progenitor cells for neovascularization. *Nat. Med.* **5,** 434–8 (1999).

103. Asahara, T. *et al.* VEGF contributes to postnatal neovascularization by mobilizing bone marrow-derived endothelial progenitor cells. *EMBO J.* **18,** 3964–72 (1999).

104. Hattori, K. *et al.* Plasma elevation of stromal cell-derived factor-1 induces mobilization of mature and immature hematopoietic progenitor and stem cells. *Blood* **97,** 3354–3360 (2001).

105. Jin, D. K. *et al.* Cytokine-mediated deployment of SDF-1 induces revascularization through recruitment of CXCR4+ hemangiocytes. *Nat. Med.* **12,** 557–567 (2006).

106. De Falco, E. *et al.* SDF-1 involvement in endothelial phenotype and ischemia-induced recruitment of bone marrow progenitor cells. *Blood* **104,** 3472–3482 (2004).

107. Peled, A. *et al.* The chemokine SDF-1 activates the integrins LFA-1 , VLA-4 , and VLA-5 on immature human CD34+ cells : role in transendothelial / stromal migration and engraftment of NOD / SCID mice. *Blood* **95,** 3289–3296 (2000).

108. Yamaguchi, J. *et al.* Stromal cell-derived factor-1 effects on ex vivo expanded endothelial progenitor cell recruitment for ischemic neovascularization. *Circulation* **107,** 1322–1328 (2003).

109. Aiuti, B. a, Webb, I. J., Bleul, C., Springer, T. & Gutierrez-Ramos, J. C. The Chemokine SDF-1 Is a Chemoattractant for Human CD34+ Hematopoietic Progenitor Cells and Provides a New Mechanism to Explain the Mobilization of CD34+ Progenitors Progenitors to Peripheral Blood. *J. Exp. Med.* **185,** 111–20 (1997).

110. Kocher, a a *et al.* Myocardial homing and neovascularization by human bone marrow angioblasts is regulated by IL-8/Gro CXC chemokines. *J. Mol. Cell. Cardiol.* **40,** 455–64 (2006).

111. Grunewald, M. *et al.* VEGF-induced adult neovascularization: recruitment, retention, and role of accessory cells. *Cell* **124,** 175–89 (2006).

112. Zentilin, L. *et al.* Bone marrow mononuclear cells are recruited to the sites of VEGF-induced neovascularization but are not incorporated into the newly formed vessels. *Blood* **107,** 3546–54 (2006).

113. Peled, A. *et al.* The chemokine SDF-1 stimulates integrin-mediated arrest of CD34(+) cells on vascular endothelium under shear flow. *J. Clin. Invest.* **104,** 1199–1211 (1999).

114. Zemani, F. *et al.* Ex vivo priming of endothelial progenitor cells with SDF-1 before transplantation could increase their proangiogenic potential. *Arterioscler. Thromb. Vasc. Biol.* **28,** 644–650 (2008).

115. Shamri, R. *et al.* Lymphocyte arrest requires instantaneous induction of an extended LFA-1 conformation mediated by endothelium-bound chemokines. *Nat. Immunol.* **6,** 497–506 (2005).

116. Laudanna, C. & Alon, R. Right on the spot. Chemokine triggering of integrin-mediated arrest of rolling leukocytes. *Thromb. Haemost.* **95,** 5–11 (2006).

117. Tang, J. *et al.* Mesenchymal stem cells over-expressing SDF-1 promote angiogenesis and improve heart function in experimental myocardial infarction in rats. *Eur. J. Cardiothorac. Surg.* **36,** 644–50 (2009).

118. Elmadbouh, I. *et al.* Ex vivo delivered stromal cell-derived factor-1alpha promotes stem cell homing and induces angiomyogenesis in the infarcted myocardium. *J. Mol. Cell. Cardiol.* **42,** 792–803 (2007).

119. Richardson, T. P., Peters, M. C., Ennett, A. B. & Mooney, D. J. Polymeric system for dual growth factor delivery. **19,** 1029–1034 (2001).

120. Yuen, W. W., Du, N. R., Chan, C. H., Silva, E. A. & Mooney, D. J. Mimicking nature by codelivery of stimulant and inhibitor to create temporally stable and spatially restricted angiogenic zones. *PNAS* **107,** 17933–17938 (2010).

121. Thevenot, P. T. *et al.* The effect of incorporation of SDF-1alpha into PLGA scaffolds on stem cell recruitment and the inflammatory response. *Biomaterials* **31,** 3997–4008 (2010).

122. Bladergroen, B. A. *et al.* In vivo recruitment of hematopoietic cells using stromal cell-derived factor 1 alpha-loaded heparinized three-dimensional collagen scaffolds. *Tissue Eng. Part A* **15,** 1591–1599 (2009).

123. Schantz, J.-T., Chim, H. & Whiteman, M. Cell guidance in tissue engineering: SDF-1 mediates site-directed homing of mesenchymal stem cells within three-dimensional polycaprolactone scaffolds. *Tissue Eng.* **13,** 2615–2624 (2007).

124. He, X., Ma, J. & Jabbari, E. Migration of marrow stromal cells in response to sustained release of stromal-derived factor-1alpha from poly(lactide ethylene oxide fumarate) hydrogels. *Int. J. Pharm.* **390,** 107–16 (2010).

125. Prokoph, S. *et al.* Sustained delivery of SDF-1α from heparin-based hydrogels to attract circulating pro-angiogenic cells. *Biomaterials* **33,** 4792–800 (2012).

126. Kimura, Y. & Tabata, Y. Controlled release of stromal-cell-derived factor-1 from gelatin hydrogels enhances angiogenesis. *J. Biomater. Sci. Polym. Ed.* **21,** 37–51 (2010).

127. Carmeliet, P. Mechanisms of angiogenesis and arteriogenesis. *Nat. Med.* **6,** 389–395 (2000).

128. Potente, M., Gerhardt, H. & Carmeliet, P. Basic and therapeutic aspects of angiogenesis. *Cell* **146,** 873–87 (2011).

129. Chen, R. R. *et al.* Integrated approach to designing growth factor delivery systems. *FASEB J.* **21,** 3896–3903 (2007).

130. Silva, E. A. & Mooney, D. J. Effects of VEGF temporal and spatial presentation on angiogenesis. *Biomaterials* **31,** 1235–41 (2010).

131. Silva, E. A. & Mooney, D. J. Spatiotemporal control of vascular endothelial growth factor delivery from injectable hydrogels enhances angiogenesis. *J. Thromb. Haemost.* **5,** 590–598 (2007).

132. Peters, M. C., Polverini, P. J. & Mooney, D. J. Engineering vascular networks in porous polymer matrices. *J. Biomed. Mater. Res.* **60,** 668–678 (2002).

133. Bae, H. *et al.* Building vascular networks. *Sci. Transl. Med.* **4,** 160ps23 (2012).

134. Phelps, E. a, Landázuri, N., Thulé, P. M., Taylor, W. R. & García, A. J. Bioartificial matrices for therapeutic vascularization. *Proc. Natl. Acad. Sci. U. S. A.* **107,** 3323–8 (2010).

CHAPTER 2:

Effects of VEGF and SDF on Recruitment of Endothelial Progenitor Cells

2.1 Purpose of Chapter

This chapter addresses the hypothesis that local, sustained delivery of Vascular Endothelial Growth Factor (VEGF) and Stromal Cell-Derived Factor (SDF) can improve endothelial progenitor recruitment to ischemic hind-limb muscle in mice by increasing their adhesion and migration, two key steps in the homing process. *In vitro* assays were used to determine the influence of SDF on the adhesion of Outgrowth Endothelial Cells (OECs) and Circulating Angiogenic Cells (CACs) to endothelial cells in both static and shear-controlled environments. VEGF was not expected to play a role in cell adhesion, and therefore was not tested in these assays. The role of both VEGF and SDF on progenitor cell migration was also determined. *In vivo*, alginate gels that steadily release VEGF and SDF were tested for the ability to enhance recruitment of OECs and CACs to ischemic and non-ischemic muscle tissue. This chapter fits into the overall hypothesis of this thesis by determining whether VEGF and SDF can enhance the recruitment efficiency of systemically delivered endothelial progenitors.

2.2 Introduction

Cardiovascular disease is the primary cause of mortality in the developed world, a significant portion of which is caused by ischemic diseases, including peripheral vascular disease[1,2]. Peripheral vascular disease is characterized by blockages in arteries of the limbs, which reduces blood flow and results in ischemic, unhealthy tissue downstream[3]. Endothelial progenitor cells can contribute to the growth of new blood vessels, potentially restoring the health of the tissue[4–6]. There are currently over 200 clinical trials

involving endothelial progenitors for the treatment of various forms of cardiovascular disease, including ischemic diseases[6–8]. Many of these clinical trials use systemic infusion of cells into the blood stream as the delivery method. Systemic infusion of progenitor cells is generally attractive because of the simple delivery procedure, but this approach often shows poor efficacy due to high cell death and lack of control over cell targeting. Despite increasing clinical investigation, there is still a need to improve the limited therapeutic efficacy associated with systemic delivery of endothelial progenitor cells.

One possibility for improving therapeutic outcomes is to actively recruit systemically delivered cells to the tissue of interest, thereby improving the targeting efficiency of cell delivery.[9] As many steps are involved in the process of cell recruitment, there is potential to influence the ability of cells to home to target tissues at multiple stages. First, a circulating cell must adhere to the inner surface of a blood vessel at a specific location[9–11]. This is followed by migration to a position where the cell can participate in regeneration, often outside of the blood vessel[9–11]. There are many signaling molecules that regulate each of these steps mentioned here, the combination of which help to form a specific microenvironment that encourages cell recruitment[11-12]. Artificially replicating or enhancing this pro-recruitment microenvironment could enhance cell targeting to that location. For these studies, SDF and VEGF were chosen for delivery because they both play significant roles in regulating endothelial progenitor cell trafficking. SDF is highly involved in the recruitment and retention of endothelial progenitors in the bone marrow, and also acts as a chemotactic factor for multiple cell types, with the ability to influence adhesion and migration. Specifically, disruption of SDF gradients in the bone marrow leads to mobilization of progenitors into the circulation, where the progenitors can then be recruited to specific tissues[13–17]. Exposure to SDF can also promote in vitro CD34+ cell adhesion to endothelial cells in flow chambers, and migration through transwells[18–21]. Local injection of SDF into muscle tissue has been shown to influence the *in vivo* recruitment of endothelial progenitors in a mouse model of ischemia[22]. VEGF, in addition to potently promoting angiogenesis, also plays a role in mobilization of progenitors from the bone marrow, and is a well-known chemoattractant for endothelial cells[23]. Further, endothelial

progenitors can migrate according to gradients of VEGF delivered from alginate hydrogels[24]. Taken together, VEGF and SDF have both been shown to regulate key steps in progenitor cell trafficking, and for this reason were selected and tested for their ability to enhance targeting.

The use of polymeric biomaterials is potentially advantageous for these studies because they can be designed to release signaling molecules in a spatiotemporally controlled manner in order to create specific microenvironments that can regulate cell behavior[25]. The controlled release of these molecules (*e.g.* growth factors and cytokines), as opposed to a bolus injection, protects them from rapid enzymatic degradation, resulting in sustained presentation over a longer therapeutic window. Our lab has extensive experience creating biomaterials that promote angiogenesis for the treatment of ischemia[26–35]. For example, poly lactide-co-glycolide (PLG) scaffolds that first release VEGF, followed by a slower release of Platelet-Derived Growth Factor, were designed to not only promote the formation of new blood vessels, but also to support the maturation of these vessels[28,30]. PLG scaffolds can also be layered to spatially separate VEGF release from release of an anti-VEGF antibody, which creates a temporally stable and spatially restricted zone of angiogenesis[36]. Alternatively, alginate hydrogels can be designed to release VEGF with a decreasing rate over time, which was the profile determined to promote the most endothelial cell sprouting in a 3D model of angiogenesis[32]. Here, I used an injectable alginate hydrogel to control the release of VEGF and SDF.

Lastly, all experiments were performed with both OEC and CAC populations. OECs and CACs are both potentially relevant as therapies for ischemic diseases, but the contributions to new blood vessel growth from each cell type differ[37–39]. OECs exhibit a high proliferative potential, allowing for significant expansion in culture and therefore a near-unlimited therapeutic cell source[38,40]. OECs can also directly participate in blood vessel formation[24,41,42]. CACs alternatively are very limited in number and do not form blood vessels, but secrete potent angiogenic factors, and hence potentially contribute to new vessel formation in a paracrine manner[43–45]. The direct comparison between OECs and CACs in these studies may therefore guide future decisions on how each of these cells types should be used therapeutically.

2.3 Materials and Methods

Cell Isolation and Characterization

Human cord blood was used for OEC/CAC isolation within 12 hours from collection. Cord blood was diluted 1:1 with Hanks Balanced Salt Solution (HBSS) and gently placed on top of Histopaque 1077 (Sigma #10771-500ml). Samples were centrifuged at 740g (OECs) and 400g (CACs) for 30 minutes with no brake. Mononuclear cells were then collected and washed with HBSS. Remaining red blood cells were lysed and cells were washed twice with HBSS. For OEC isolation, cells were resuspended in EGM-2MV (Lonza #CC-3202) supplemented with 10% FBS and plated on Collagen coated dishes (BD #354400). Media was changed after two days, and every day until colonies appeared (day 10-14). Colonies were replated and maintained in EGM-2MV media while in use; OECs were used between passages 2 and 6. For CAC isolation, cells were plated on fibronectin-coated dishes (BD #356008) in EGM-2MV without hydrocortisone and supplemented with 10% FBS. Additional media was added to the cells on day 4, and attached cells at day 7 were immediately used for experiments.

Human B-lymphocytes were obtained from Coriell Cell Repository (#GM20431) and were cultured in RPMI 1640 with 2mM L-glutamine and 15% FBS. Culture of cord blood cells was exempt from Institutional Review Board approval, and lymphocyte cell culture was approved by the Institutional Review Board at Harvard University.

OEC and CAC surface marker expression was characterized via flow cytometry. Antibodies to the following markers were used for detection: CD31 (BD Pharmingen #555445), CD45/CD14 (BD #340040), VEGFR2 (R&DSystems # FAB357P), CXCR4 (R&DSystems #FAB170P), CD34 (BD Pharmingen #555821), ICAM (BDPharmingen #559047), VCAM (BDBiosciences #555645), and β2 integrin (CalBiochem #217660). ICAM, VCAM and β2 integrin required the application of a secondary antibody for fluorescent detection (Invitrogen #A11029). Flow cytometry data was collected on a BD LSRFortessa (Franklin Lakes, New Jersey) and analyzed with FlowJo software (Tree Star, Inc. Ashland,

OR). Relative OEC and CAC integrin expression was characterized using an antibody-based adhesion array according to the manufacturers protocol (Millipore #ECM535). Briefly, single cell suspensions of OECs or CACs were plated into the wells provided, which were coated with an antibody for each assayed integrin. After 1hour, un-attached cells were gently rinsed. OECs or CACs which had been captured by the integrin antibody were then lysed and stained with the provided CyQuantGR® dye, and fluorescence was measured on a plate reader (Bio-Tek Synergy H1 Plate Reader, Winooski, VT) at excitation 485nm and emission 528nm.

Luciferase OEC Transduction

Reporter gene constructs Luciferase plasmid pGreenFire1-CMV (cat# TR011PA-1) and packing plasmid pPACKH1-XL HIV (cat# LV510A-1) were purchased from System Bioscience. To produce the second-generation replication-incompetent lentivirus, 1.5 million 293TN cells (Cat. # LV900A-1) were seeded onto 10 cm petri-dishes in 10 ml DMEM (10%FBS, 1x glutamine, 1x PenStrep) per dish and incubated for 24 hours at 5% CO2, 37°C until 50-70% confluency. On day 2, media was changed to DMEM (10% FBS, 1x glutamine, without PenStrep). To create a plasmid mix, 400µl DMEM (without FCS, glutamine and PenStrep), 6µl of Luciferase plasmid (2µg/dish), and 20µl pPACK Packaging Plasmid Mix (10µg/dish) was added to a polystyrene tube and mixed gently. In a second tube, 400µl DMEM (without FCS, glutamine and PenStrep) and 30µl Lipofectamine 2000 (cat# 11668-027) were mixed gently. These two solutions were combined and incubated at room temperature for 15 minutes. The mixture was added drop-wise to the 293TN cells in a petri-dish, gently mixed by tilting, and then allowed to incubate for 48 hours at 5% CO2, 37°C. The viral supernatant was collected 48 hours after transfection and passed through a 0.2µm filter prior to aliquoting and storing in polystyrene tubes at -80°C.

5ml of thawed viral supernatant, 15µl of protamine sulfate (concentration 4µg/µl, Life cell technologies, cat# A11559IK), and 5ml EBM-2 + 10%FBS was added to 70% confluent OECs in a T75 flask and incubated at 5% CO2, 37°C. After 48 hours, the cells were washed twice with PBS, and media was

changed to EGM-2MV (without antibiotics or hydrocortisone). Luciferase expression was verified with a plate reader (Bio-Tek Synergy H1 Plate Reader, Winooski, VT) using Bright-Glo™ Luciferase Assay System (Promega, Cat# E2610) following manufactures instructions.

Adhesion Assay

HMVECs (Lonza #CC-2543) or HUVECs (Lonza # C2517A) were grown to confluence on 12mm diameter, Human Collagen IV (BD #354245) coated glass cover slips in 24 well plates with EGM-2MV (Lonza #CC-3202) or EGM-2 (Lonza # CC-3162) media, respectively (n=6 for each condition assayed in each experiment). For some conditions, media in contact with endothelial cells was supplemented with 50ng/ml TNFα (Peprotech #300-01A) for 8 hours before beginning experiments. OECs/CACs were fluorescently labeled with octadecyl-rhodamine (Life Technologies # O-246) for visualization, and trypsinized and prepared to a single cell suspension in EBM-2 + 5%FBS. OECs/CACs were then gently applied on top of HMVECs or HUVECs. SDF (R&D #350-NS) presentation on the surface of endothelial cells was achieved by incubating HMVECs or HUVECs with 500ng/ml SDF for 1 hour prior to starting experiments. The SDF in solution was then rinsed with fresh media, and all wells were changed to EBM-2 + 5%FBS at the start of the experiment. For conditions with SDF present during adhesion, 100ng/ml SDF was added to the HMVECs or HUVECs immediately before application of the OECs/CACs. A β2 antibody[46,47] (CalBiochem #217660) was also used to block adhesion of OECs/CACs, and was given to these cells for 5 minutes prior to their application on top of HMVEC or HUVEC monolayers. OECs and CACs were allowed to adhere for 30 or 60 minutes. At the end of this time, cover slips were removed from the well, gently rinsed in PBS, and then fixed in 20% methanol in PBS for 5 minutes. Cover slips were then mounted on glass slides with ProLong gold Anti-fade Reagent with Dapi (Life Technologies #P36935), and kept at room temperature in the dark for 24 hours and at 4^{o}C thereafter. Cell adhesion was quantified by imaging each 12mm slide 6 times, and the mean number of cells per image for each slide was used to determine the mean and standard deviation for each condition (Zeiss Axio Observer Z1, Thornwood, NY; Image J software). Each experiment was repeated 2-6 times.

ICAM Adhesion Assay

Non-tissue culture treated plates were placed in a plasma generator (SPI Plasma-Prep II Plasma Etcher, West Chester, PA) for 45 seconds to render the surface hydrophilic for ICAM protein (eBioscience # BMS313) adsorption. 5mg/ml recombinant human soluble ICAM was diluted in PBS and quickly applied to the well plate surface following plasma exposure; alternatively 1% BSA in PBS was applied to the wells as a negative control. Plates were then placed at 4^{o}C overnight to allow protein adsorption. Prior to starting the experiment, protein was aspirated from each well and blocking buffer (PBS with 1% BSA) was applied for 1 hour at room temperature to block the plate surface where ICAM had not adsorbed. Blocking buffer was aspirated and 300ul of adhesion buffer (HBSS with 0.1% BSA and 25mM HEPES) was applied to each well. Other conditions include the addition of SDF and 100ng/ml in adhesion buffer, 2mM $MnCl_2$ in adhesion buffer, or 5mM EDTA diluted in PBS without Calcium and Magnesium. OECs/CACs were trypsinized and resuspended in adhesion buffer. For conditions using blocking β2 integrins, 0.5ug of β 2 blocking antibody was applied to the OEC/CAC cell suspension 5 minutes before placing cells in the well plate. OECs/CACs were allowed to adhere for 30-60 minutes at 37^{o}C and 5% CO_2. Wells were then gently washed with PBS three times to remove non-adherent cells. 100ul of TrypLE Select without phenol red (Life Technologies #12563029) was added to each well and placed in the incubator for 5 minutes to detach adherent cells. 50ul of adhesion buffer was then added to each well, along with 50ul of lysis buffer (3mM Na_2HPO_4, 0.8mM NaH_2PO_4, 0.1M NaCl, 0.25%v/v Triton-100) with 1ul of CyQuant GR dye(Life Technologies #C7026). The plate was allowed to sit at room temperature for 15 minutes protected from light. Lysed OEC/CAC cell suspensions in each well were then mixed thoroughly and pipetted into a 96 well black plate. Fluorescence was read at excitation 485nm and emission 528nm for quantification (Bio-Tek Synergy H1 Plate Reader, Winooski, VT).

Flow Adhesion Assay

COMSOL MultiPhysics 4.2 software (COMSOL, Inc. Burlington, MA) was used to verify laminar flow properties of chosen dimensions for PDMS-based parallel flow channels. A model was created using Laminar Flow and Transport of Dilute Species physics settings, and the chosen channel geometry and flow parameters were input into the model. The model was solved, and shear forces and flow velocities were calculated. Stamps for PDMS flow chambers were cut out of 80μm thick MACtac (#8389-00-2411) to the dimensions verified by the COMSOL model using a cutting plotter (Graphtec #CE5000-60). Stamps were 1cm wide and 2cm long with triangular caps at the ends, and were placed on silica wafers to create a mold. PDMS (Sylgard® 184, Dow Corning #3097358-1004) was poured over the mold, degassed, and cured overnight at 65^{o}C. The PDMS channels were irreversibly bonded to a glass slide after plasma treatment. HMVECs were then cultured to confluence on the collagen-coated glass surface with EGM-2MV media flowed over the surface at 0.1dyne/cm^{2}. One million CFSE-stained (eBioscience # 65-0850-84) OECs or CACs were then flowed over the surface for 20 minutes in EBM-2 + 5% FBS. SDF was presented on the surface of HMVECs by flowing 500ng/ml SDF over the surface for 1 hour prior to beginning the experiment. Free SDF in the device was rinsed prior to adding OECs or CACs. Alternatively, SDF was presented in solution by adding 100ng/ml SDF to the suspension of OECs or CACs as they flowed over the HMVEC surface. Flow continued for 20 minutes after cell administration to rinse any unattached cells. Dapi was then added to the devices and cells were fixed with 0.5% paraformaldehyde. 30-60 images, in areas where HMVEC confluence was confirmed, were captured for each device to quantify cell adhesion. Each experiment was repeated three times.

Transwell Migration

Transwell membranes with 8μm pores (Corning # 3422) were used to assess OEC migration, while membranes with 5μm pores (Corning #3421) were used for CAC migration. Transwell membranes were coated with 5μg/ml Collagen IV in 10mM acetic acid overnight at 4^{o}C, and were then rinsed thoroughly

with PBS. EBM-2 media with 5% FBS was supplemented with 50ng/ml VEGF (R&D Systems #293-VE), 100ng/ml SDF or the combination (n=6-10 individual membranes), and this was applied to the bottom of the wells. Single cell suspensions of either OECs or CACs were prepared and 50,000 cells were applied to the top of 6mm diameter membranes. Plates were then allowed to incubate at 37^{o}C and 5% CO_2 for 4 hours. For OECs, cells remaining on the top of membranes were removed by wiping with a cotton swab, leaving migrated cells on the bottom of the membrane for quantification. Membranes were then removed from the transwell, mounted on glass slides with ProLong Gold Anti-Fade with Dapi and covered with a glass coverslip. Slides were protected from light and allowed to sit at room temperature for 24 hours before being stored at 4^{o}C until imaging. To quantify migration, 7 fields of view per membrane were imaged under dapi fluorescence. For CACs, cells that migrated through the membrane to the bottom of the transwell were counted.

Alginate Gel Preparation

Gels were prepared as previously described[32,48]. In brief, Ultra-pure MVG alginate was obtained from Pronova (# 4200106). MVG alginate was irradiated at 3MRad to obtain low molecular weight polymer chains. 1% of carboxylic acid groups on both high and low molecular weight alginates were oxidized to aldehyde groups with sodium periodate, to produce a hydrolytically labile polymer backbone[49]. The reaction was stopped with the addition of ethylene glycol after 17 hours. Alginate polymers were then dialyzed in 3000MWCO membranes for 3 days with repeated water exchange, frozen and lyophilized for storage. One day prior to use, both HMW and LMW alginate were reconstituted with EBM-2 to 2%w/v. VEGF and SDF were then added to a mixture of 75% LMW and 25% HMW alginates. 40µl of 0.21g/ml $CaSO_4$ was added per 1ml of alginate to crosslink the gel and was mixed between two 1ml syringes connected with a Leur-Lok union. Gels were allowed to crosslink for at least 30 minutes prior to use.

Cytokine Release from Alginate Gel

5μCi of ^{125}I-radiolabeled VEGF was purchased from Perkin Elmer (#NEX328025UC), and SDF (R&D Systems #350-NS) was custom labeled with ^{125}I by Lofstrand Labs Ltd (Gaithersburg, MD). Alginate gels were prepared as described above, with 3ug of unlabeled-VEGF or 2ug of unlabeled-SDF and approximately 0.05μCi of either ^{125}I-VEGF or SDF added per 50ul of alginate prior to cross-linking with $CaSO_4$. Immediately after the addition of $CaSO_4$, a 25G needle was connected to the 1ml syringe containing the alginate, and 50ul volume gels were distributed into polypropylene tubes. Gels were allowed to crosslink in the tubes for 1 hour before 2 ml of PBS containing Ca^{2+} and Mg^{+} with 1% BSA was gently added to each tube. CPM of the radiolabeled protein released into the supernatant and remaining in the gel were measured at multiple time points with a gamma counter (1470 WIZARD, PerkinElmer, Waltham, MA).

Hind-limb Ischemia Mouse Model and Muscle Tissue Processing

All animal experiments were performed in accordance with IACUC approved protocols. Hind-limb ischemia surgery was performed on C57BL6/J mice (#000664, Jackson Laboratory, Bar Harbor, ME) less than 10 weeks old, as previously described[31,48]. Briefly, mice were given an intraperitoneal injection of a Ketamine/Xylazine cocktail to induce anesthesia. An incision was then made at the inner thigh, exposing the underlying muscle and the external iliac artery and vein, and the hypogastric artery and vein. Two ligatures were placed around the external iliac artery and vein and one was placed around the femoral artery and vein. The external iliac vessel was cut between the two suture knots. Alginate gels containing 2ug of SDF and 3ug of VEGF or control gels (no factors) were then injected intramuscularly under the ligation site. The incision was closed with 7mm staples. One day after surgery, OECs or CACs in culture were stained for 10 minutes with 3ul of Vybrant™ DiD dye per million cells (Molecular Probes #V-22887), and were delivered to the mouse blood stream using an intracardiac injection to prevent first pass accumulation in the lungs. At 48 hours, the semimembranosus, semitendinosus, gracilis and adductor

muscles surrounding the vessel ligation site on the ischemic limb and the same muscles from the contralateral, non-ischemic limb were collected and enzymatically digested with 250 U/ml Collagenase II (Life Technologies #17101-015) in DMEM for 2 hours at 37^{o}C with agitation followed by trituration with glass pasteur pipette. Samples were then subjected to a second digestion step with 50U/ml Collagenase II and 1U/ml dispase II (Roche #04942078001) in DMEM at 37^{o}C for 2 hours with agitation, and were vortexed at high speed for 1 minute before being passed through 40µm filters in preparation for flow cytometry analysis. Alternatively, gastrocnemius muscles isolated from ischemic and contralateral, non-ischemic hind-limbs were processed for frozen tissue sectioning. Muscles were cryoprotected in 30% sucrose in PBS at 4^{o}C overnight, and then in 50% OCT compound (Tissue-Tek #27050) + 15% sucrose in PBS at 4^{o}C overnight, before being embedded and frozen in OCT compound. Samples were cut perpendicular to muscle fibers, midway through the gastrocnemius muscle into 10µm thick sections and placed on glass slides. Cryosections were rehydrated in 70% ethanol, and PBS. Rehydrated sections were permeabilized in blocking buffer (1% BSA fraction V (Sigma #85040) + 10% normal goat serum (Jackson ImmunoResearch Laboratories #005-000-001) in PBS, containing 0.2% TritonX-100 (Sigma-Aldrich #X100)). A primary mouse anti-human CD31 antibody (BD #555444) was applied to detect OECs, followed by a goat anti-mouse Alexafluor647-conjugated secondary antibody (Life Technologies #A21235), used for visualization under fluorescence. Cell nuclei were stained during cover slip mounting with ProLong Gold Anti-fade with Dapi (Invitrogen #P36935). Muscles were imaged at 4x and 20x magnification with a Nikon Eclipse E800 microscope (Nikon Instruments Inc., Melville, NY) equipped with an Olympus DP70 camera.

Additionally, Luciferase-transduced OECs were systemically delivered via intracardic injection one day after ischemia surgery to assay for localization to the ischemic hind-limb. At 48 hours following surgery, RediJect D-Luciferin Ultra Bioluminescent Substrate (Perkin Elmer #760505) was delivered into the intra-peritoneal cavity (150mg Luciferin / kg body weight) 10 minutes prior to animal sacrifice. Mouse

hind-limbs were detached and skin was removed prior to imaging with an InVivo Imaging System (IVIS Spectrum, Perkin Elmer, Waltham, MA).

Flow Cytometry of Cells Isolated from Hind-limb Muscle

Single cell suspensions of digested muscle were analyzed via flow cytometry for the presence of DiD-labeled OECs or CACs. Fluorescently labeled antibodies for CD11b (eBioscience #25-0112), F4/80 (eBiosceince #12-4801), and Gr1 (eBioscience #11-5931) were used to stain for inflammatory cell presence in the samples. Briefly, blocking buffer (10%NGS + 1%BSA in PBS) was applied to the cell suspension for 15 minutes at room temperature. 0.25ug of each antibody was the applied to the individual cell suspensions and these were placed on ice for 45 minutes. Cells were then washed three times in PBS with 0.1% BSA before flow cytometry was collected with a BD LSRFortessa (Franklin Lakes, New Jersey) and analyzed with FlowJo software (Tree Star, Inc. Ashland, OR

Statistical Analysis

Data was compared using a Students unpaired t-test (two-tailed), with a p-value less than 0.05 considered significant. A 3-way ANOVA was used to compare contributions from and interactions between different test factors in *in vivo* experiments using IBM SPSS Software. ANOVA statistical evaluations were performed in consultation with a biostatistician at Harvard Catalyst.

2.4 Results

OEC and CAC Characterization

The expression of surface markers commonly used to characterize endothelial progenitors was first analyzed on OECs and CACs to confirm their identities (Figure 2.1A-B). Flow cytometry analysis confirms a high percentage of OECs expressed typical endothelial markers, including CD31, VE-Cadherin, and VEGFR-2, a smaller percent expressed CD34, and no expression of CD45 or CD14 was detected. CAC populations alternatively showed moderate percentages staining positive for CD31 and VEGFR-2, but high percentages staining positive for CD45 and CD14, hematopoietic and myeloid lineage markers, respectively. A high percentage of both OECs and CACs expressed CXCR4, the receptor for SDF (75% and 85%, respectively).

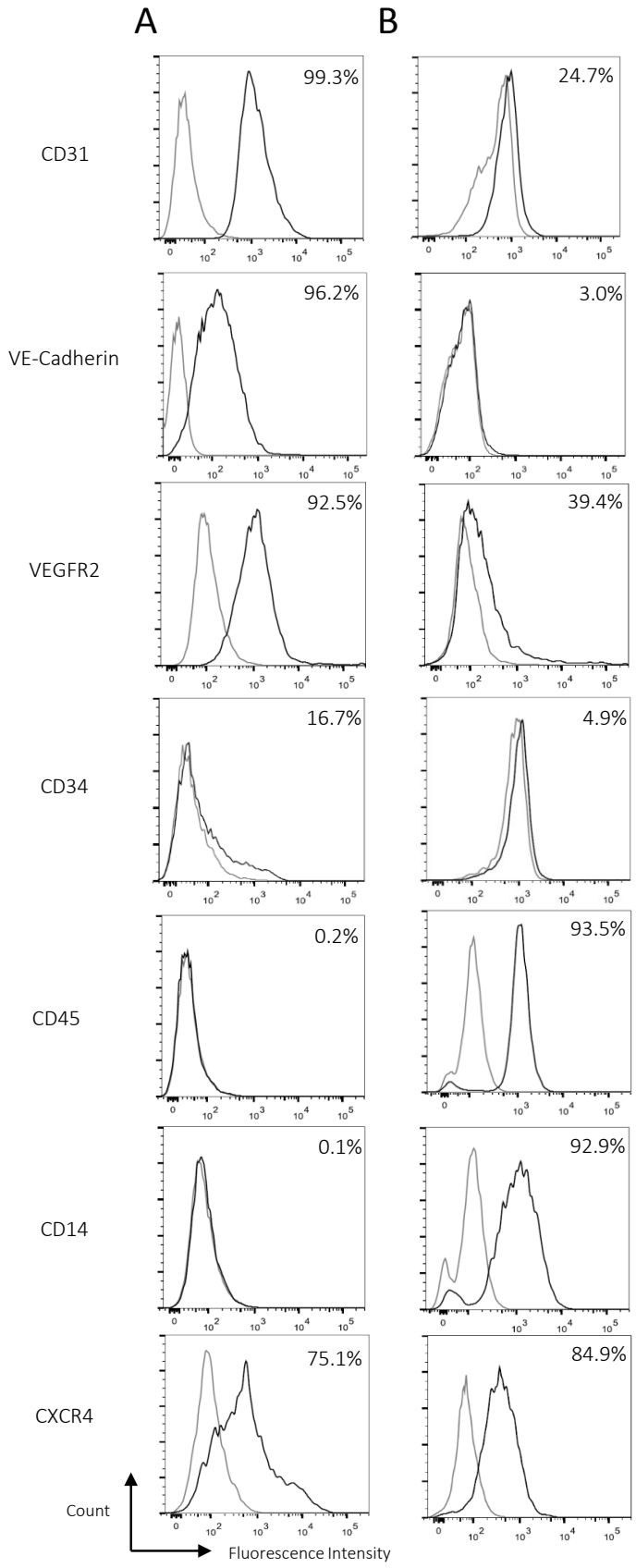

Figure 2.1. Flow cytometry characterization of OECs (A) and CACs (B). Representative histograms of relative expression of endothelial and hematopoietic markers used to characterize progenitors. Antibody-stained sample (black line) and isotype control (grey line).

In vitro Adhesion Models

As adhesion of progenitors to endothelial cells in blood vessels is an important initial step in the recruitment of these cells, OECs and CACs were assayed for their ability to adhere to cultured human microvascular endothelial cells (HMVECs). When HMVECs were pre-treated with TNFα, an inflammatory cytokine, to mimic the inflammation typical of ischemic tissues, the expression of ICAM and VCAM were increased, as expected (Figure 2.2A-B). TNFα stimulation of HMVECs led to increased adhesion of both OECs and CACs to endothelial monolayers compared to untreated endothelial cells (Figure 2.2C; Suppl Figure 2.1). OEC adhesion was increased by a factor of 1.6, while CAC adhesion was increased by a factor of 6 with TNFα stimulation. For comparison, lymphocyte adhesion increased by 11 times when endothelial cells were stimulated with TNFα (Figure 2.2C). Since TNFα stimulation causes up-regulation of adhesion molecules on the endothelial surface, and also leads to increased OEC and CAC adhesion, it is likely that integrin-adhesion molecule interactions are involved in this process. A common interaction mediating adhesion of circulating cells involves β2 integrins (αL β2 and αM β2) and ICAM[10,50]. Almost all CACs expressed high levels of β2, while OECs were either negative or expressed low levels (Figure 2.2D). In addition, CACs express other integrins, such as α4, α5β1, β3, β4, and β6, to a greater extent than OECs (Suppl Figure 2.2). These differences may be responsible for the larger increase in adhesion for CACs compared to OECs following TNFα stimulation of HMVECs. β2 blocking antibodies, applied at saturating concentrations, reduced adhesion of both OECs and CACs in a statistically significant manner (Figure 2.2E-G). To further probe the role of β2 integrins, since the reduction in adhesion of OECs with β2 integrins blocking antibodies was modest, recombinant human soluble ICAM (rhsICAM) protein was added to OECs as an alternative method of blocking β2 integrins. The addition of rhsICAM reduced adhesion of OECs to HMVECs to the same level as β2 blocking antibody (82% of control; Suppl Fig 2.3). Blocking β2 integrins on CACs reduced adhesion to 40% of the control on non-stimulated HMVECS, and to 65% of the control with TNFα-stimulated HMVECs (Figure 2F). Adhesion results were replicated with CACs seeded on Human Umbilical Vein Endothelial Cells

(HUVECs), verifying that the adhesion behavior was not specific to one endothelial cell type (Figure 2.2G). Additionally, as a positive control, lymphocytes were also subjected to β2 blocking before application onto TNFα-stimulated HMVECs. Lymphocyte adhesion was reduced to 55% of the control level following the addition of β2 blocking antibodies (Figure 2.2H). These results suggest that β2 integrin is more responsible for CAC than OEC adhesion to endothelial cells. CACs may be more responsive to the ICAM level on endothelial cells than OECs in part because they rely on β2 integrins for adhesion to a greater extent than OECs.

Finally, in order to specifically assay the β2 integrin-ICAM interaction in OEC and CAC adhesion, these cells were tested for their ability to adhere directly to an ICAM-coated surface (Suppl Figure 2.4 - ICAM deposition method verification). Similar to adhesion assays with endothelial cells, adhesion of both OECs and CACs was reduced when β2 blocking antibodies were added to the cells prior to seeding onto the ICAM surface (Figure 2.2I-J). To eliminate all integrin involvement during adhesion, EDTA was added to the adhesion solution. EDTA did not reduce adhesion of OECs or CACs to a greater extent than β2 blocking antibodies alone, suggesting that the only integrin both OECs and CACs use to adhere to ICAM surfaces is the β2 integrin, as expected. OECs and CACs were also added to BSA-coated wells as a negative control to assess the background level of adhesion to the well plate surface. OECs and CACs demonstrated the lowest levels of adhesion to BSA-coated wells.

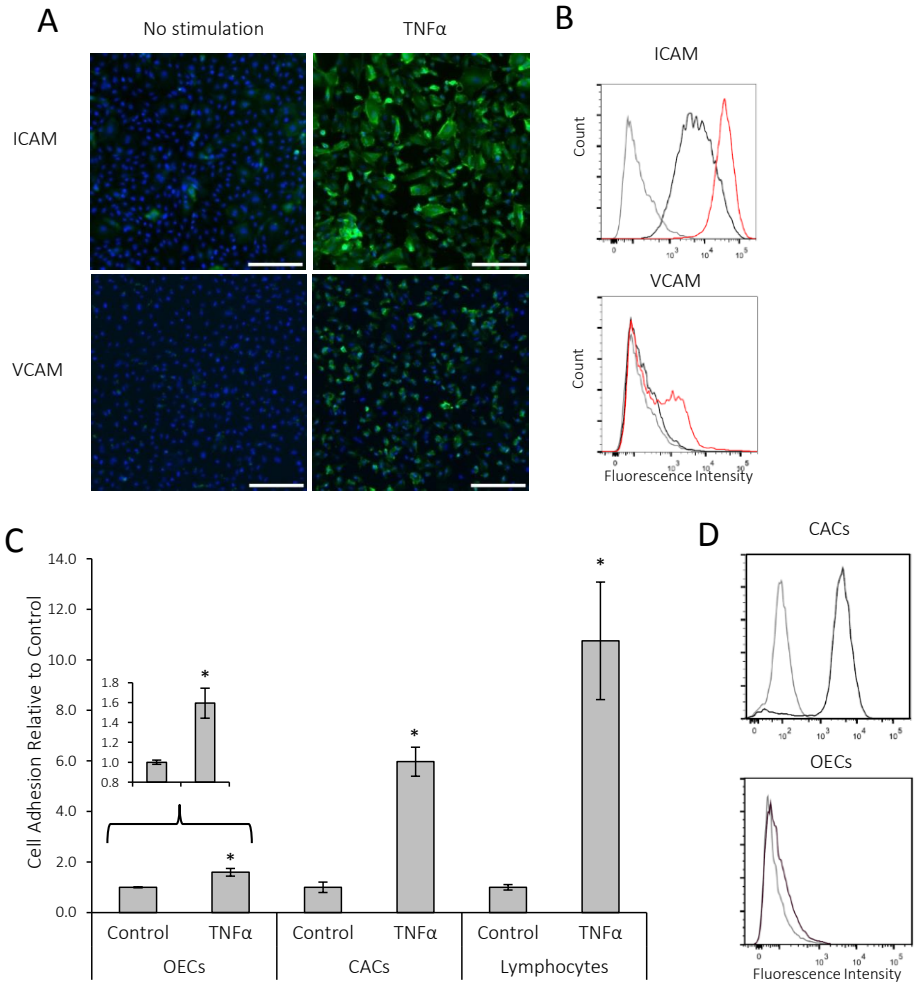

Figure 2.2. Adhesion of OECs and CACs to endothelial cells, and role of B2 integrins. A) Immunohistochemical staining of ICAM and VCAM on HMVECs treated with 50ng/ml TNFα for 8 hours or control (No Stimulation). Scale bars are 200µm. B) Representative histograms of flow cytometry characterization of ICAM and VCAM expression on HMVECs after TNFα stimulation (red line) or no stimulation (black line); grey line is isotype control. C) Adhesion of OECs, CACs and lymphocytes to HMVECs grown in regular media (Control) or media supplemented with TNFα. Cell counts are normalized to the control to compare the relative increase in adhesion to activated endothelial cells. Inset is magnified view of OEC adhesion. D) Representative histograms from flow cytometry characterization of β2 integrin expression on OECs and CACs. Antibody-stained sample (black line) and isotype control (grey line).

Figure (2.2 Continued)

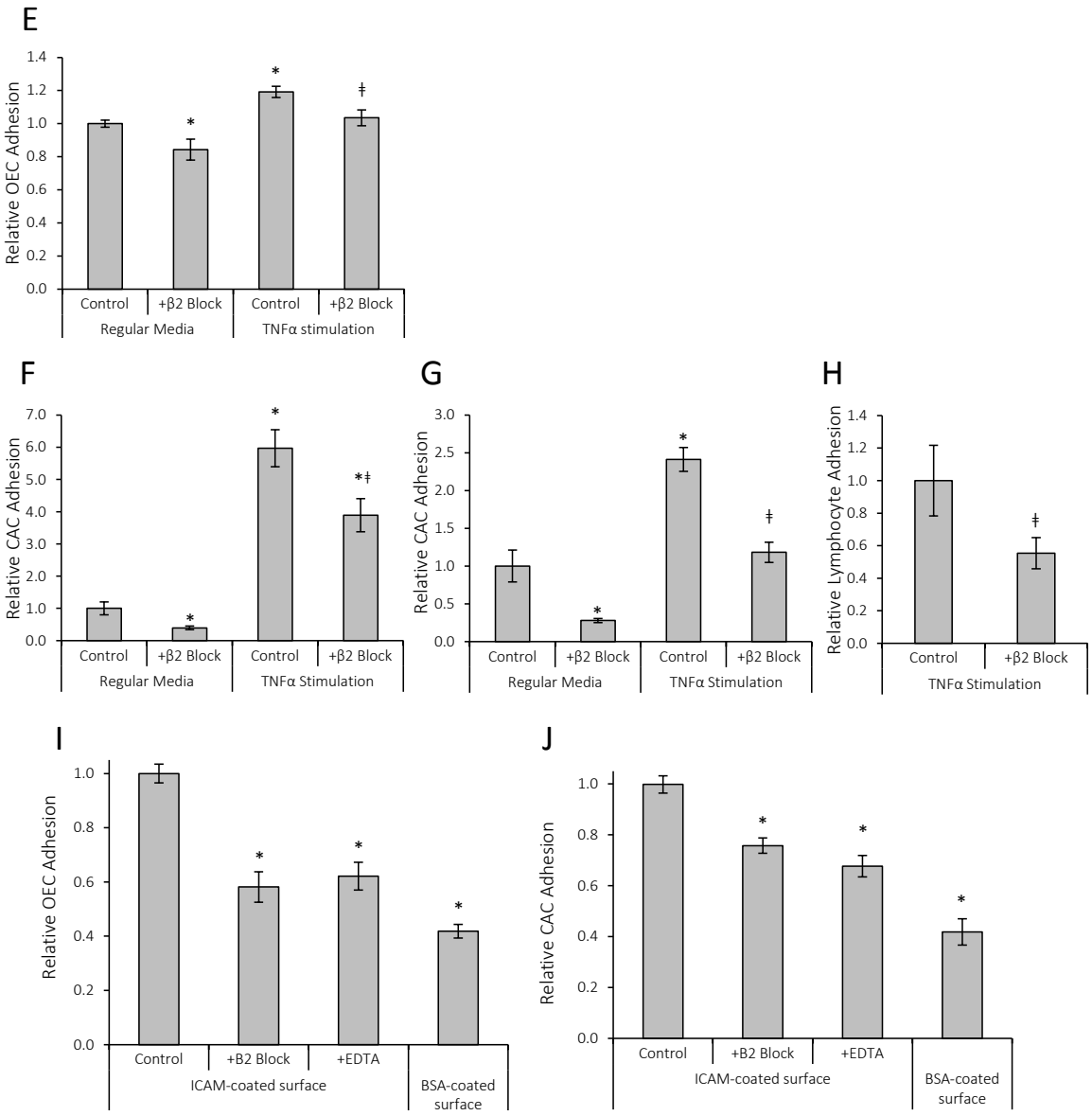

Figure 2.2 (Continued). E-H) Adhesion of OECs to HMVECs (E), CACs to HMVECs (F), CACs to HUVECs (G), and lymphocytes to HMVECs (H) with and without application of a β2 integrin blocking antibody, and with or without TNFα stimulation of endothelial cells. I-J) Adhesion of OECs (I) and CACs (J) to surfaces coated with 5mg/ml recombinant human soluble ICAM protein or BSA as the negative control. 2mM $MnCl_2$ was added as the positive control to activate integrins, and 5mM EDTA was added to prevent integrin-based adhesion. Results were combined from 2-10 experiments with n=6 for each experiment. Data is plotted as Mean ± SEM. * $p < 0.05$ compared to control, ‡ $p < 0.05$ compared to TNFα-stimulated control.

Effects of SDF on OEC and CAC Adhesion

SDF is involved in endothelial progenitor trafficking and is also known to activate integrins on lymphocytes to increase adhesion to endothelial cells[51,52]. We therefore tested the ability of SDF to increase adhesion of OECs and CACs. VEGF is not expected to affect adhesion by OECs or CACs and was therefore not tested in these assays. SDF was presented on the surface of endothelial cells by pre-incubating HMVECs with 500ng/ml SDF for 1 hour and was then rinsed before applying OECs or CACs. Alternatively, SDF was continuously present in the adhesion buffer solution during OEC and CAC adhesion. For OECs, SDF modestly increased adhesion only when it was presented on the surface of unstimulated endothelial cells. OEC adhesion was higher in all three conditions when HMVECs were stimulated with TNFα, and no statistically significant effect of SDF on adhesion was found in this setting (Figure 2.3A). In contrast, CAC adhesion to unstimulated endothelial cells increased both when SDF was presented in solution during adhesion (1.8X) and on the surface (2.7X, Figure 2.3B). CAC adhesion was dramatically increased in all these conditions following TNFα stimulation of endothelial cells, and adhesion of CACs was only further increased when SDF was presented in solution.

SDF was also tested for the ability to increase OEC and CAC adhesion to ICAM surfaces. OEC adhesion was increased modestly with SDF, but the effect was only statistically significant when SDF was presented from the adhesion surface (Figure 2.3C). In contrast, CAC adhesion to ICAM-coated dishes doubled when SDF was present in solution (Figure 2.3D). As a positive control, $MnCl_2$ was added to activate integrins, which resulted in increased adhesion of both OECs and CACs, although the effect was more dramatic for CACs, in agreement with the above finding that CACs express higher levels of adhesion-mediating β2 integrins. These results provide further support for an increased responsiveness of CACs, compared to OECs, to adhesive cues.

Finally, to better mimic the *in vivo* process of adhesion that progenitors must undergo during recruitment, flow-based adhesion assays were conducted in PDMS-based parallel-plate flow channels (Suppl Figure

2.5). HMVEC monolayers were grown to confluence with media flowing over the surface, with a resulting shear stress of 0.1dyn/cm^2. The effects of SDF on progenitor adhesion, when presented both on the surface and in solution during adhesion, were tested in these devices. SDF has differential effects on lymphocyte adhesion depending on the presentation[51], which may also be possible to observe for OECs and CACs. OECs showed an increase in adhesion when SDF was presented in solution, but only surface presentation of SDF resulted in a statistically significant increase (Figure 2.3E). CACs demonstrated the same trend, where only surface presentation led to a statistically significant increase in adhesion. CAC adhesion was increased by 4-fold, whereas OEC adhesion was increased less than 3-fold in this assay, consistent with previous results where CACs showed higher sensitivity to SDF (Figure 2.3F).

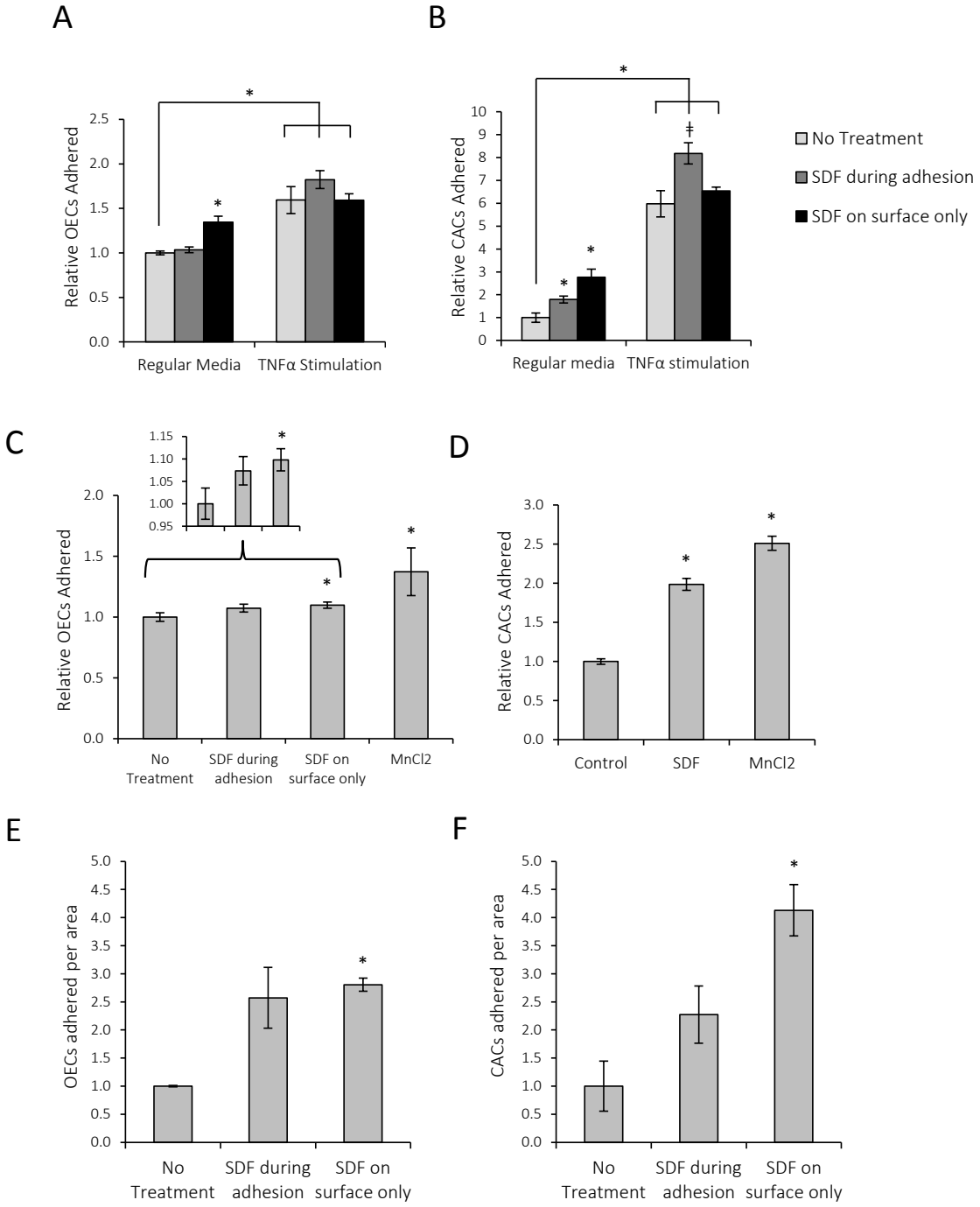

Figure 2.3. SDF effects on OEC and CAC adhesion. A-B) Adhesion of OECs (A) and CACs (B) to HMVECs with SDF presented in solution during adhesion or on the surface of HMVECs. C-D) Adhesion of OECs (C) and CACs (D) to ICAM-coated surfaces with SDF presented in solution or on the surface. Data are presented as Mean ± SEM from a minimum of 3 separate experiments with n=6 for each experiment. E-F) Adhesion of OECs (E) and CACs (F) to HMVECs under flow conditions with SDF presented in solution during adhesion or on the surface. Shear stress at the surface was 0.1dyn/cm^2 and flow velocity was 0.2mm/sec. For each experiment, 30-60 images were captured for each condition to quantify cell adhesion per area; each experiment was repeated three times. * $p < 0.05$ compared to control, ‡ $p < 0.05$ compared to TNFα-stimulated control.

OEC and CAC Migration in Response to VEGF and SDF

Migration of OECs or CACs into ischemic tissue is also an important step in the recruitment of these cells. VEGF and SDF were tested for their ability to promote migration of OECs and CACs in transwell assays. OECs demonstrated a 25% increase in migration towards a source of SDF (100ng/ml), and a 31% increase in migration towards VEGF (50ng/ml) (Figure 2.4A). When VEGF and SDF were presented in combination, each at the same concentration used individually, OEC migration doubled, suggesting a synergistic effect of the two growth factors. CACs demonstrated a nearly three-fold increase in migration when SDF was present, while VEGF had no effect on migration , and the combination of VEGF and SDF did not increase CAC migration significantly above the condition with SDF alone (Figure 2.4B).

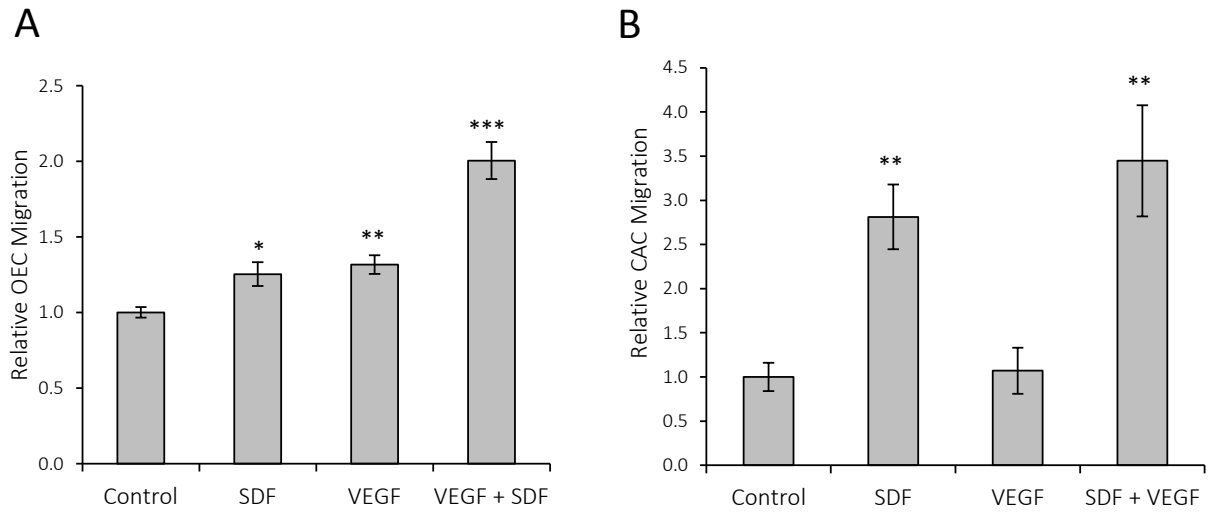

Figure 2.4. OEC and CAC migration toward SDF and VEGF. Quantification of relative migration in transwells toward 100ng/ml SDF, 50ng/ml VEGF or the combination for OECs (A) and CACs (B). Data are shown as Mean ± SEM from one experiment, with n = 6-10. * $p < 0.05$, ** $p < 0.01$, *** $p < 0.001$.

VEGF and SDF Delivery System

Hydrogels to provide a sustained and localized release of VEGF and SDF were next characterized. Injectable alginate gels were fabricated from a combination of 1% oxidized, low and high molecular weight polymer chains and were cross-linked with calcium ions[32,48]. The use of a hydrogel for growth

factor and cytokine delivery creates a depot for localized and sustained release[25,48]. The release kinetics of VEGF and SDF were individually quantified by incorporating ^{125}I-radiolabeled protein into alginate gels, and measuring the amount released into PBS supplemented with 1% BSA at multiple time points with a gamma counter. SDF exhibited a burst release of ~50% gels over the period of a few days, followed by a continuous slow release for several weeks (Figure 2.5A). VEGF exhibited similar release kinetics, with faster release in the first few days and slower, steady release at later time points, as expected[48] (Figure 2.5B). The sustained release demonstrated by VEGF and SDF from these gels *in vitro* is expected to translate to an extended release *in vivo*, as was shown previously[48].

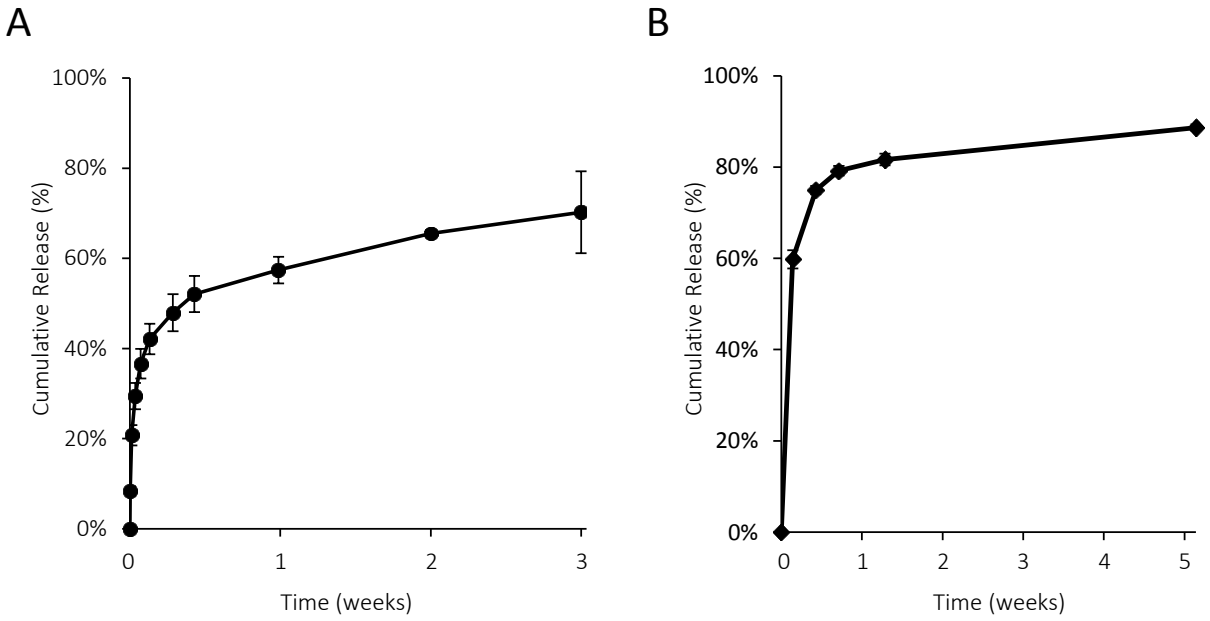

Figure 2.5. Characterization of cytokine and growth factor release from injectable alginate hydrogels. A-B) Cumulative release of SDF (A) and VEGF (B). Mean ± SD.

In Vivo OEC and CAC Recruitment to Non-Ischemic Limbs

To determine the effect of local presentation of VEGF and SDF on the recruitment of OECs and CACs, alginate gels loaded with a combination of VEGF and SDF were injected into one hind-limb of mice. The other, non-treated limb, served as the control. One day following gel injection, DiD-labeled OECs or

CACs were delivered to the bloodstream via intracardiac injection. Intracardiac injections were found to dramatically reduce cell accumulation in the lungs compared to tail vein injections (Suppl Fig 2.6A-B).

Accumulation of OECs and CACs in the semimembranosus, semitendinosus, gracilis and adductor muscles surrounding the gel injection site was quantified 24 hours after cell delivery by retrieving muscle tissue, digesting to single cells, and using flow cytometry analysis (Figure 2.6A). Gel injection alone appeared to modestly increase the number of accumulated OECs and CACs, but not in a statistically significant manner. Generally, there was a trend for both OECs and CACs to accumulate to greater numbers in limbs treated with VEGF and SDF compared to control gel injections (Figure 2.6B-C). Further, the ratio of the mean number of cells accumulated in the test limb over the contralateral limb is always higher for the VEGF and SDF conditions versus control conditions (7.6 vs 2.2, respectively for OECs, and 3.6 vs 1.9 respectively for CACs). Infiltration of inflammatory cell populations into the hind-limbs was also characterized, as VEGF and SDF are known to recruit a variety of inflammatory cells[53–57]. Interestingly, when CACs were delivered to the blood stream and allowed to accumulate in non-ischemic limbs at sites of alginate gel injection, there was a subsequent large influx of both CD11b+ myeloid-lineage cells and F4/80+ cells, presumably macrophages, whereas extremely low inflammatory cell influx was observed with OEC delivery (Figure 2.6D-E). In the contralateral limb the average percentage of CD11b positive cells was 3% and F4/80 positive cells was 0.5%. When CACs were transplanted, statistically significant differences between the test limbs and contralateral limbs were found for both CD11b+ and F4/80+ cells, regardless of whether gels contained VEGF and SDF or were blank. No statistically significant differences between test limbs and contralateral limbs were found for either gel condition or inflammatory cell type when OECs were transplanted. There was a trend of increased Gr1+ cell accumulation at the gel injection site compared to the contralateral limb, but no statistically significant differences were found for either CAC or OEC delivery. Further, no difference in the level of inflammatory cell recruitment was found between limbs receiving VEGF and SDF-delivering gels and control gels, for either cell type. While the number of CACs present in non-ischemic muscle varied

considerably between mice, the number of CACs recruited for each individual mouse strongly and positively correlated with the presence of CD11b+ cells (R^2 = 0.69, Figure 2.6F), F4/80+ cells (R^2 = 0.94, Figure 2.6G), and Gr1+ cells (R^2 = 0.89, Figure 2.6H) in that particular limb. For each CAC found in the hind-limb, there were approximately 680 Cd11b+ cells, 220 F4/80+ cells, and 40 Gr1+ cells. Delivery of OECs did not result in the same strong, linear correlation for either CD11b+ cells (R^2 = 0.44, Figure 2.6I), F4/80+ cells (R^2 = 0.43, Figure 2.6J). The R^2 value for Gr1+ cells after OEC delivery is artificially high (R^2 = 0.74), because it is strongly influenced by the single data point associated with ~2500 OECs collected; without it, R^2 = 0.06 (Figure 2.6K). Application of the linear correlation for each immune cell type would suggest that for each OEC found in the hind-limb, there were approximately 24 CD11b+ cells and 18 F4/80+ cells, and 0.5 Gr1+ cells, approximately 1-2 orders of magnitude fewer than for CACs.

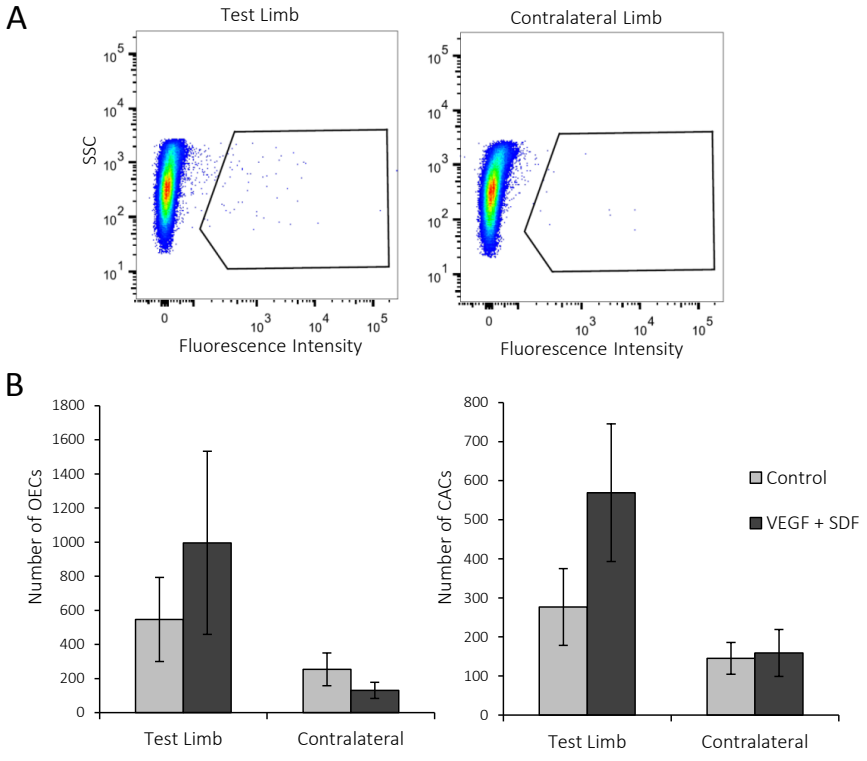

Figure 2.6. OEC and CAC recruitment to non-ischemic mouse hind-limbs with VEGF and SDF delivery. A) Flow cytometry plots of DiD positive cells collected from mouse hind-limb muscles where gel was injected (Test Limb) or from the Contralateral Limb. B-C) Quantification of the total number of OECs (B) and CACs (C) recovered from mouse hind-limb muscle surrounding the alginate gel injection site (test limb) or the muscle from the contralateral limb. 750,000 OECs or 200,000 CACs were systemically delivered into separate groups of mice. Data is shown as Mean ± SEM, n=4.

Figure 2.6 (Continued)

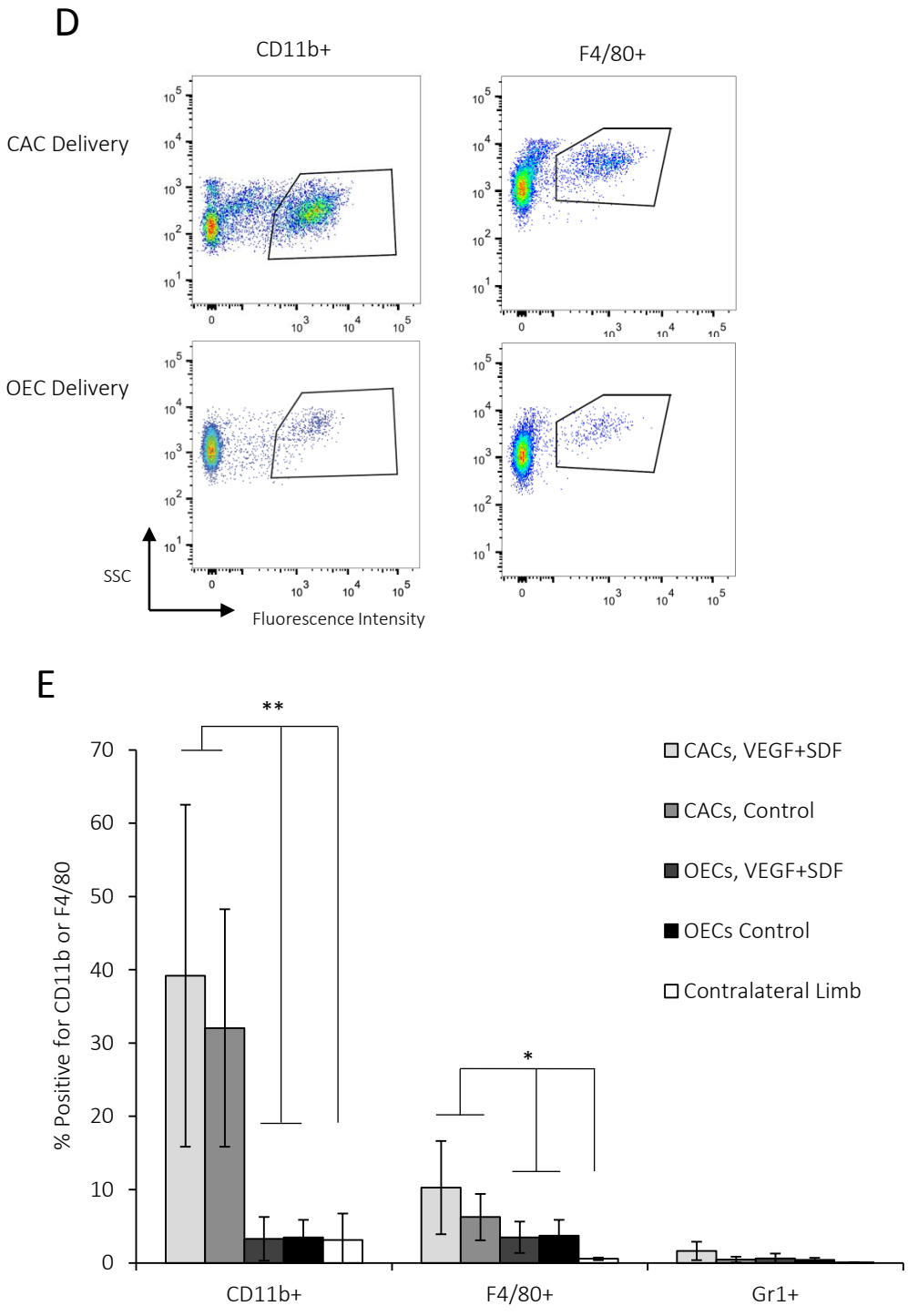

Figure 2.6 (Continued). D) Flow cytometry characterization of myeloid lineage cells (CD11b+) and F4/80+ cells collected from hind-limb muscle tissue surrounding the gel injection. E) Quantification of the percentage of total cells in the tissue surrounding alginate gel injection site that stained positive for CD11b, F4/80, or Gr1 after systemic injection of OECs and CACs. Mean ± SD, n=4. * $p < 0.05$, ** $p < 0.01$

Figure 2.6 (Continued)

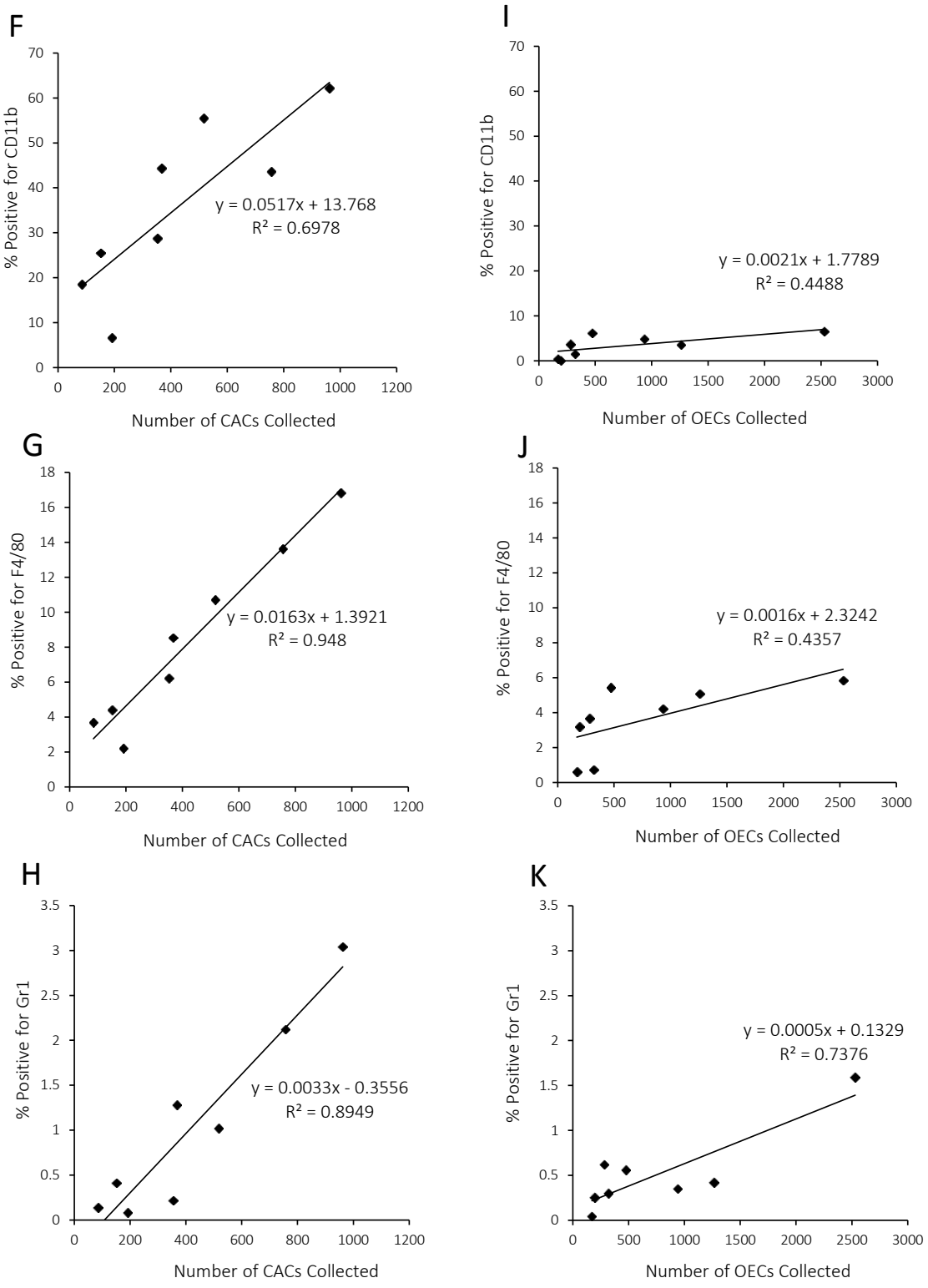

Figure 2.6 (Continued). F-K) Plots of number of CACs or OECs collected in each limb and the percentage of cells in the tissue that were positively stained for CD11b, F4/80, and Gr1. Correlation plots shown, with linear-fit equation and R^2 value indicated on each chart.

In Vivo OEC and CAC Recruitment to Ischemic Limbs

Recruitment of OECs and CACs to ischemic muscle, in the absence of VEGF and SDF stimulation, was next analyzed. Mice were subjected to complete ligation of the external iliac artery and vein in order to induce hindlimb ischemia (Figure 2.7A). Blood flow to the test limb was reduced to 25% of the contralateral limb (Figure 2.7B), as expected for this model[31,58]. Either during surgery, or on day 7 or 14 following surgery, mice also received an injection of blank alginate (no VEGF or SDF). OECs or CACs were delivered on day 1, 8 and 15 post-surgery, and were allowed to accumulate in limbs for 24 hours before muscle tissue was collected for analysis (See figure 2.7C for timeline). The numbers of both OECs and CACs accumulating in the ischemic hindlimb muscle tissue were increased dramatically at Day 2 (Figure 2.7D-E). The recruitment of OECs to ischemic limbs still remained high when cells were delivered on day 8 (with limbs collected on day 9), but the effect of ischemia on recruitment was lost when cells were delivered on day 15. Cell accumulation in the contralateral, control limb was low for all conditions and time points, suggesting the impact of ischemia on cell accumulation is a local effect, with little systemic spill-over impact (Figure 2.7F). To qualitatively confirm results using labeled cells, luciferase-expressing OECs were additionally delivered on day 1 post-surgery, and analyzed using non-invasive imaging. Preferential accumulation in the ischemic hind-limbs, compared to the contralateral limb, was again noted (Figure 2.7G). Additionally, immunohistochemistry was used to locate systemically OECs within the muscle tissue (Suppl Figure 2.7). OECs were identified within tissue sections, but were often difficult to find because typically 0-2 cells were present within each 10μm section. Although the number of cells per section was very low, it was quantitatively consistent with the total number of OECs collected from muscle for flow cytometry analysis being evenly distributed throughout the tissue volume.

To determine if cells are simply trapped in blood vessels which may be altered in the ischemic tissue, OECs that had been previously fixed with 1% paraformaldehyde for 10 minutes were injected into the blood stream of mice one day after ischemia surgery. The accumulation of fixed cells was compared to

the recruitment of regular, non-fixed OECs. The average number of fixed OECs accumulated in the ischemic limb was lower than the average number of regular OECs, although this difference was not statistically significant (Figure 2.7H). As an additional test for passive accumulation in the ischemic hind-limb, fluorescent beads with either a 6μm or 15μm diameter were systemically delivered one day following surgery. Quantification of 6μm bead accumulation in the hind-limb muscles revealed no preference for accumulation in the ischemic or contralateral, non-ischemic limb (Figure 2.7I). Specifically, the ratio of the number of 6μm beads found in the ischemic limb to the contralateral limb was 1.01 ± 0.21 (Mean ± SEM, n=5). Alternatively, the larger 15μm beads, which are approximately the same size as both OECs and CACs, resulted in severe injury or death to 3 out of 4 mice, most likely due to entrapment and blockage of vital blood vessels. The single surviving mouse showed no preference for bead accumulation in the ischemic or contralateral limb, while the number of beads detected was extremely low (approximately 30 times fewer than the number of 6μm beads found in the limbs).

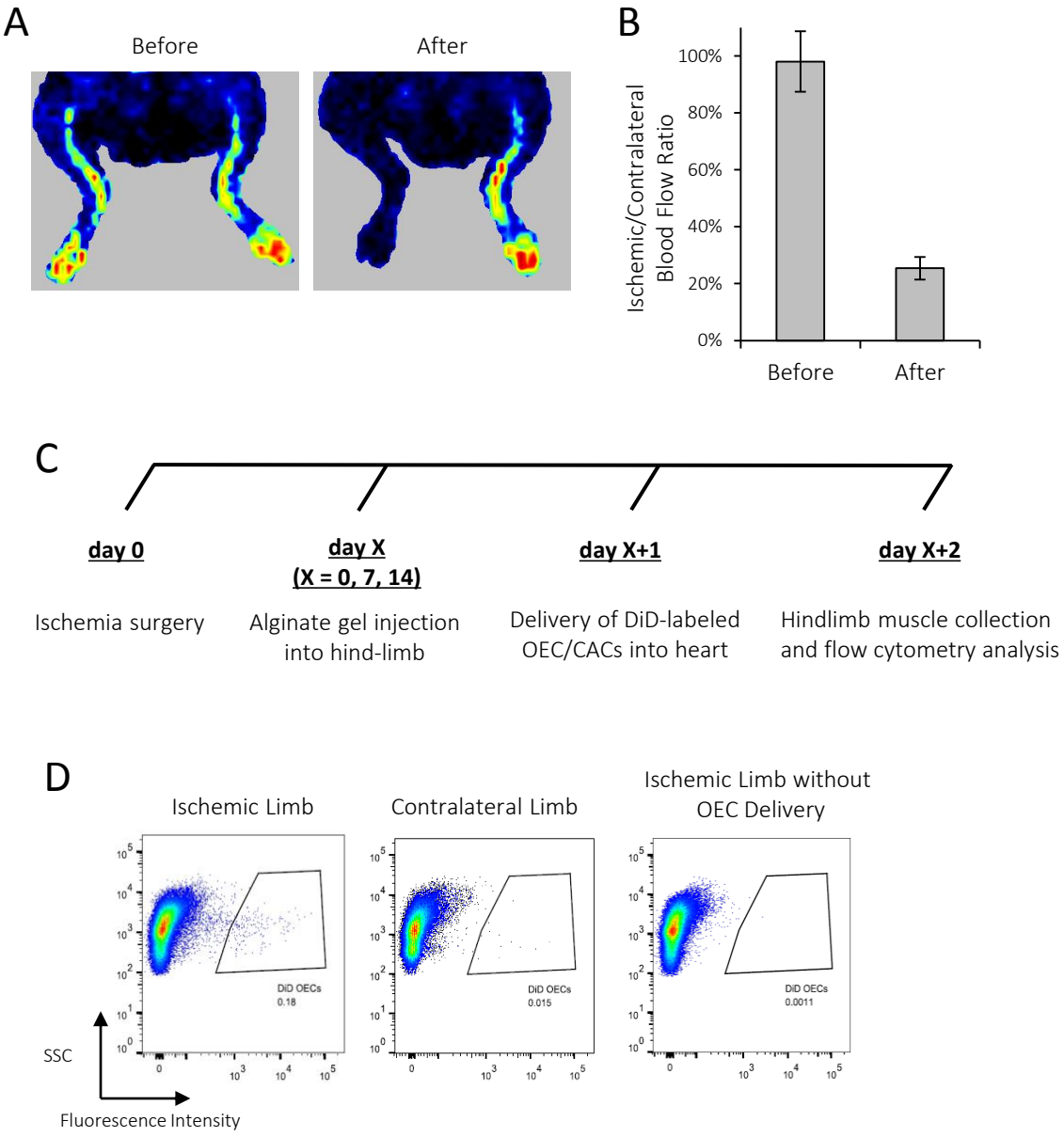

Figure 2.7. Recruitment of progenitors to hind-limb muscle tissue after ischemia surgery. A) LDPI images of blood perfusion in mouse limbs before and after surgery. B) Quantification of blood perfusion before and after surgery. Mean ± SD, n=20. C) Experimental timeline. D) Flow cytometry plots of DiD-labeled OECs collected from mouse muscle in the ischemic limb (left), contralateral limb (center) and from an ischemic limb without OECs delivered (negative control, right). Dot plots are shown as fluorescence intensity vs. side scatter.

Figure 2.7 (Continued)

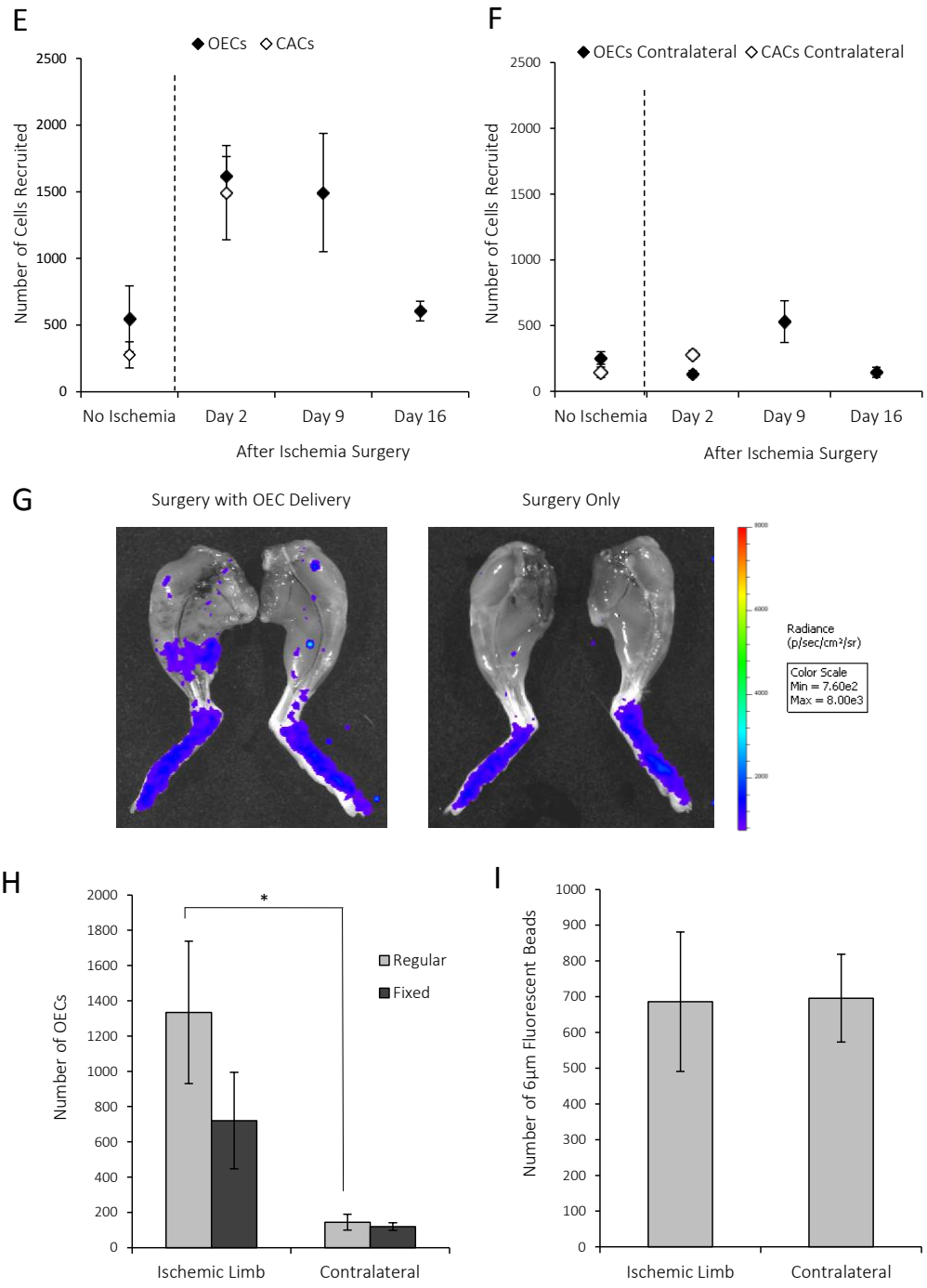

Figure 2.7 (Continued). E-F) Number of OECs and CACs accumulated in mouse hind-limbs when injected at various time-points after surgery in the ischemic (E) and the contralateral limbs (F). Data are shown as Mean ± SEM, n=6. G) IVIS images of hind-limbs of mice following systemic delivery of luciferase-transduced OECs. Both the ischemic limb (left) and contralateral limb (right) are shown (left image), and hind-limbs from a control mouse which underwent surgery but did not receive OECs (right image). H) Quantification of OEC accumulation on day 2 in the ischemic and contralateral limbs after delivery of regular or paraformaldehyde-fixed cells Mean ± SEM, n=10. I) Number of 6µm-diameter fluorescent beads accumulated on day 2 in the ischemic and contralateral limbs. Mean ± SEM, n=10.

As ischemia surgery is expected to lead to inflammation[59] (Figure 2.8A), immune cell infiltration into the ischemic tissue following hind-limb ischemia surgery was characterized. A dramatic influx of cells was observed within two days (Figure 2.8B-D), and CD11b+ myeloid lineage cells constituted approximately half of the total cells collected from the ischemic limb at this time (Fig. 2.8E). The number of CD11b+ cells remained high at day 9, and decreased at day 16. F4/80+ cells, presumably macrophages, were also present in large numbers early, and showed a reduced presence over time (Figure 2.8F). Cells positive for Gr1 accumulated to significant numbers at day 2, but returned close to baseline by day 9 (Figure 2.8G). The number of inflammatory cells in the contralateral limb remained very low at all time points. Specifically, CD11b+ cells ranged from 5-10%, F4/80+ cells decreased from 7% on day two to 1.4% on day 16, and Gr1+ cells decreased from 1.4% to 0%, which were almost all significantly less than the measured values for the ischemic limb. Last, the kinetics of inflammatory cell accumulation in the ischemic tissue was similar to that observed with infused OECs (Fig. 2.7E).

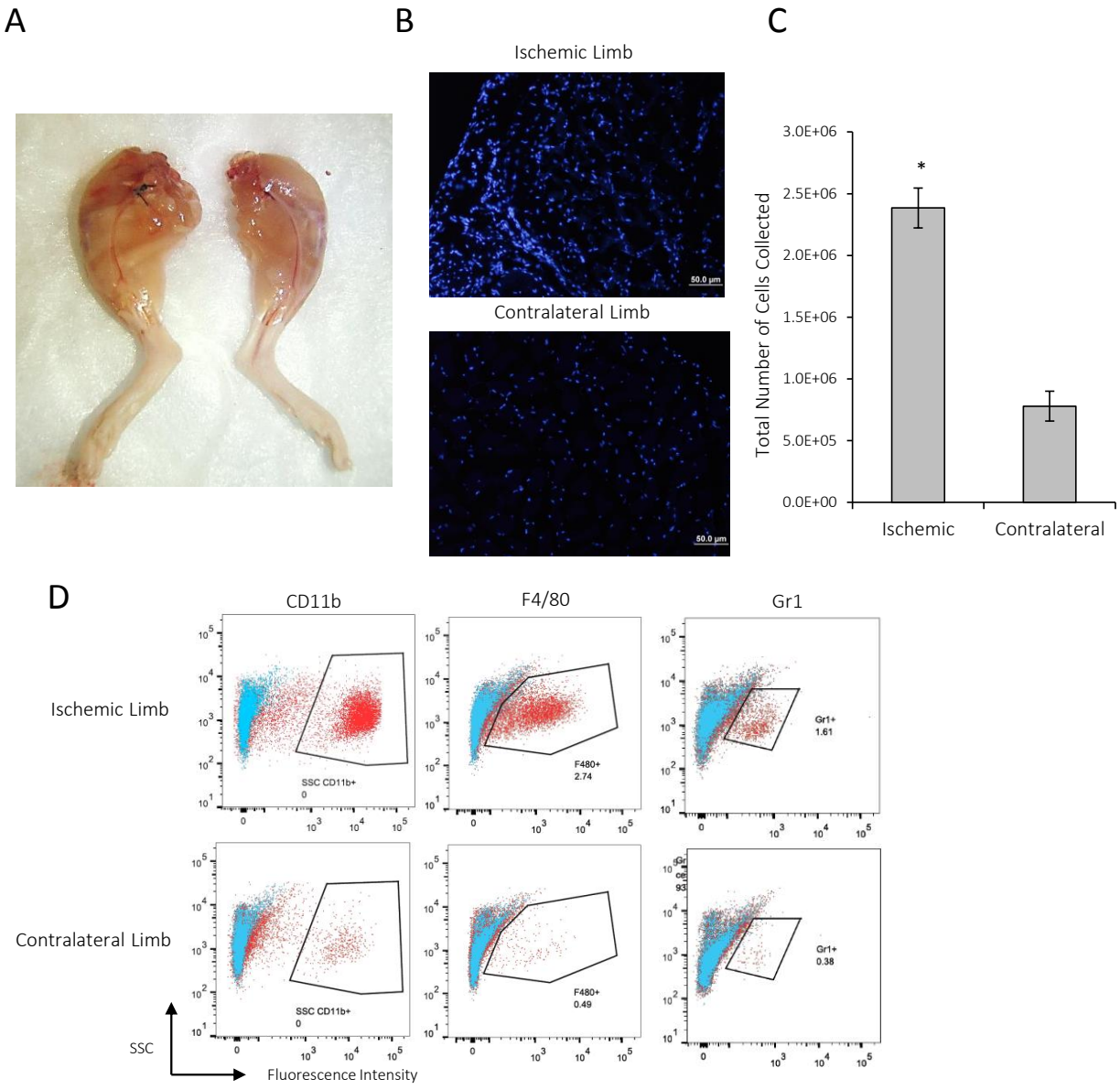

Figure 2.8. Characterization of inflammatory cell infiltration due to ischemia. A) Photograph of ischemic, swollen limb two days after surgery (left) and the contralateral, healthy limb (right). B) Cell accumulation, as analyzed using DAPI-stained tissue sections from the ischemic limb compared to the contralateral, healthy limb. Scale bars are 50 C) Average number of cells collected from ischemic and contralateral limbs two days after surgery. Mean ± SEM, n=12. D) Flow cytometry plots for analysis of CD11b, F4/80 and Gr1 stained cells collected from ischemic and healthy limbs (contralateral) two days after surgery. Blue is unstained; Red is antibody stained.

Figure 2.8 (Continued)

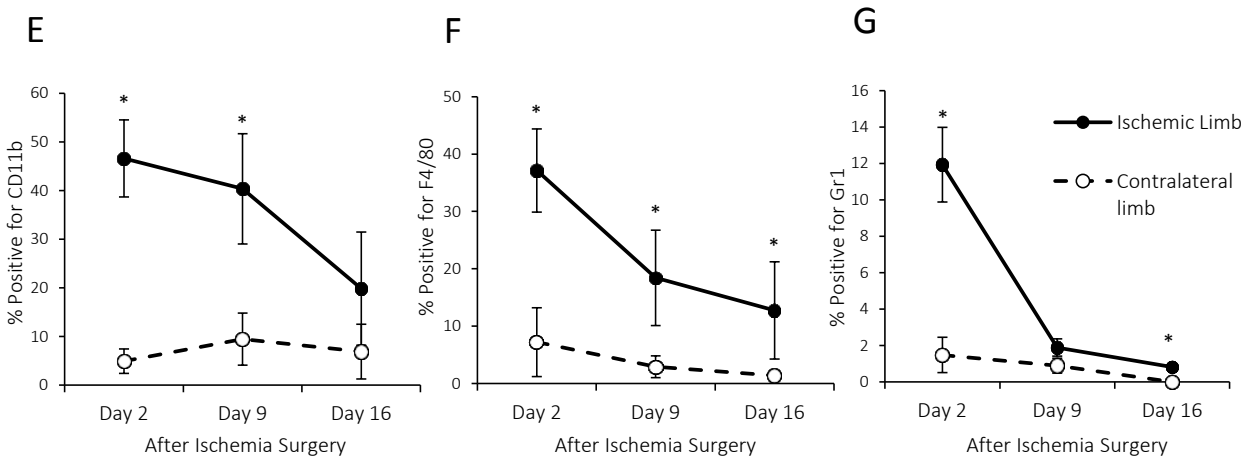

Figure 2.8 (Continued). E-G) Time course quantification of the percentage of cells in both the ischemic limb, and contralateral, control limb that stained positive for CD11b (E), F4/80 (F), and Gr1 (G) as a function of time. Mean ± SD, n=6. * $p < 0.05$.

SDF and VEGF-releasing Alginate Hydrogels for OEC and CAC Recruitment to Ischemic Limbs

Since OEC recruitment to ischemic limbs is highest immediately after surgery, this time point was chosen to test whether VEGF and SDF-releasing alginate gels could enhance recruitment of OECs and CACs. Similar to the timeline shown in Figure 2.7C, some mice underwent hind-limb ischemia surgery immediately before receiving an intramuscular injection of alginate gel containing VEGF and SDF, or a control gel without growth factors. One day following surgery, OECs or CACs were delivered into the circulation, and 24 hours later muscle tissue was collected and analyzed. OEC accumulation in both ischemic muscle and non-ischemic muscle was modestly increased with VEGF and SDF releasing gels, while CAC accumulation approximately doubled with VEGF and SDF delivery (Figure 2.9A). A 3-way ANOVA (3 factors: Cell Type, Treatment, Ischemia; 2 levels: OECs *vs.* CACs, VEGF+SDF *vs.* Control, and Ischemia *vs.* Non-Ischemic) was used to compare differences between conditions, as well as determine if there were interactions between factors. Full-factorial analysis showed that all possible interactions between pairs of factors were not statistically significant (Cell Type * Treatment: p=0.317; Cell Type * Ischemia: p=0.863; Treatment * Ischemia: p=0.977). Interaction effects were then excluded, and a 3-way ANOVA of the main effects was performed (Suppl Table 1). By this analysis, significant

differences were found between the recruitment of CACs and OECs (p=0.022), as well as the effect of VEGF and SDF gels compared to control gels (p=0.050, Figure 2.9B and Suppl Table 2.1). Lastly, we quantified inflammatory cell infiltration in muscle with VEGF and SDF delivery. There was a trend towards increasing accumulation of inflammatory cells with VEGF/SDF delivery, but the only statistically significant difference was in accumulation of F4/80+ cells at day 2 (Figure 2.9C-E).

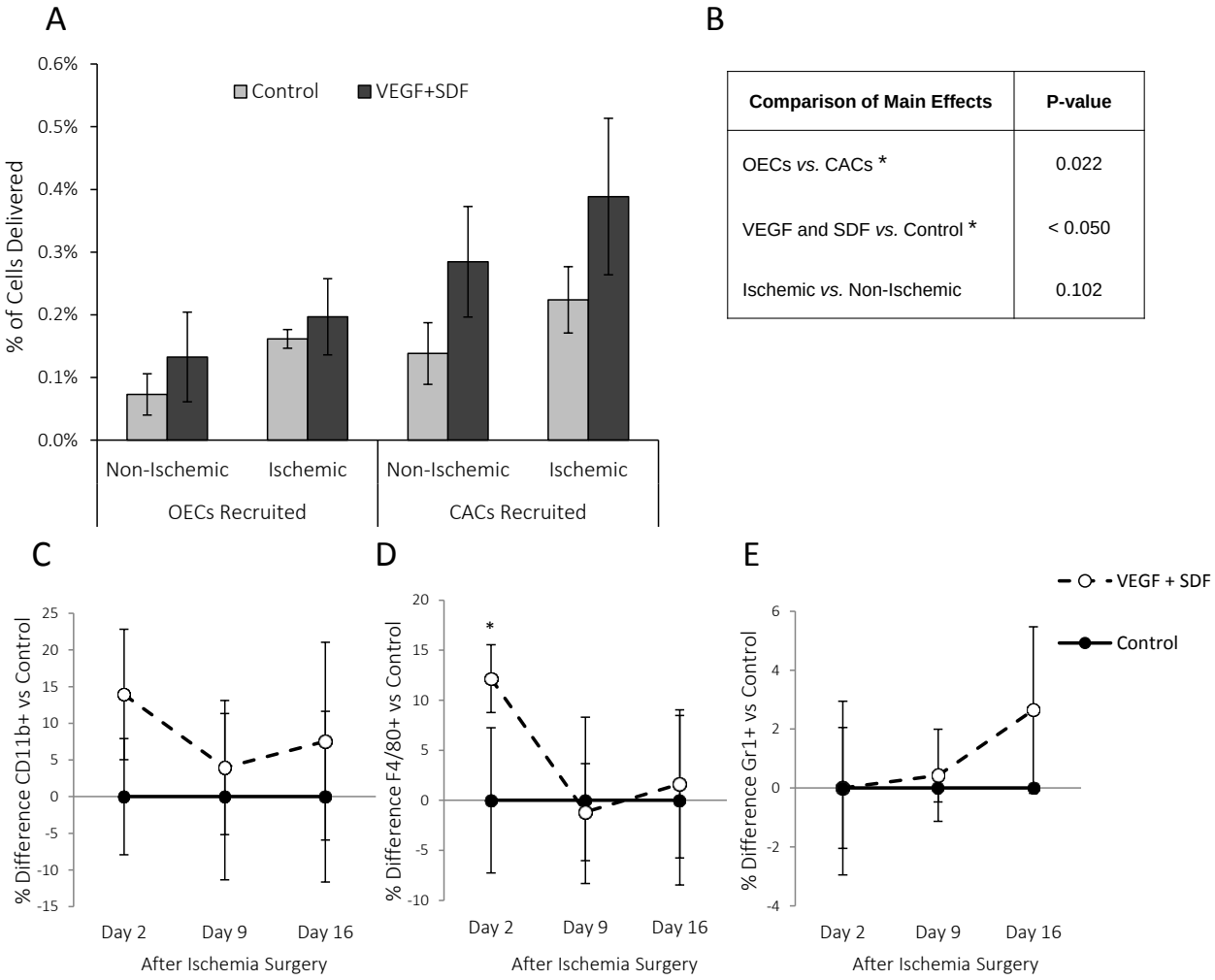

Comparison of Main Effects	P-value
OECs *vs.* CACs *	0.022
VEGF and SDF *vs.* Control *	< 0.050
Ischemic *vs.* Non-Ischemic	0.102

Figure 2.9. OEC and CAC recruitment, and inflammatory cell infiltration, into ischemic and non-ischemic limbs with VEGF+SDF delivery via alginate gels. A) Percentage of total transplanted cells recruited to hind-limbs after injection of alginate gels releasing VEGF and SDF or control gels (no growth factors). Gels were injected into non-ischemic, healthy limbs (n = 4) and in separate mice, gels were injected into hind-limbs following ischemia surgery (n = 6). Mean ± SEM. B) P-values from 3-way ANOVA Regression Analysis of main effects of Cell Type, VEGF+SDF treatment, and Ischemia (See Supplemental Table 2.1). * p <0.05. C-E) Percentage difference between the total cells in ischemic muscle tissue from animals treated with VEGF+SDF gel condition normalized to untreated ischemic limbs, that stained positive for CD11b (C), F4/80 (D) and Gr1 (E). Mean ± SD, n=6. * p < 0.05.

2.5 Discussion

The data from these experiments together demonstrate that the targeting efficiency of circulating endothelial progenitors to ischemic tissue *in vivo* can be enhanced by local delivery of VEGF and SDF, which were shown to affect the adhesion and migration of these cells *in vitro.* Specifically, CACs adhesion was more responsive to HMVECs that have been activated by TFNα in static *in vitro* adhesion assays compared to OECs, likely due to differences in β2 integrin expression on each progenitor cell type. SDF presented on the surface of HMVECs significantly increased adhesion of both OECs and CACs in flow-based adhesion assays. SDF also enhanced migration of CACs, while the combination of VEGF and SDF increased migration of OECs to a greater extent than either factor alone. These *in vitro* results led us to investigate the potential of local, sustained presentation of VEGF and SDF to increase recruitment of OECs and CACs to both ischemic and non-ischemic muscle tissue in a mouse model. Local delivery of VEGF and SDF from alginate gels increased accumulation of both cell types, as compared to control gels, in a statistically significant manner as indicated by 3-way ANOVA. A similar trend, in terms of enhanced accumulation, was noted in both ischemic tissue and normal tissue. Further, CACs accumulated to a greater extent than OECs across all conditions. Entrapment of OECs within vessels of the ischemic tissue accounted for approximately half of the total cell accumulation in the limb. This is likely similar for CACs, since their size is comparable to OECs. Overall, the fraction of transplanted OECs or CACs recruited to ischemic tissue was extremely low for all conditions, highlighting the inefficiency of this cell delivery method, even with use of recruitment signals. Lastly, the effect of VEGF and SDF on inflammatory cell infiltration into ischemic and normal tissue was also quantified. Ischemia alone led to significant infiltration of CD11b+, F4/80+, and Gr1+ cells from days 2-16. VEGF and SDF gels only increased F4/80+ cell accumulation in ischemic limbs at day 2, although not at days 9 and 16, and did not alter immune cell infiltration in non-ischemic limbs. Quite interestingly, CAC accumulation at the gel injection site in non-ischemic limbs induced a significantly higher level of immune cell infiltration

compared to OECs. The number of CACs in the muscle tissue was also strongly correlated with the percent of CD11b+, F4/80+ and Gr1+ cells.

In vitro adhesion assays demonstrated that TNFα stimulation of endothelial cells significantly increased adhesion of both OECs and CACs, although to a much greater extent for CACs. This larger increase in adhesion for CACs correlated with higher surface expression of integrins involved in adhesion processes for other types of circulating cells, including β2 and α4 integrins[50]. Studies with CD34+ cells demonstrated that both β2 and α4 integrins play a role in adhesion to endothelial cells[18], but α4 integrin is not expressed on OECs, therefore only the effect of β2 integrin on adhesion was examined. Addition of β2 blocking antibodies reduced CAC adhesion close to the level of reduction shown for lymphocytes, while OEC adhesion was only minimally reduced. OEC adhesion remained high after blocking β2 integrin, likely because OECs develop other adhesive interactions with endothelial cells, possibly through PECAM. Although both OECs and CACs are isolated from the blood, these results suggest that CACs exhibit adhesion behavior more similar than OECs to a typical blood leukocyte, and are therefore likely more responsive to activation by chemokines.

The effect of SDF on adhesion behavior of OECs and CACs was demonstrated using both static and flow-based *in vitro* assays. SDF was presented both on the surface of endothelial cells and in solution during adhesion. These conditions were chosen to replicate possible modes of SDF exposure to progenitor cells *in vivo*. The shear force on the cells in the flow assays was lower than physiological shear levels ($0.1 dyn/cm^2$ *vs.* $1 dyn/cm^2$), but this was necessary to allow cells to come into contact with the flow chamber surface and is comparable to the shear used in other studies[50,51,60]. Similar to the paradigm for chemokine exposure effects on adhesion of lymphocytes and CD34+ cells, in which surface presentation of SDF activates β2 integrins to a pro-adhesive, extended state[18,51,61], surface presentation of SDF led to a significant increase in adhesion of both OECs and CACs to unstimulated endothelial cells in both static and flow-based assays. CACs were shown to be more responsive than OECs to SDF in the static assay, while in the flow assay both cell types demonstrated a similar response. Adhesion also increased slightly

when SDF was present in solution, although this was not statistically significant for either cell type. CD34+ cells in flow-based adhesion assays show increased adhesion for both modes of SDF exposure, with a greater effect when the chemokine was surface-presented, similar to the results shown here[18–20]. This behavior is contrasted with lymphocytes, where presentation of soluble SDF activates β2 integrins to a 'high-affinity state', which, contrary to the name, does not promote adhesion to endothelial cells (specifically when the cells are pre-exposed and then the source of SDF is removed)[51]. My finding that soluble SDF did not significantly enhance OEC or CAC adhesion suggests that β2 integrins on endothelial progenitors may be activated to this high affinity state, in a similar manner as lymphocytes, but in this case the SDF source was not removed. The small effect of soluble SDF on OEC/CAC adhesion may be caused by SDF in the media adsorbing to the surface of the endothelial cells, although this was not measured in these assays. When progenitors are placed on top of TNFα stimulated endothelial cells in static assays, in contrast, adhesion increased when SDF was present in solution, although this was only significant for CACs. It's likely that no effect was observed with surface presentation of SDF for OECs or CACs because the amount of SDF adsorbed to the endothelial surface relative to the high expression of ICAM was too low to cause a change in adhesion. Overall, the results from these *in vitro* assays demonstrate that SDF exposure can increase adhesion of both cell types, and suggest the possibility that OECs and CACs may be responsive to SDF stimuli *in vivo*.

Migration of OECs and CACs towards VEGF and SDF was assessed in transwell assays, as a model of the second step in the recruitment process. CACs only migrated significantly in response to SDF, while the combination of VEGF and SDF enhanced OEC migration more than either factor alone. These results are in agreement with previous research demonstrating that SDF is a known chemoattractant for many circulating cell types, including CD34+ cells, and VEGF is a chemoattractant for endothelial cells[19,24,31,62–66]. VEGF and SDF together have a substantial synergistic effect on OEC migration. It is possible that this combination may influence *in vivo* recruitment of OECs primarily through migration, and compensate for the slightly lower responsiveness of these cells to adhesive cues. Transwell assays do not mimic the *in*

vivo environment in which progenitors would be migrating out of a blood vessel, but they do provide a simple method to determine which cytokines and combinations of cytokines can exert chemotactic effects on OECs and CACs. A more relevant and quantitative model would include the ability to assay effects of flow on a cell's ability to migrate, the role of chemokine gradients (rather than just concentration) on migration[67]. A better model might also include an endothelial monolayer for the progenitors to migrate through, or may replicate the 3D tissue environment in which cells migrate after extravasation from a blood vessel[19,66,68]. (Please see *Appendix D* for a summary of other systems which were modeled or used to various degrees for assaying OEC migration.) While VEGF and SDF have differential effects on adhesion and migration of OECs and CACs, the *in vitro* data together imply that this combination of factors displays potential to effect recruitment of both cell types *in vivo*.

OEC and CAC accumulation *in vivo* was significantly increased with local presentation of VEGF and SDF. The injectable alginate hydrogels, capable of providing sustained release of VEGF and SDF, have previously been measured to yield approximately 100ng/ml VEGF in hind-limb tissue at the 48 hour time point analyzed here, when used in this same animal model[48]. SDF has similar release characteristics as VEGF, and is therefore also assumed to be present in a significant concentration *in vivo.* A statistically rigorous 3-way ANOVA demonstrated that, overall, VEGF and SDF delivery had a significant effect on the accumulation of progenitors in muscle tissue at this time point. A similar trend was seen in both ischemic and non-ischemic muscle, with an approximate 2-fold increase in progenitor accumulation with VEGF and SDF delivery. To achieve statistically significant comparisons within each group (e.g. CAC delivery in non-ischemic limbs, control *vs.* VEGF/SDF delivery), due to the high variance associated with this experimental method, experiments would have required 24-70 mice per condition, and so were not performed. The results of these *in vivo* experiments are in agreement with the increased adhesion and migration of progenitors found with VEGF and/or SDF treatment *in vitro*. Finally, ANOVA analysis revealed that CACs accumulated to a significantly greater extent *in vivo* than OECs, in agreement with the increased responsiveness of CAC adhesion to the inflammatory state of HMVECs and to SDF

presentation *in vitro*. Although CACs were only responsive to SDF, and not VEGF, *in vitro*, the effect of SDF delivery alone was not evaluated *in vivo*. Based on *in vitro* results, CACs would be expected to accumulate to a similar extent with SDF delivery alone, while OEC accumulation may decrease slightly. Also, my findings for the effects of SDF are in agreement with previous recruitment experiments performed with CD34+ cells[19,54,63,69]. Many past studies use histologic analysis to identify progenitors in the tissue of interest, and often focus on cell location rather than quantitative evaluation[56,69,70]. While identification of fluorescently labeled progenitors was possible, results are likely sensitive to the experimental timeline. Alginate gels, alternatively, are capable of sustained cytokine release over a longer time period. In this study, only one experimental timeline between gel injection and cell infusion (24 hours) and tissue collection (another 24 hours) was investigated, but at multiple time points following ischemia. This study did not evaluate the length of time over which the VEGF and SDF were present in sufficient concentration to affect cell recruitment. Clinically, if VEGF and SDF are released slowly and remain active over a long time period, it could be possible to have one gel injection, with multiple cell infusion treatments at different time points. Lastly, while a number of studies have examined biological interactions between VEGF and SDF, the use of these cytokines in combination for the recruitment of endothelial progenitor cells has not been investigated[71–74].

Ischemia alone led to a significantly higher accumulation of OECs and CACs in ischemic limbs compared to the contralateral, control limbs. OECs that had been previously fixed in paraformaldehyde also accumulated to a greater extent in ischemic tissue, although only to ~1/2 the level found with viable cells, suggesting that physical changes in the vascular network of the ischemic muscle play some role in the increased accumulation of cells in this condition. It is important to note that while a statistically significant increase in accumulation of viable OECs was found in the ischemic limb compared to the contralateral limb, this difference was not statistically significant for fixed OECs. Since fixed cells cannot use integrin-adhesion molecule interactions for recruitment, accumulation must occur by entrapment. 6μm beads accumulated equivalently in the ischemic and contralateral limbs, suggesting that blood vessel

diameter is not reduced to below 6μm. Alternatively, 15μm beads, similar in size to OECs and CACs, resulted in paralysis or death of the animals, which was not too surprising since a typical capillary is 5-10μm in diameter[50]. In addition to size affecting cell accumulation, viable cells are more pliable than beads. Paraformaldehyde treatment cross-links cell proteins and likely stiffens the cell, which in turn could increase the number accumulated in ischemic tissue. Further, it may still be possible for a cell that is physically entrapped to exert a therapeutic effect[75,76]. These cells can secrete angiogenic factors and contribute to new blood vessel growth through a paracrine mechanism[24,77], and once physically entrapped in a capillary may be more responsive to migratory and regenerative cues presented from the gels. For example, VEGF exposure on OECs trapped in capillaries could activate these cells to directly participate in new blood vessel growth. Overall, while a significant fraction of delivered cells were trapped in ischemic limbs, rather than actively recruited, both modes of accumulation may permit endothelial progenitor participation in blood vessel regeneration.

The effects of ischemia and VEGF/SDF delivery on immune cell infiltration of muscle were also assessed in these studies. Ischemia caused a significant increase in the overall cell number, a large fraction of which was inflammatory cells, including CD11b+, F4/80+ and Gr1+ cells. These cells, likely myeloid lineage cells (CD11b), macrophages (F4/80), and granulocytes (Gr1, most commonly neutrophils in this setting), are recruited in response to injury and hypoxia resulting from ischemia[59,78,79]. They are highly responsive to cytokines, including VEGF and SDF, and also secrete a variety of cytokines which help repair and restore damaged tissues[78,80–82] . The presence of these cells peaked at day 2, and then decreased over 2 weeks. This is in agreement with the expected time course for immune cell infiltration after an acute ischemic injury[83,84]. Interestingly, the time course of OEC accumulation into ischemic limbs was similar. Delivery of VEGF and SDF gels at various time points after ischemia surgery only had an effect on the infiltration of F4/80+ cells at day 2, and not on later days. It is likely that signaling from the exogenously delivered VEGF and SDF was overwhelmed by the multitude of cytokines secreted in response to ischemia[80]. Inflammatory monocytes, which likely comprise a large fraction of the CD11b+

population, for example, traffic mainly in response to Monocyte Chemoattractant Protein-1 following ischemia[85–87]. VEGF and SDF also did not affect immune cell infiltration into non-ischemic limbs. Most often, studies on cytokine influence on immune cell infiltration into biomaterials typically use immunohistochemistry to identify various cell populations[57,88,89]. Using this kind of analysis for my studies may have revealed local differences in cell recruitment due to VEGF and SDF delivery, as has been shown previously[57]. Alternatively, the flow cytometry analysis used here assessed the total cell population present throughout the entire muscle. The muscle tissue was collected and fully digested, with only some pieces of ligament not passing through a 40μm filter in the final processing step. This method is sensitive for the detection of low cell numbers, but again, has high variability between samples. Taken together, these results demonstrated that ischemia plays a large role in the infiltration of immune cells into muscle tissue, while VEGF/SDF delivery has a lesser impact.

Remarkably, the systemic delivery of CACs in non-ischemic mice resulted in significant accumulation of CD11b+ and F4/80+ cells in the site of gel injection in the hind-limb muscle. Again, inflammatory cell accumulation was not dependent on whether mice received either VEGF+SDF or control gel injections. The number of CD11b+, F4/80+ and Gr1+ cells accumulated in the muscle strongly correlated to the number of CACs in the tissue. Each CAC present in the hind-limb muscle was associated with 680 CD11b+ cells, 220 F4/80+ cells, and 40 Gr1+ cells. While cause and effect were not established in these studies, CACs may secrete cytokines that enhance immune cell infiltration or activate an inflammatory response. Endothelial progenitors are most often assayed for secretion of angiogenic factors (VEGF, PDGF, FGF, HGF, IL-8, etc.), but have also been shown to secrete factors that attract monocytes and macrophages (MCP-1 and MIP-1), as well as other inflammatory cytokines (IL-12, IP-10)[24,77,90,91]. Strikingly, no increase in immune cell infiltration was observed with systemic OEC delivery, even though they also secrete IL-8, IL-12, and IL-6[24]. Surprisingly little has been published demonstrating cause and effect of specific cytokines secreted from delivered CACs (or OECs) on the inflammatory or angiogenic

environment. My experiments suggest that the cytokines secreted from a very small number of recruited cells can dramatically influence the inflammatory state of the tissue.

In summary, these studies demonstrate that accumulation of transplanted endothelial progenitors can be enhanced using local delivery of VEGF and SDF. The efficiency of cell accumulation, even in the optimal conditions, was extremely low for both cell types. However, as was observed with CAC transplantation studies, the local accumulation of a few cells can be correlated with a substantial influence on the local biology. Even modest improvements in the delivery of endothelial progenitor cells to ischemic tissue therefore may have a therapeutic effect on blood vessel growth and regeneration. The following chapter examines the potential contributions of OECs and CACs to new blood vessel growth, and the effect of VEGF and SDF on those contributions.

2.6 References

1. Kochanek, K. D., Xu, J., Murphy, S. L. & Minin, A. M. Deaths : Final Data for 2009. *Natl. Vital Stat. Reports* **60,** (2011).

2. Morbididty and Mortality: 2012 Chartbook on Cardiovascular, Lung and Blood Diseases. (2012). at <http://www.nhlbi.nih.gov/resources/docs/cht-book.htm>

3. About Peripheral Artery Disease. *Am. Hear. Assoc.* (2013). at <http://www.heart.org/HEARTORG/Conditions/More/PeripheralArteryDisease/About-Peripheral-Artery-Disease-PAD_UCM_301301_Article.jsp>

4. Tongers, J., Roncalli, J. G. & Losordo, D. W. Role of endothelial progenitor cells during ischemia-induced vasculogenesis and collateral formation. *Microvasc. Res.* **79,** 200–6 (2010).

5. Möbius-Winkler, S., Höllriegel, R., Schuler, G. & Adams, V. Endothelial progenitor cells: implications for cardiovascular disease. *Cytom. Part A J. Int. Soc. Anal. Cytol.* **75,** 25–37 (2009).

6. Fadini, G. P., Losordo, D. & Dimmeler, S. Critical reevaluation of endothelial progenitor cell phenotypes for therapeutic and diagnostic use. *Circ. Res.* **110,** 624–37 (2012).

7. ClinicalTrials.gov. (2013).

8. Raval, Z. & Losordo, D. W. Cell therapy of peripheral arterial disease: from experimental findings to clinical trials. *Circ. Res.* **112,** 1288–302 (2013).

9. Chavakis, E., Urbich, C. & Dimmeler, S. Homing and engraftment of progenitor cells: a prerequisite for cell therapy. *J. Mol. Cell. Cardiol.* **45,** 514–22 (2008).

10. Caiado, F. & Dias, S. Endothelial progenitor cells and integrins: adhesive needs. *Fibrogenesis Tissue Repair* **5,** 4 (2012).

11. Hristov, M., Erl, W. & Weber, P. C. Endothelial progenitor cells: mobilization, differentiation, and homing. *Arterioscler. Thromb. Vasc. Biol.* **23,** 1185–9 (2003).

12. Hristov, M., Zernecke, A., Liehn, E. A. & Weber, C. Regulation of endothelial progenitor cell homing after arterial injury. *J. Thromb. Haemost.* **98,** 274–277 (2007).

13. Petit, I. *et al.* G-CSF induces stem cell mobilization by decreasing bone marrow SDF-1 and up-regulating CXCR4. *Nat. Immunol.* **3,** 687–694 (2002).

14. Lévesque, J.-P., Hendy, J., Takamatsu, Y., Simmons, P. J. & Bendall, L. J. Disruption of the CXCR4/CXCL12 chemotactic interaction during hematopoietic stem cell mobilization induced by GCSF or cyclophosphamide. *J. Clin. Invest.* **111,** 187–196 (2003).

15. Hattori, K. *et al.* Plasma elevation of stromal cell-derived factor-1 induces mobilization of mature and immature hematopoietic progenitor and stem cells. *Blood* **97,** 3354–3360 (2001).

16. Jin, D. K. *et al.* Cytokine-mediated deployment of SDF-1 induces revascularization through recruitment of CXCR4+ hemangiocytes. *Nat. Med.* **12,** 557–567 (2006).

17. Shi, Q. *et al.* Evidence for circulating bone marrow-derived endothelial cells. *Blood* **92,** 362–7 (1998).

18. Peled, A. *et al.* The chemokine SDF-1 stimulates integrin-mediated arrest of CD34(+) cells on vascular endothelium under shear flow. *J. Clin. Invest.* **104,** 1199–1211 (1999).

19. Peled, A. *et al.* The chemokine SDF-1 activates the integrins LFA-1 , VLA-4 , and VLA-5 on immature human CD34+ cells : role in transendothelial / stromal migration and engraftment of NOD / SCID mice. *Blood* **95,** 3289–3296 (2000).

20. Zemani, F. *et al.* Ex vivo priming of endothelial progenitor cells with SDF-1 before transplantation could increase their proangiogenic potential. *Arterioscler. Thromb. Vasc. Biol.* **28,** 644–650 (2008).

21. Jo, D.-Y., Rafii, S., Hamada, T. & Moore, M. a S. Chemotaxis of primitive hematopoietic cells in response to stromal cell–derived factor-1. *J. Clin. Invest.* **105,** 101–111 (2000).

22. Yamaguchi, J. -i. Stromal Cell-Derived Factor-1 Effects on Ex Vivo Expanded Endothelial Progenitor Cell Recruitment for Ischemic Neovascularization. *Circulation* **107,** 1322–1328 (2003).

23. Pitchford, S. C., Furze, R. C., Jones, C. P., Wengner, A. M. & Rankin, S. M. Differential mobilization of subsets of progenitor cells from the bone marrow. *Cell Stem Cell* **4,** 62–72 (2009).

24. Silva, E. a, Kim, E.-S., Kong, H. J. & Mooney, D. J. Material-based deployment enhances efficacy of endothelial progenitor cells. *PNAS* **105,** 14347–14352 (2008).

25. Augst, A. D., Kong, H. J. & Mooney, D. J. Alginate hydrogels as biomaterials. *Macromol. Biosci.* **6,** 623–633 (2006).

26. Fischbach, C. & Mooney, D. J. Polymers for pro- and anti-angiogenic therapy. *Biomaterials* **28,** 2069–2076 (2007).

27. Lee, K. Y., Peters, M. C., Anderson, K. W. & Mooney, D. J. Controlled growth factor release from synthetic extracellular matrices. *Nature* **408,** 998–1000 (2000).

28. Richardson, T. P., Peters, M. C., Ennett, A. B. & Mooney, D. J. Polymeric system for dual growth factor delivery. **19,** 1029–1034 (2001).

29. Murphy, W. L., Peters, M. C., Kohn, D. H. & Mooney, D. J. Sustained release of vascular endothelial growth factor from mineralized poly(lactide-co-glycolide) scaffolds for tissue engineering. *Biomaterials* **21,** 2521–2527 (2000).

30. Chen, R. R., Silva, E. a, Yuen, W. W. & Mooney, D. J. Spatio-temporal VEGF and PDGF delivery patterns blood vessel formation and maturation. *Pharm. Res.* **24,** 258–264 (2007).

31. Chen, R. R. *et al.* Integrated approach to designing growth factor delivery systems. *FASEB J.* **21,** 3896–3903 (2007).

32. Silva, E. A. & Mooney, D. J. Effects of VEGF temporal and spatial presentation on angiogenesis. *Biomaterials* **31,** 1235–41 (2010).

33. Silva, E. a & Mooney, D. J. Spatiotemporal control of vascular endothelial growth factor delivery from injectable hydrogels enhances angiogenesis. *J. Thromb. Haemost. JTH* **5,** 590–598 (2007).

34. Borselli, C. *et al.* Functional muscle regeneration with combined delivery of angiogenesis and myogenesis factors. *Proc. Natl. Acad. Sci. U. S. A.* **107,** 3287–3292 (2010).

35. Hao, X. *et al.* Angiogenic effects of sequential release of VEGF-A165 and PDGF-BB with alginate hydrogels after myocardial infarction. *Cardiovasc. Res.* **75,** 178–185 (2007).

36. Yuen, W. W., Du, N. R., Chan, C. H., Silva, E. A. & Mooney, D. J. Mimicking nature by codelivery of stimulant and inhibitor to create temporally stable and spatially restricted angiogenic zones. *PNAS* **107,** 17933–17938 (2010).

37. Hur, J. *et al.* Characterization of two types of endothelial progenitor cells and their different contributions to neovasculogenesis. *Arterioscler. Thromb. Vasc. Biol.* **24,** 288–93 (2004).

38. Yoder, M. C. *et al.* Redefining endothelial progenitor cells via clonal analysis and hematopoietic stem/progenitor cell principals. *Blood* **109,** 1801–1809 (2007).

39. Prater, D. N., Case, J., Ingram, D. a & Yoder, M. C. Working hypothesis to redefine endothelial progenitor cells. *Leukemia* **21,** 1141–1149 (2007).

40. Ingram, D. a *et al.* Identification of a novel hierarchy of endothelial progenitor cells using human peripheral and umbilical cord blood. *Blood* **104,** 2752–2760 (2004).

41. Melero-Martin, J. M. *et al.* In vivo vasculogenic potential of human blood-derived endothelial progenitor cells. *Blood* **109,** 4761–8 (2007).

42. Melero-Martin, J. M. *et al.* Engineering robust and functional vascular networks in vivo with human adult and cord blood-derived progenitor cells. *Circ. Res.* **103,** 194–202 (2008).

43. Asahara, T. *et al.* Isolation of Putative Progenitor Endothelial Cells for Angiogenesis. *Science.* **275,** 964–966 (1997).

44. Ziegelhoeffer, T. *et al.* Bone marrow-derived cells do not incorporate into the adult growing vasculature. *Circ. Res.* **94,** 230–8 (2004).

45. Rehman, J. Peripheral Blood "Endothelial Progenitor Cells" Are Derived From Monocyte/Macrophages and Secrete Angiogenic Growth Factors. *Circulation* **107,** 1164–1169 (2003).

46. Berman, E., Xie, Y. & Muller, W. A. Roles of Platelet/Endothelial Cell Adhesion Molecule-1 (PECAM-1, CD31) in Natural Killer Cell Transendothelial Migration and B2 Integrin Activation. *J. Immunol.* **156,** 1515–1524 (1996).

47. Kaneko, M., Horie, S., Kato, M., Gleich, G. J. & Kita, H. A Crucial Role for B2 lntegrin in the Activation of Eosinophils Stimulated by IgG. *J. Immunol.* **155,** 2631–2641 (1995).

48. Silva, E. A. & Mooney, D. J. Spatiotemporal control of vascular endothelial growth factor delivery from injectable hydrogels enhances angiogenesis. *J. Thromb. Haemost.* **5,** 590–598 (2007).

49. Bouhadir, K. H. *et al.* Degradation of partially oxidized alginate and its potential application for tissue engineering. *Biotechnol. Prog.* **17,** 945–950 (2001).

50. Lucila, S. M. & von Andrian, U. H. Immunological Adhesion and Homing. *Encycl. Life Sci.* **21,** 1–16 (2005).

51. Shamri, R. *et al.* Lymphocyte arrest requires instantaneous induction of an extended LFA-1 conformation mediated by endothelium-bound chemokines. *Nat. Immunol.* **6,** 497–506 (2005).

52. Laudanna, C. & Alon, R. Right on the spot. Chemokine triggering of integrin-mediated arrest of rolling leukocytes. *Thromb. Haemost.* **95,** 5–11 (2006).

53. Chen, R. R. *et al.* Host immune competence and local ischemia affects the functionality of engineered vasculature. *Microcirculation* **14,** 77–88 (2007).

54. Lau, T. T. & Wang, D. Stromal cell-derived factor-1 (SDF-1): homing factor for engineered regenerative medicine. *Expert Opin. Biol. Ther.* **11,** 189–97 (2011).

55. Goncharova, V. & Khaldoyanidi, S. K. A novel three-dimensional flow chamber device to study chemokine-directed extravasation of cells circulating under physiological flow conditions. *J. Vis. Exp.* e50959 (2013). doi:10.3791/50959

56. Prokoph, S. *et al.* Sustained delivery of SDF-1α from heparin-based hydrogels to attract circulating pro-angiogenic cells. *Biomaterials* **33,** 4792–800 (2012).

57. Thevenot, P. T. *et al.* The effect of incorporation of SDF-1alpha into PLGA scaffolds on stem cell recruitment and the inflammatory response. *Biomaterials* **31,** 3997–4008 (2010).

58. Borselli, C. *et al.* Functional muscle regeneration with combined delivery of angiogenesis and myogenesis factors. *PNAS* **107,** 3287–3292 (2010).

59. Eltzschig, H. K. & Carmeliet, P. Hypoxia and inflammation. *N. Engl. J. Med.* **364,** 656–65 (2011).

60. Sigal, a *et al.* The LFA-1 integrin supports rolling adhesions on ICAM-1 under physiological shear flow in a permissive cellular environment. *J. Immunol.* **165,** 442–52 (2000).

61. Grabovsky, V. *et al.* Subsecond induction of alpha4 integrin clustering by immobilized chemokines stimulates leukocyte tethering and rolling on endothelial vascular cell adhesion molecule 1 under flow conditions. *J. Exp. Med.* **192,** 495–506 (2000).

62. Stellos, K. *et al.* Platelet-derived stromal cell-derived factor-1 regulates adhesion and promotes differentiation of human CD34+ cells to endothelial progenitor cells. *Circulation* **117,** 206–215 (2008).

63. Elmadbouh, I. *et al.* Ex vivo delivered stromal cell-derived factor-1alpha promotes stem cell homing and induces angiomyogenesis in the infarcted myocardium. *J. Mol. Cell. Cardiol.* **42,** 792–803 (2007).

64. Kucia, M. *et al.* CXCR4–SDF-1 signalling, locomotion, chemotaxis and adhesion. *J. Mol. Histol.* **35,** 233–245 (2004).

65. Kim, C. H. & Broxmeyer, H. E. In vitro behavior of hematopoietic progenitor cells under the influence of chemoattractants: stromal cell-derived factor-1, steel factor, and the bone marrow environment. *Blood* **91,** 100–110 (1998).

66. Aiuti, B. a, Webb, I. J., Bleul, C., Springer, T. & Gutierrez-Ramos, J. C. The Chemokine SDF-1 Is a Chemoattractant for Human CD34+ Hematopoietic Progenitor Cells and Provides a New Mechanism to Explain the Mobilization of CD34+ Progenitors Progenitors to Peripheral Blood. *J. Exp. Med.* **185,** 111–20 (1997).

67. Mosadegh, B. *et al.* Generation of stable complex gradients across two-dimensional surfaces and three-dimensional gels. *Langmuir* **23,** 10910–10912 (2007).

68. Tayalia, P., Mendonca, C. R., Baldacchini, T., Mooney, D. J. & Mazur, E. 3D Cell-Migration Studies using Two-Photon Engineered Polymer Scaffolds. *Adv. Mater.* **20,** 4494–4498 (2008).

69. Yamaguchi, J. *et al.* Stromal cell-derived factor-1 effects on ex vivo expanded endothelial progenitor cell recruitment for ischemic neovascularization. *Circulation* **107,** 1322–1328 (2003).

70. Kalka, C. *et al.* Transplantation of ex vivo expanded endothelial progenitor cells for therapeutic neovascularization. *PNAS* **97,** 3422–7 (2000).

71. Salcedo, R. *et al.* Vascular endothelial growth factor and basic fibroblast growth factor induce expression of CXCR4 on human endothelial cells: In vivo neovascularization induced by stromal-derived factor-1alpha. *Am. J. Pathol.* **154,** 1125–1135 (1999).

72. Yu, J.-X. *et al.* Combination of stromal-derived factor-1alpha and vascular endothelial growth factor gene-modified endothelial progenitor cells is more effective for ischemic neovascularization. *J. Vasc. Surg.* **50,** 608–16 (2009).

73. Hiasa, K. *et al.* Gene transfer of stromal cell-derived factor-1alpha enhances ischemic vasculogenesis and angiogenesis via vascular endothelial growth factor/endothelial nitric oxide synthase-related pathway: next-generation chemokine therapy for therapeutic neovasculariz. *Circulation* **109,** 2454–2461 (2004).

74. Kijowski, J. *et al.* The SDF-1-CXCR4 axis stimulates VEGF secretion and activates integrins but does not affect proliferation and survival in lymphohematopoietic cells. *Stem Cells* **19,** 453–466 (2001).

75. Gnecchi, M., Zhang, Z., Ni, A. & Dzau, V. J. Paracrine mechanisms in adult stem cell signaling and therapy. *Circ. Res.* **103,** 1204–19 (2008).

76. Cheng, A. S. & Yau, T. M. Paracrine effects of cell transplantation: strategies to augment the efficacy of cell therapies. *Semin. Thorac. Cardiovasc. Surg.* **20,** 94–101 (2008).

77. Majka, M. Numerous growth factors, cytokines, and chemokines are secreted by human CD34+ cells, myeloblasts, erythroblasts, and megakaryoblasts and regulate normal hematopoiesis in an autocrine/paracrine manner. *Blood* **97,** 3075–3085 (2001).

78. Hoefer, I. E. *et al.* Leukocyte subpopulations and arteriogenesis: specific role of monocytes, lymphocytes and granulocytes. *Atherosclerosis* **181,** 285–93 (2005).

79. Pober, J. S. & Sessa, W. C. Evolving functions of endothelial cells in inflammation. *Nat. Rev. Immunol.* **7,** 803–15 (2007).

80. Shireman, P. K. The chemokine system in arteriogenesis and hind limb ischemia. *J. Vasc. Surg.* **45,** A48–56 (2007).

81. Chambers, S. E. J., O'Neill, C. L., O'Doherty, T. M., Medina, R. J. & Stitt, A. W. The role of immune-related myeloid cells in angiogenesis. *Immunobiology* **218,** 1370–5 (2013).

82. Jaipersad, A. S., Lip, G. Y., Silverman, S. & Shantsila, E. The role of monocytes in angiogenesis and atherosclerosis. *J. Am. Coll. Cardiol.* (2013). doi:10.1016/j.jacc.2013.09.019

83. Nahrendorf, M. *et al.* The healing myocardium sequentially mobilizes two monocyte subsets with divergent and complementary functions. *J. Exp. Med.* **204,** 3037–47 (2007).

84. Frangogiannis, N. G., Smith, C. W. & Entman, M. L. The inflammatory response in myocardial infarction. *Cardiovasc. Res.* **53,** 31–47 (2002).

85. Auffray, C. *et al.* Monitoring of blood vessels and tissues by a population of monocytes with patrolling behavior. *Science (80-.).* **317,** 666–70 (2007).

86. Willenborg, S. *et al.* CCR2 recruits an inflammatory macrophage subpopulation critical for angiogenesis in tissue repair. *Blood* **120,** 613–25 (2012).

87. Shi, C. & Pamer, E. G. Monocyte recruitment during infection and inflammation. *Nat. Rev. Immunol.* **11,** 762–74 (2011).

88. De Falco, E. *et al.* SDF-1 involvement in endothelial phenotype and ischemia-induced recruitment of bone marrow progenitor cells. *Blood* **104,** 3472–3482 (2004).

89. Schantz, J.-T., Chim, H. & Whiteman, M. Cell guidance in tissue engineering: SDF-1 mediates site-directed homing of mesenchymal stem cells within three-dimensional polycaprolactone scaffolds. *Tissue Eng.* **13,** 2615–2624 (2007).

90. Di Santo, S. *et al.* Novel cell-free strategy for therapeutic angiogenesis: in vitro generated conditioned medium can replace progenitor cell transplantation. *PLoS One* **4,** e5643 (2009).

91. Suh, W. *et al.* Transplantation of endothelial progenitor cells accelerates dermal wound healing with increased recruitment of monocytes/macrophages and neovascularization. *Stem Cells* **23,** 1571–8 (2005).

CHAPTER 3:

Endothelial Progenitor Cell Contribution to New Blood Vessel Growth and the Effects of VEGF and SDF

3.1 Purpose of Chapter

This chapter addresses the hypothesis that Outgrowth Endothelial Cells (OECs) and Circulating Angiogenic Cells (CACs) have distinct roles in contributing to angiogenesis, which can be altered by the presence of Vascular Endothelial Growth Factor (VEGF) and Stromal Cell-Derived Factor (SDF). To address this hypothesis, I used a 3-dimentional, *in vitro* sprouting assay as a model to understand the potential contributions to angiogenesis by OECs and CACs that have been exposed to VEGF and SDF. Further, I demonstrated the functional ability of VEGF+SDF-recruited OECs and CACs to restore perfusion *in vivo*. This chapter fits into the overall hypothesis of this thesis by examining if VEGF and SDF promote progenitor cell contribution to new blood vessel growth.

3.2 Introduction

Since the discovery of endothelial progenitor cells, interest in using these cells therapeutically for various forms of cardiovascular disease has grown[1–5]. However, the mechanism(s) by which endothelial progenitors contribute to new blood vessel growth is unclear. Early reports revealed that infused progenitors could be located in ischemic tissue at sites of new blood vessel growth, suggesting direct participation in vessel formation[1,6]. However, years of follow-up research revealed that 'endothelial progenitors' used by different researchers were actually several distinct cell types, which could underlie the many discrepancies between various studies utilizing these cells. Outgrowth Endothelial Cells (OECs) and Circulating Angiogenic Cells (CACs) are two types of 'endothelial progenitors,' however, these two

cell types appear to differ in how they can contribute to new blood vessel growth[7]. Only OECs demonstrate high proliferative capacity and the ability to directly form new blood vessels, while CACs resemble monocytes and secrete many cytokines, which may act in a paracrine fashion on resident endothelial cells (See Chapter 1 for more information on these cell types)[7]. This chapter uses *in vitro* assays to clarify the roles of OECs and CACs in contributing to angiogenic sprouting. In addition, as the previous chapter demonstrated that Vascular Endothelial Growth Factor (VEGF) and Stromal Cell-Derived Factor (SDF) can impact adhesion and migration of OECs and CACs, their effect on the angiogenic potential of these cells *in vitro* and *in vivo* were studied.

The sprouting assay used in these studies replicates the initial stages of angiogenesis, including the loosening of inter-endothelial contacts and vessel destabilization, followed by endothelial cell migration and the formation of sprouts, similar to the *in vivo* process[8]. This assay uses endothelial cell-seeded beads suspended in a 3D fibrin matrix, and can be used to study the dynamics of endothelial cell interactions and relationships between tip cells and stalk cells, and key cell signaling events[9,10]. Multiple cell types can be combined to study direct cell-cell interactions, and this assay can be used to study angiogenic effects of secreted cytokines from support cells[11,12]. Qualitative interactions between mature endothelial cells and OECs and CACs have been previously reported, but not a quantitative analysis[12]. Further, sprouting assays can be used to determine the potency of externally applied angiogenic factors, and are often predictive of the *in vivo* response to those factors[11,13,14]. Here, I used the sprouting assay to determine the effect of VEGF and SDF on endothelial cell sprouting. The effect of VEGF concentration, spatial and temporal gradients on sprouting of mature endothelial cells has previously been explored[13,14]. A minimum level of VEGF is necessary for endothelial cells to participate in sprouting angiogenesis *in vitro* and *in vivo*[13,14]. Data supporting a direct angiogenic role for SDF mainly comes from studies of endothelial cell tube formation on 2D matrigel surfaces, while a variety of other studies suggest that SDF indirectly promotes angiogenesis by regulating trafficking of various stem and progenitor cells to sites of new vessel growth[15–20]. A direct effect of SDF on sprouting angiogenesis has not been reported, nor has the impact of a combination of VEGF and SDF. Lastly, the effect of VEGF and SDF on the profile of secreted factors

from endothelial progenitors was measured to determine if exposure to these factors enhances endothelial sprouting in a paracrine manner.

The regenerative capacity of OECs and CACs accumulated in ischemic hind-limbs and exposed to VEGF and SDF was also demonstrated in an *in vivo* model. In this model, OECs or CACs were systemically delivered following surgery, and preferentially accumulated in the ischemic tissue (as shown in Chapter 2). Perfusion was then measured to quantify functional blood vessel regeneration over time. This model has been used to test the angiogenic strength of growth factors and other molecules delivered from polymer scaffolds[10,13,21–23]. Angiogenic factors that showed potency in *in vitro* sprouting assays correspondingly showed improved perfusion *in vivo*[11,13,14]. OECs and CACs have also previously demonstrated therapeutic efficacy in this model when delivered locally from a alginate scaffold[12]. Here, the baseline perfusion recovery with VEGF and SDF-loaded alginate gels was quantified, and then OECs or CACs were infused to determine if there were additive regenerative capabilities.

3.3 Materials and Methods

OEC/CAC Cell Isolation and Culture

As described in Chapter 2, human cord blood was used for OEC/CAC isolation within 12 hours from collection. Cord blood was diluted 1:1 with Hanks Balanced Salt Solution (HBSS) and gently placed on top of Histopaque 1077 (Sigma #10771-500ml). Samples were centrifuged at 740g (OECs) and 400g (CACs) for 30 minutes with no brake. Mononuclear cells were then collected and washed with HBSS. Remaining red blood cells were lysed and cells were washed twice with HBSS. For OEC isolation, cells were resuspended in EGM-2MV (Lonza #CC-3202) supplemented with 10% FBS and plated on Collagen coated dishes (BD #354400). Media was changed after two days, and every day until colonies appeared (day 10-14). Colonies were replated and maintained in EGM-2MV media while in use; OECs were used between passages 2 and 6. For CAC isolation, cells were plated on fibronectin-coated dishes (BD

#356008) in EGM-2MV without hydrocortisone and supplemented with 10% FBS. Additional media was added to the cells on day 4, and attached cells at day 7 were immediately used for experiments.

Human Microvascular Endothelial Cells (HMVECs, Lonza # CC-2543) and Human Umbilical Vein Endothelial Cells (HUVECs, Lonza # C-2517A) were cultured in EGM-2MV from Lonza and EGM-2 (Lonza # CC-3162), respectively, and were used between passages 3 and 6.

Collection of Conditioned Media and Analysis

OECs and CACs were rinsed thoroughly with PBS to remove all growth factors included in the culture medium. 5ml of EBM-2 (Lonza #CC-3156) containing 0.5% FBS was added per $75cm^2$, and cells were allowed to condition the media for 48 hours at 37^oC in 5% CO_2. Conditioned media was collected and immediately used for analysis or frozen and stored at -20^oC. Secreted cytokines were measured using a human angiogenesis array according to the manufacturer's protocol (Affymetrix Transignal™ Angiogenesis Antibody Array # MA6310). Briefly, membranes arrays were soaked for 1 hour at room temperature with the provided blocking buffer, followed by 3 rinses with the provided Wash Buffer II. Arrays were then soaked with 2ml of conditioned media at room temperature for 2 hours, with slow shaking, followed by three 5 minute rinses with Wash Buffer I and one 5 minute rinse with Wash Buffer II (standard washing method). The provided primary, biotin-conjugated antibodies were then applied to the arrays and incubated for two hours at room temperature with slow shaking, followed by the standard washing method. The provided streptavidin-HRP working solution was then prepared and 2 ml were added to each array and incubated at room temperature for 60 minutes, followed by the standard washing method. Equal volumes of Detection Buffers A and B were then mixed and added to each array for 5 minutes at room temperature. Excess Detection Buffer mixture was then removed and arrays were imaged with a chemiluminescent imaging system (FluorChem™ M Imager, ProteinSimple, San Jose, CA) with increasing exposure times until sufficient signal was detected. Array images were analyzed and quantified using ImageJ software. ELISA Development Kits were purchased from Peprotech for cytokines that were

detected with the Angiogenesis Array, including FGFb (#900-M08), IL-12 (#900-M96), IL-8 (#900-M18), VEGF (#900-M10), PlGF (#900-K307), and Leptin (#900-K90). ELISA plates were developed according to manufacturer's protocols. Briefly, capture antibodies were applied to high-bind well plates (Nunc Maxisorp #439454) and allowed to adsorb overnight at room temperature. After rinsing wells, standards and conditioned media samples were then added to individual wells in duplicate, and incubated at room temperature for 2 hours. Samples were then aspirated and plates were washed four times with 0.05% Tween in PBS. Detection Antibody was then applied to each well and allowed to incubate for two hours at room temperature, followed by washing as described previously. Avidin-HRP conjugate was then applied to each well for 30 minutes at room temperature, followed by application of ABTS Liquid Substrate Solution (Sigma # A3219). Color development was monitored and absorbance at 405nm and 650nm was read every 5 minutes with a plate reader until sufficient color developed (Bio-Tek Synergy H1 Plate Reader, Winooski, VT).

Sprouting Assays

Sprouting assays were performed similarly to those previously described[13,14,24]. Here, HMVECs, HUVECs or cord blood-isolated OECs between passage 2 and 6, or CACs, were seeded onto collagen-coated dextran beads (Cytodex^{TM}3 Microcarriers, GE Healthcare # 17-0485-01) that were approximately 200μm in diameter. In some conditions, OECs were stained with octadecyl rhodamine B chloride dye (Life Technologies #O-246) overnight at 1nM and seeded onto beads in a 1:1 ratio with unstained HMVECs or HUVECs. Cells were trypsinized from a T75 flask, and added to a small spinner flask with 7 ml of growth media and beads. The spinner flask was placed in an incubator at 37^{o}C on a stir plate and alternated between 2 minutes spinning at 60rpm and 28 minutes at rest for 4 hours, followed by 20 hours spinning at 60rpm. Cell-seeded beads were then transferred into T25 flasks with fresh media and placed on an orbital shaker until cells became confluent. For conditions with rhoadimine –stained OECs and unstained HUVECs or HMVECs co-seeded on the beads, the percentage of each cell type on the beads was measured by flow cytometry prior to beginning assays (BD LSRFortessa, Franklin Lakes, New

Jersey). 1ml of bead suspension was then gently mixed with 3ml of 2mg/ml fibrinogen (Millipore #EMD 341576) and 400µl of 500µg/ml aprotinin (Sigma #A4529-5MG) in a 15 ml tube. 250µl of this fibrinogen-aprotinin-bead solution was then gently mixed with 200µl of a 2U/ml thrombin (Sigma #F3879-250MG) solution in a 24 well plate to form a fibrin gel. Gels were allowed to solidify in the incubator at 37^{o}C for 10 minutes. 600µl of media was gently added on top of the fibrin gel (EBM2 + 5% FBS was used as the control media, with SDF = 100ng/ml, VEGF = 50ng/ml, or the combination added as test conditions). Media was changed every 24 hours for 3 days. Increasing, stable, and decreasing profiles of SDF (10-100-190ng/ml on day 1-2-3, or 100-100-100ng/ml, or 190-100-10ng/ml, respectively) were also overlaid on top of a decreasing VEGF profile (95-50-5ng/ml) to test for effects of temporally-controlled cytokine presentation on sprouting. Alternatively, 50,000 OECs or CACs in 600µl of control media were seeded on top of fibrin gels containing HUVEC-covered beads to assay for angiogenic effects of secreted cytokines. Polyclonal antibodies were also applied to wells containing OECs or CACs on top of the fibrin gel to block secreted cytokines. PlGF (Peprotech #500-P226), FGFb (Peprotech #500-P18), IL-8 (Peprotech #500-P28), and Leptin (R&D Systems #44802) antibodies were used at 1, 0.4, 0.2, and 2µg/ml, respectively, and were reapplied in fresh control media every 24 hours for 3 days. At 24, 48 or 72 hours, fibrin gels were rinsed twice with PBS and then 4% paraformaldehyde in PBS was added to fix the cells. Plates were stored at 4^{o}C until quantification. The number of sprouts per bead was counted on a Zeiss Axio Observer Z1 microscope (Zeiss, Thornwood, NY). A sprout was defined as more than one cell protruding from the bead while remaining connected to the bead surface, as previously described[13,24]. Approximately 200 beads per well were counted, with n = 4 wells per condition.

Time Lapse Imaging of OEC Sprouting

Sprouting assays were prepared as described above. A 24-well plate of OEC-seeded beads in fibrin gel was then placed in a live-cell imaging chamber on a Zeiss Axio Observer Z1 microscope, pre-warmed to 37^{o}C and set to 5% CO_2. Metamorph Imaging Software (Molecular Devices, Sunnyvale, CA) was used to set up the time lapse image capture. 200µm stacks (10µm steps) of phase contrast images over ten fields

of view, each containing one cell-seeded bead, were imaged per well, with 4 wells imaged per condition (120 positions total for 3 conditions). Image stacks were captured every 20 minutes for 24 hours. For each bead, the time at which the first OEC protruded from the bead was recorded as the sprout initiation time. The number of sprouts per bead at 8 hours was also quantified.

Alginate Gel Preparation

Gels were prepared as previously described[14,23]. In brief, Ultra-pure MVG alginate was obtained from Pronova (# 4200106). MVG alginate was irradiated at 3MRad to obtain low molecular weight polymer chains. 1% of carboxylic acid groups on both high and low molecular weight alginates were oxidized to aldehyde groups with sodium periodate, to produce a hydrolytically labile polymer backbone[25]. The reaction was stopped with the addition of ethylene glycol after 17 hours. Alginate polymers were then dialyzed in 3000MWCO membranes for 3 days with repeated water exchange, frozen and lyophilized for storage. One day prior to use, both HMW and LMW alginate were reconstituted with EBM-2 to 2%w/v. VEGF and SDF were then added to a mixture of 75% LMW and 25% HMW alginates. 40µl of 0.21g/ml $CaSO_4$ was added per 1ml of alginate to crosslink the gel, and the solution was mixed between two 1ml syringes connected with a Leur-Lok union. Gels were allowed to crosslink for at least 30 minutes prior to use.

Hind-limb Ischemia Model

All animal experiments were performed in accordance with IACUC approved protocols. Hind-limb ischemia surgery was performed on C57BL6/J mice (Jackson Laboratories #000664) or C.B-17 SCID mice (Taconic #CB17SC-F) less than 10 weeks old, as previously described[13,23]. Briefly, mice were given an intraperitoneal injection of a Ketamine/Xylazine cocktail to induce anesthesia. An incision was then made at the inner thigh, exposing the underlying muscle and the external iliac artery and vein, and the hypogastric artery and vein. Two ligatures were placed around the external iliac artery and vein and one was placed around the femoral artery and vein. The external iliac vessel was cut between the two suture

knots. Alginate gels containing 2ug of SDF, 3ug of VEGF, the combination or control gels (no factors) were then injected intramuscularly under the ligation site. The incision was closed with 7mm staples. Mice were imaged with a Laser Doppler Perfusion Imaging (LDPI) system (PeriScan PIM II, Perimed Instruments, Ardmore, PA) prior to performing surgery, and 1 week intervals after surgery for 4 or 5 weeks. C57BL6/J mice were used to test the gel delivery system alone (n = 5), while SCID mice were used for experiments with human cells (n = 7) to eliminate the adaptive immune reaction by T and B cells in response to human-mouse HLA incompatibilities, although natural killer cells are still present[26]. One day after surgery, OECs or CACs in culture were stained for 10 minutes with 3ul of Vybrant™ DiD dye per million cells (Molecular Probes #V-22887), and were delivered to the blood stream of SCID mice using an intracardiac injection to prevent first pass accumulation in the lungs. Mice were humanely sacrificed by CO_2 inhalation at the end of experiments. Muscles surrounding the vessel ligation site, including the semimembranosus, semitendinosus, gracilis and adductor muscles, in the ischemic limb, and the same muscle in the contralateral limb were collected and zinc formalin fixed (Anatech Ltd #170) for 24 hours. Muscles were then transferred to a 70% ethanol solution prior to paraffin embedding and sectioning.

Immunohistochemical Analysis

Paraffin embedding and sectioning was performed by the Dana Farber / Harvard Cancer Center Histopathology Core (P30 CA06516). 5μm thick paraffin sections, cut perpendicular to muscle fiber direction were analyzed for blood vessel density as described previously[12,14,21,27,28]. Briefly, slides were soaked in xylene to remove excess paraffin and then rehydrated in decreasing ethanol solutions (100%-95%-70%), followed by a 30 minute Citrate Buffer (10mM Tri-sodium citrate, pH = 6) epitope retrieval step (20 minutes boiling, 10 minutes at room temperature). After washing in Tris Buffer (0.15M Tris-HCl, 0.1M NaCl, 0.05% Tween 20, pH = 7.6) and applying Blocking Buffer (10% Normal Goat Serum, 1% BSA in Tris Buffer), rat anti-mouse CD31 antibody (BD # 557355) was applied overnight at 4^{o}C for the detection of endothelial cells. Slides were then washed again, and an AlexaFluor-568 goat anti-rat

secondary (Life Technologies #A-11077) was applied for 1 hour at room temperature. Following a final wash, slides were mounted with ProLong gold Anti-fade Reagent with Dapi (Life Technologies #P36935) and protected from light until imaged. Muscle sections were imaged on a Zeiss Axio Observer (Zeiss, Thornwood, NY) equipped with a Hamamatsu Orca-Flash 4.0 sCMOS camera (Hamamatsu Photonics, Bridgewater, NJ). Blood vessel density was quantified from 6 images per mouse (taken from 4 sections per animal), 4 mice per condition.

Statistical Analysis

Data was compared using a Students unpaired t-test (two-tailed), with a p-value less than 0.05 considered significant.

3.4 Results

OEC and CAC Sprouting Potential

OECs or CACs were mixed with 100µm collagen coated beads in a spinning flask, alternating between static and spinning states over 4 hours, sufficient time to allow cell seeding[13,14]. OECs readily adhered to the beads, and proliferated on the beads until forming a confluent layer of cells (Figure 3.1A-B), similar to previously reported bead coating by HMVECs and HUVECs[9,13,14]. In contrast, CACs adhered poorly to beads. A few beads were found with one or two CACs adhered, but the majority of beads were empty with individual cells still floating in suspension (Figure 3.1C-D). CACs were not used further in sprouting assays, because the beads never became confluent with cells. Sprouting assays were initiated with OEC-covered beads by suspending the beads in a 3D fibrin matrix. OECs then migrated from the beads and formed sprouts, mimicking the initial stages of angiogenesis (Figure 3.1E-F).

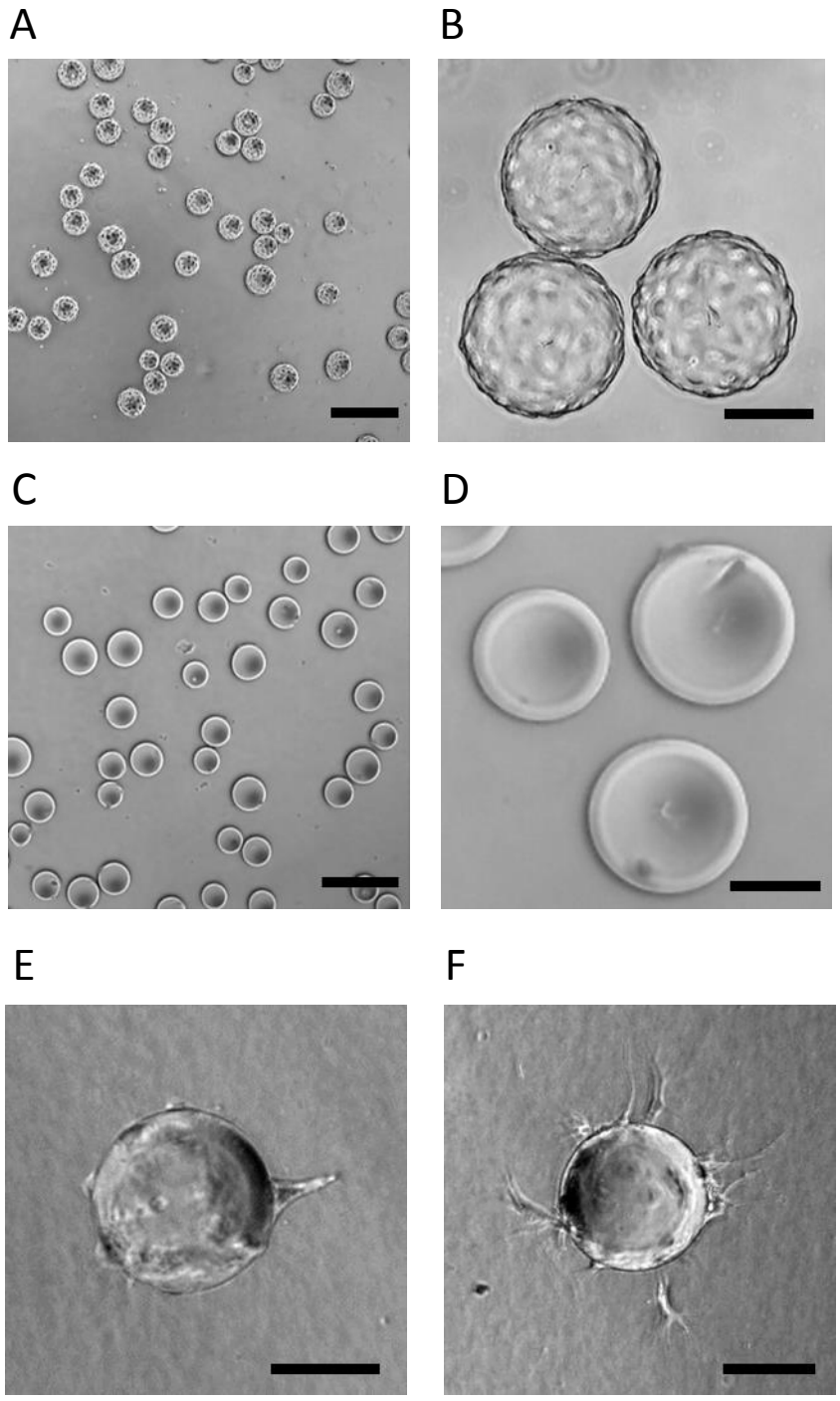

Figure 3.1. Phase contrast images of OECs and CACs after cell seeding procedure on 200µm diameter, collagen-coated dextran beads and OEC sprout examples. A-B) OECs adhered to beads and proliferated until confluent. Scale bars are 500µm (A) and 100µm (B). C-D) CACs did not adhere or proliferate on beads. Scale bars are 500µm (C) and 100µm (D). E-F) Sprouts formed by OECs after seeding in fibrin gel. One sprout (E) and multiple sprouts (F). Scale bars are 100µm.

Effects of VEGF and SDF on Endothelial Sprouting

Sprouting assays were used to compare the potential angiogenic ability of OECs, HUVECs and HMVECs, and to determine the effects of VEGF and SDF on this ability. Beads coated with OECs, HUVECs and HMVECs were placed within a fibrin gel matrix, and VEGF (50ng/ml), SDF (100ng/ml) or the combination was added to the media on top of the fibrin gel for 3 days. SDF did not support sprout formation by any cell type, whereas VEGF, a known angiogenic cytokine, induced sprout formation by all three cell types (Figure 3.2A-C). Surprisingly, the combination of VEGF and SDF promoted the most sprout formation by all three cell types. In addition to the positive effect of a constant presence of SDF with VEGF, the temporal presentation of SDF may be important for sprouting. This effect is observed with VEGF alone, where a decreasing concentration of VEGF over time is known to stimulate the best sprout formation by HMVECs[14]. The effect of increasing, decreasing or stable profiles of SDF, overlaid on a decreasing profile of VEGF was tested at the day 3 time point (Suppl Figure 3.1A). All profiles of SDF supported more sprout formation by OECs, HUVECS, and HMVECs compared to VEGF alone, except for a decreasing SDF profile with HMVECs (Suppl Figure 3.1B-D). These data suggest that SDF must be present and also maintained at a sufficient level after initial sprout formation in order to have an overall effect.

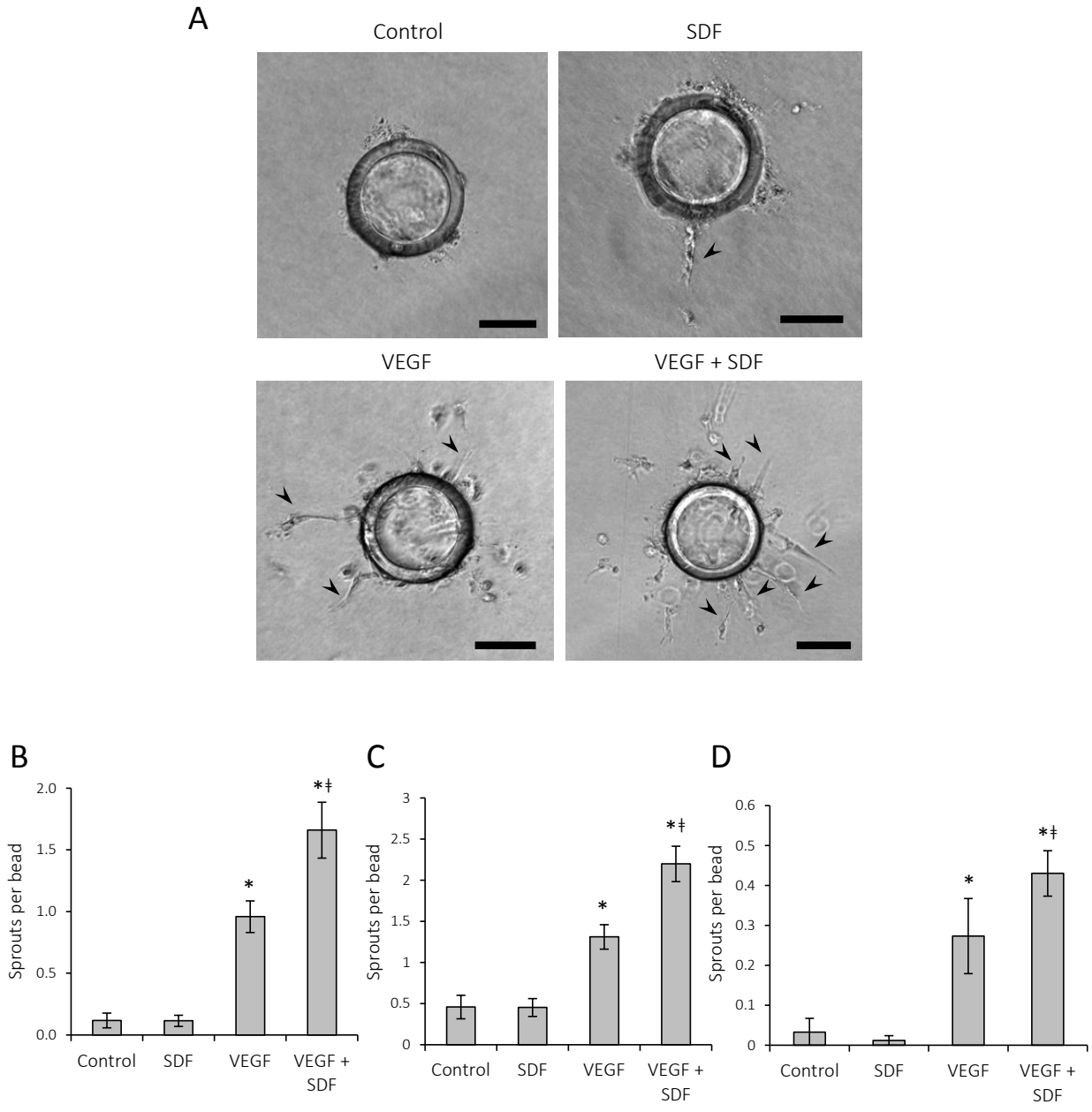

Figure 3.2. Endothelial sprouting behavior in response to SDF, VEGF and the combination at 72 hours. A) Images of OEC sprouts formed after exposure to control media, or media supplemented with 100ng/ml SDF, 50ng/ml VEGF, or the combination. Arrowheads indicate sprouts. Scale bars are 100µm. B-D) Quantification of the number of sprouts per bead formed by OECs (B), HUVECs (C), and HMVECs (D). Mean ± SD, n=4. * $p < 0.05$ compared to control condition, ‡ $p < 0.05$ compared to VEGF condition.

The positive effect of VEGF and SDF on endothelial sprouting may be achieved by promoting faster and more continuous sprout formation, or by maintaining sprouts longer. To understand if the combination of VEGF and SDF had an effect on the kinetics of initial sprout formation, time lapse microscopy was used to image OECs in this sprouting assay. The time at which the first cell protruded from the bead was recorded as the sprout initiation time. The SDF alone condition was not tested here since it did not lead to an increase in sprouting over the control in the earlier study (Figure 3.2). Both VEGF and VEGF+SDF conditions showed faster sprout initiation times relative to the control, with VEGF alone reducing the initiation time by one hour, and combining SDF with VEGF further reduced this time by an additional 50 minutes (Figure 3.3A-B). The total effect of reduced initiation time on sprouting could be observed by 8 hours, where both conditions with VEGF already showed significantly more sprouts per bead relative to the control (Figure 3.3C). To investigate sprout maintenance over time, the number of sprouts per bead was compared at 24, 48 and 72 hour time points (Figure 3.4A-C). At 24 hours, more sprouts formed when VEGF was present, compared to control and SDF alone, a possible continued effect of reduced sprout initiation time. OECs also demonstrated the highest sensitivity to VEGF in the first 24 hours as measured by the number of sprouts formed relative to the control (OECs – 5:1, HMVECs – 3:1, HUVECs – 2.2:1). While VEGF and VEGF+SDF conditions displayed similar levels of sprouting at 24 and 48 hours, by 72 hours, the number of sprouts per bead in the VEGF condition dropped significantly for HUVECs and HMVECs, and dropped only slightly for OECs. In comparison, the number of sprouts in the condition with VEGF and SDF barely decreased for HUVECs and HMVECs, and instead slightly increased for OECs. Even though all three cell types exhibited significant differences between the VEGF+SDF and VEGF alone conditions at 72 hours, OECs showed the most robust response to VEGF+SDF between 48 and 72 hours in terms of sprout maintenance. Together, these data demonstrate that the combination of VEGF and SDF potently promotes sprouting by all three cells types, possibly by multiple mechanisms, including a reduced sprout initiation time, enhanced maintenance of sprouts that have formed and/or by encouraging continuous sprouting over time.

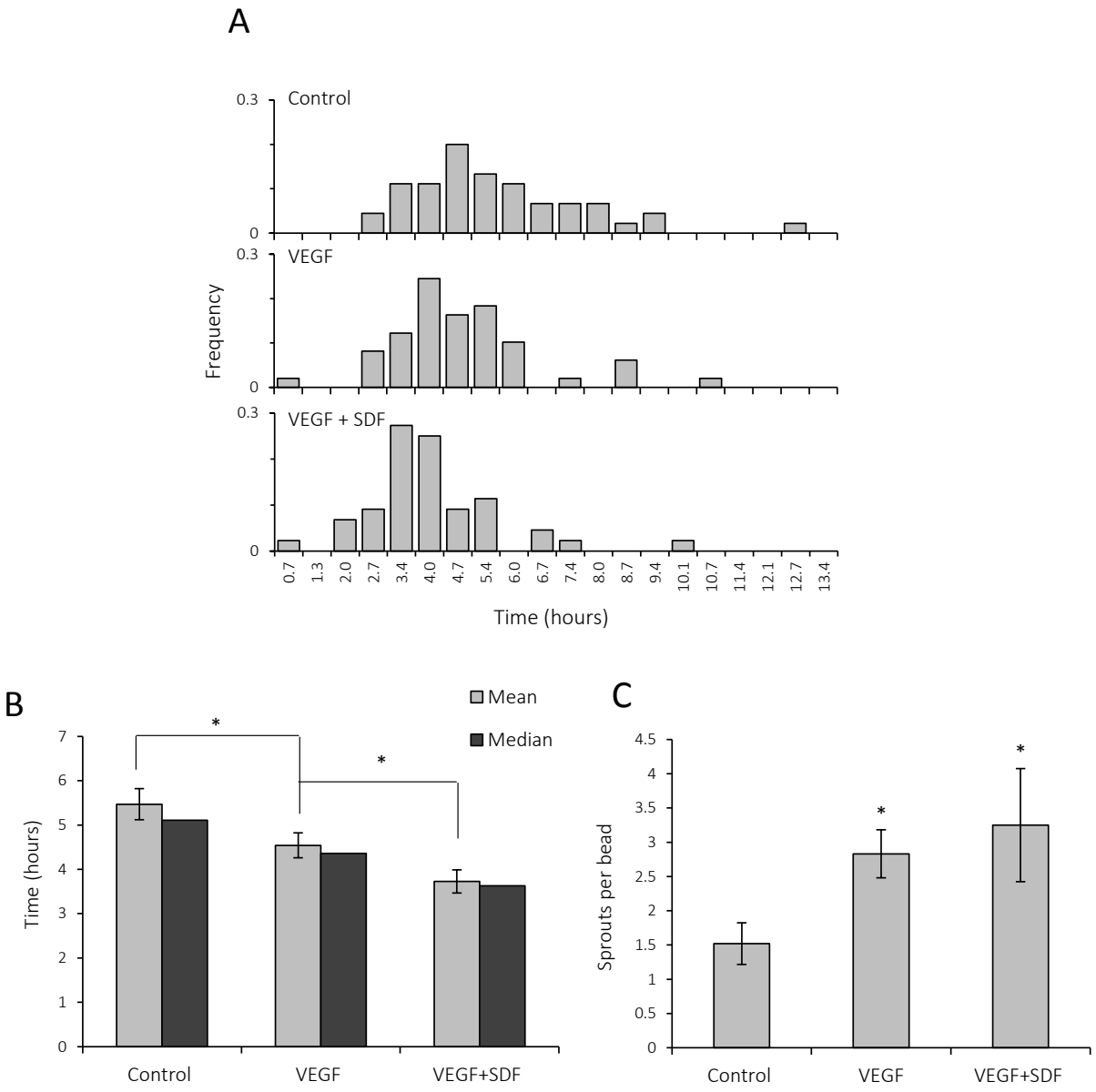

Figure 3.3. Kinetics of initial OEC sprout formation. A) Histograms of sprout initiation time for OECs with control media, or media supplemented with VEGF or VEGF+SDF. B) Population mean and median sprout initiation times. Mean ± SEM, Control (n=45), VEGF (n=49), VEGF+SDF (n=44). C) Quantification of the number of sprouts per bead formed after 8 hours. Mean ± SD, n=4. * $p < 0.05$.

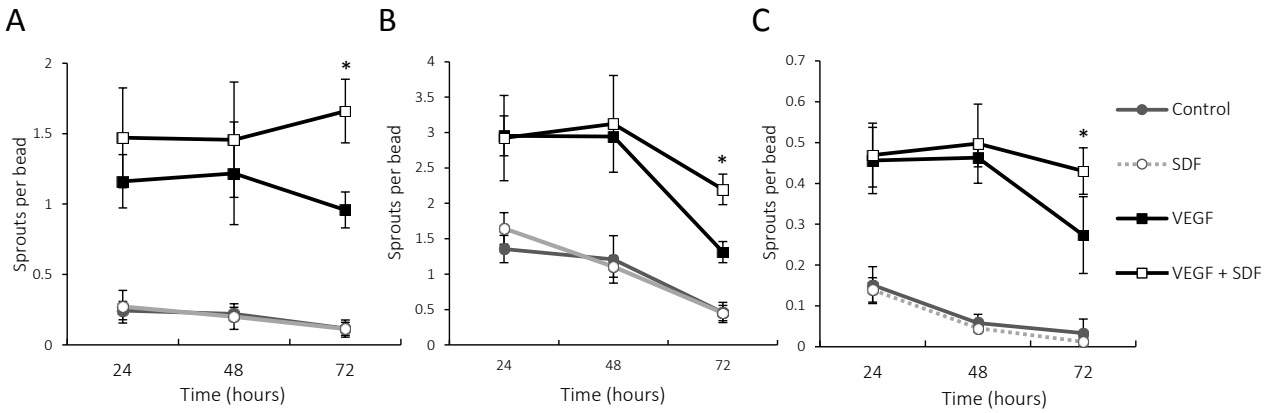

Figure 3.4. Effect of VEGF and SDF on sprouting at 24, 48, and 72 hours. A-C) Quantification of the number of sprouts formed by OECs (A), HUVECs (B) and HMVECs (C). Mean ± SD, n=4. * $p < 0.05$ compared to all other conditions.

We next directly compared the sprouting potential of OECs and mature endothelial cells by seeding either OECs and HMVECs or OECs and HUVECs onto the beads together (Figure 3.5A). When OECs and HMVECs were cultured together, the combination of VEGF and SDF still promoted more sprouting than VEGF alone (Figure 3.5B). OECs typically took the tip cell position in sprouts, and even sprouts which had a HMVEC as the tip cell were often supported at the stalk by an OEC; many sprouts were completely formed by OECs (Figure 3.5C-D). The percentage of sprouts with OECs *vs*. HMVECs as the tip cell was subsequently quantified. Even though only 38% of the cells initially on the beads were OECs, as determined by flow cytometry prior to placing beads in fibrin gels, at 24, 48 and 72 hours 60-70% percent of the sprouts had an OEC as the tip cell in both the VEGF and VEGF+SDF conditions (Figure 3.5E). Similar trends were revealed when OECs and HUVECs were seeded on the beads together. At 72 hours, the combination of VEGF and SDF promoted the most sprout formation, followed by VEGF alone, while control and SDF alone conditions showed significantly fewer sprouts (Figure 3.5F). Prior to placing beads in the fibrin matrix, 45% of the cells on the beads were OECs. After 72 hours, OECs were found in the tip cell location in approximately 60% of the sprouts in the VEGF and VEGF+SDF conditions (Figure 3.5G). Direct comparison of OECs to mature endothelial cell types in these assays demonstrates the greater sprouting potential of OECs.

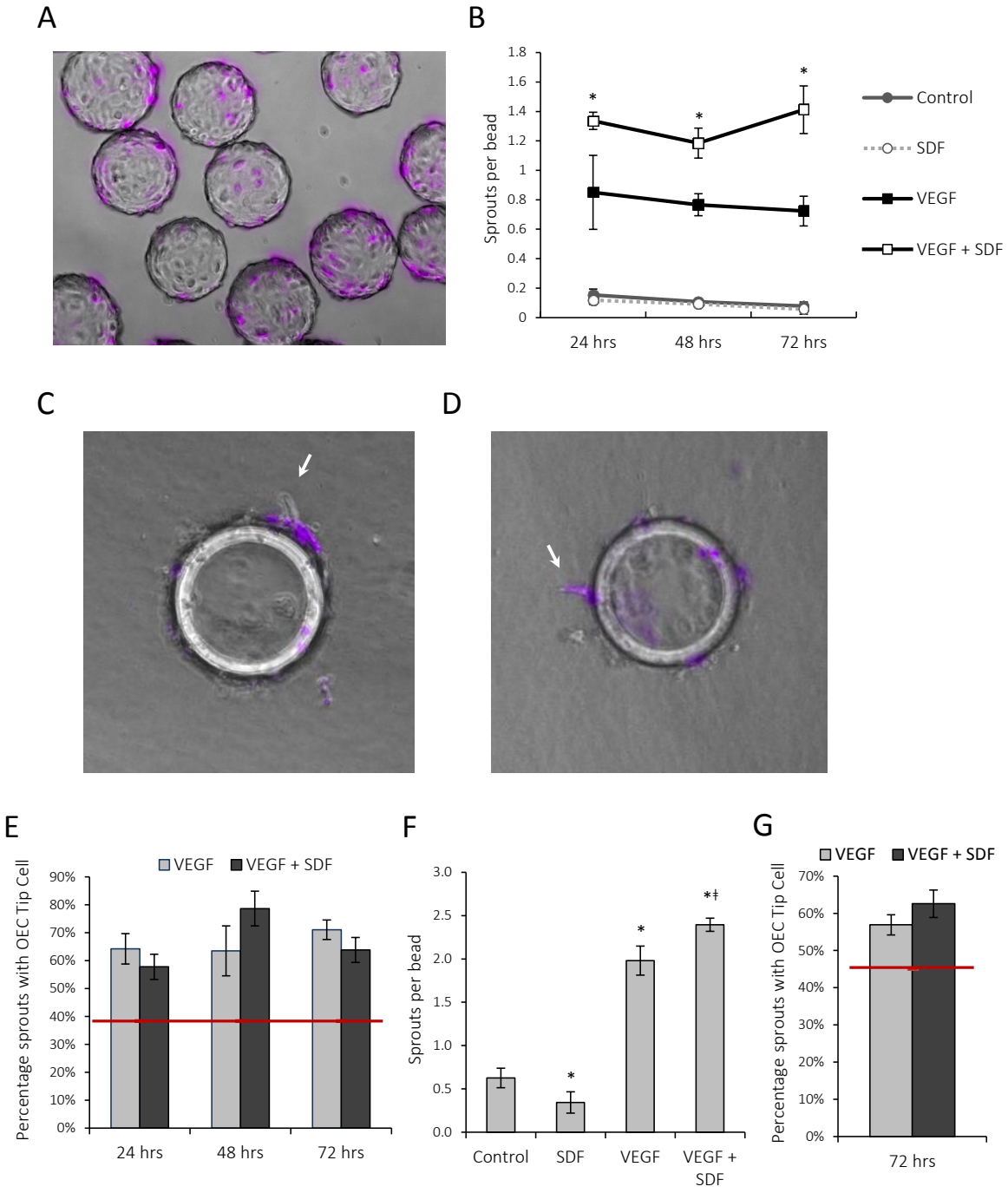

Figure 3.5. Direct comparison of OEC sprouting with HUVECs and HMVECs. A) Phase contrast image of OECs and HMVECs seeded onto 200µm beads, with image of fluorescently labeled OECs overlaid. B) Quantification of total sprouts per bead formed by OECs and HMVECs at 24, 48 and 72 hours. Mean ± SD, n = 4. * $p < 0.05$ compared to all other conditions. C) Sprout formed by a HMVEC and supported by an OEC at the base. D) Sprout formed by OECs. E) Percentage of sprouts with an OEC as the tip cell when seeded with HMVECs. Red line indicates initial percentage of cells that were OECs. F) Total number of sprouts per bead formed by OECs and HUVECs at 72 hours. Mean ± SD, n = 4. * $p < 0.05$ compared to control condition, ‡ $p < 0.05$ compared to VEGF condition. G) Percentage of sprouts with an OEC as the tip cell when seeded with HUVECs. Red line indicates initial percentage of cells that were OECs.

Paracrine Support of Angiogenesis by OECs and CACs

In addition to OECs directly participating in angiogenesis, secreted factors from OECs and CACs may contribute to new blood vessel formation in a paracrine fashion. To test this possibility, OECs and CACs were seeded on top of fibrin gels which contained HUVEC-coated beads; both VEGF and control conditions were tested. The number of sprouts per bead was counted after three days. Again, VEGF increased sprouting compared to the control when no progenitors were seeded on top of the gel. In both VEGF and control conditions, the presence of OECs increased sprouting by 35%, while CAC presence doubled the number of sprouts formed (Figure 3.6A). To determine if OECs and CACs secreted angiogenic factors, an ELISA-based array for angiogenic cytokines was used to analyze conditioned medium from both cell types. Both OECs and CACs were found to secrete TIMP-2, IL-8, VEGF, FGFb and IL-12. OECs also secreted PlGF, IL-6, TNFα, and FGFa, while CACs secreted leptin (Figure 3.6B; Suppl Figure 3.2A). The level of these secreted cytokines, collected from three independent experiments for each cell type, was also quantitatively measured using standard ELISA plates. The relative levels of cytokines secreted from OECs and CACs demonstrated the same trend as was measured with the angiogenesis array (Figure 3.6C). Both cell types secreted VEGF, FGFb, IL-12 and IL-8; here, CACs secreted more IL-8 than OECs. Only OECs secreted PlGF and only CACs secreted leptin. When OECs and CACs were exposed to VEGF and SDF, the angiogenesis array suggested that relative amount of many secreted cytokines increased, including PlGF, IL-8, IL-6, FGFb and FGFa from OECs and IL-8, FGFb, IL-12, and leptin from CACs (Suppl Figure 3.2A-B). ELISA analysis confirmed a slight increase in IL-8 secretion from OECs, and an increase in FGFb, IL-12 and leptin from CACs, while the other measured factors remained unchanged (Suppl Figure 3.2C). A number of these factors are known to have angiogenic activity, and their secretion by OECs or CACs could enhance new blood vessel formation by host endothelial cells. In order to determine the relative potency of these factors, PlGF, IL-8, FGFb, Leptin, and VEGF as a positive control, each at 10ng/ml, were added to fibrin gels containing HUVEC-coated beads. At this concentration, FGFb, Il-8 and VEGF significantly increased sprouting by HUVECs,

while PlGF and Leptin showed only modest effects (Figure 3.6D). Further, blocking antibodies were applied to neutralize the positive effect of each of these factors when secreted from OECs or CACs (Figure 3.6E). Blocking PlGF, FGFb, IL-8, or all three in combination significantly reduced HUVEC sprouting when OECs were placed on top of the fibrin. Similarly, blocking IL-8, FGFb, Leptin or the combination also significantly reduced HUVEC sprouting when CACs were on top of the fibrin.

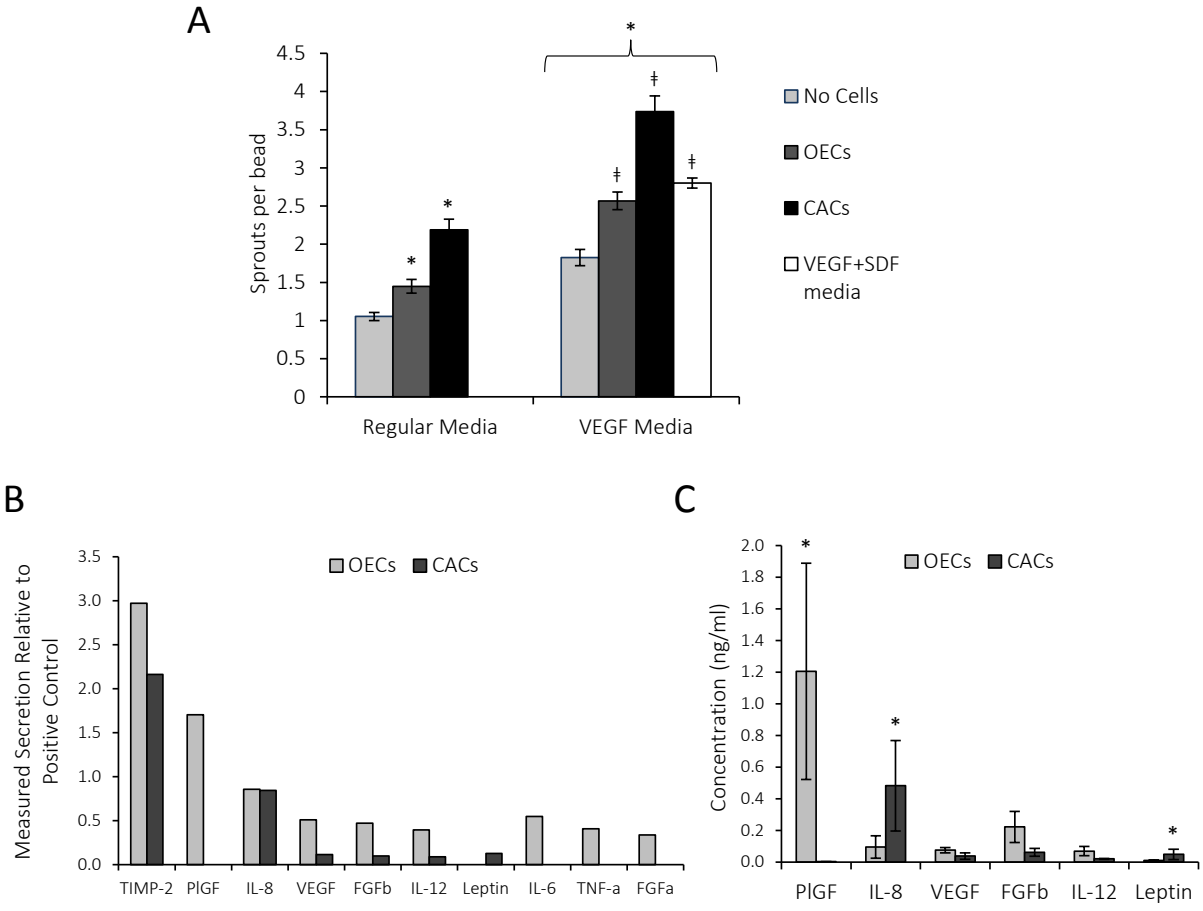

Figure 3.6. Paracrine effects of factors secreted by OECs and CACs. A) The number of sprouts per bead formed by HUVECs when 50,000 OECs or CACs were placed on top of the fibrin gel for 3 days. Potency of secreted factors from OECs and CACs are shown in comparison to the enhanced sprouting potential achieved with VEGF+SDF media. Regular media is EBM-2+5%FBS, VEGF media has 50ng/ml VEGF added to regular media. SDF was used as normal at 100ng/ml. Mean ± SD, n = 4. * $p < 0.05$ compared to regular media with no cells, ǂ $p < 0.05$ compared to VEGF media with no cells. B) Secretion of angiogenic factors from OECs and CACs as measured on an ELISA-based array. Adjusted for cell number, and plotted relative to positive control condition on the array (See Supplemental Figure 2). C) ELISA detection of factors secreted from OECs and CACs. Adjusted for cell number. Mean ± SD, n = 3.

Figure 3.6 (Continued)

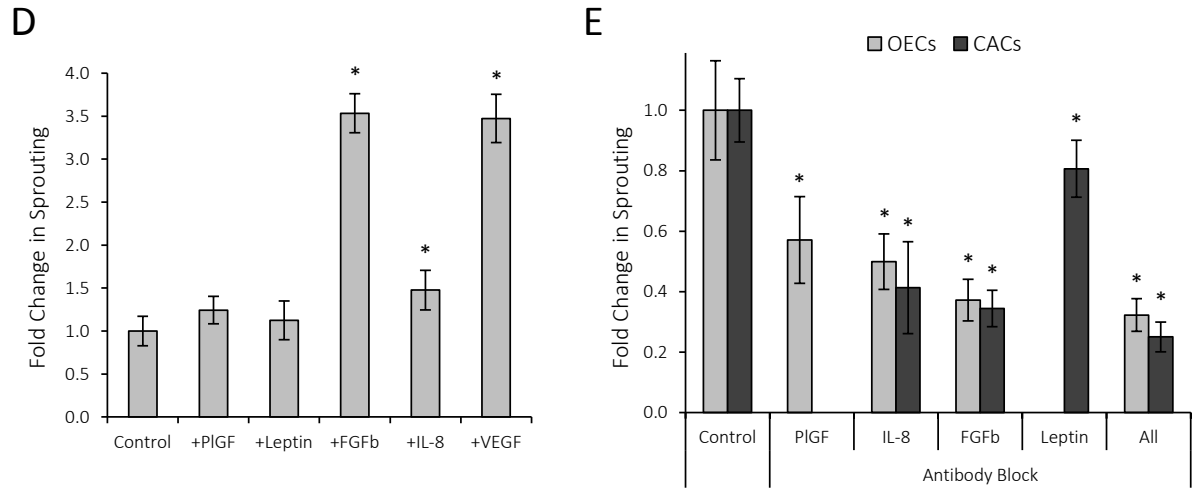

Figure 3.6 (Continued). D) Relative increase in HUVEC sprouting over the control with the addition of various angiogenic factors each at 10ng/ml. Mean ± SD, n = 4. E) Relative reduction in sprouting with the application of blocking antibodies for factors secreted by OECs or CACs. The combination condition (*All*) indicates blocking of PlGF, IL-8 and FGFb for OECs and IL-8, FGFb, and Leptin for CACs. Mean ± SD, n = 4. * $p < 0.05$.

These *in vitro* data together confirmed that OECs can directly participate in sprout formation, while CACs do not. On the other hand, CACs more potently promoted endothelial cell sprouting *in vitro*, on a per cell basis compared to OECs, likely due to secretion of factors that acted in a paracrine manor. Exposure to VEGF and SDF increased OEC sprout formation, and also slightly increased secretion of angiogenic factors from both cell types, which could potentially influence their contributions to new blood vessel growth.

In Vivo Effects of VEGF and SDF Delivery

As I am proposing to utilize VEGF and SDF delivery to enhance the localization and function of transplanted OECs and CACs, it will be important to understand the role of these factors when used alone to treat ischemic tissues. Sustained local delivery of VEGF from polymer scaffolds has previously been shown to promote angiogenesis and restore perfusion in a mouse model of hind-limb ischemia[13,14,21,23]. I have found that VEGF and SDF together potently promote angiogenic sprouting *in vitro*, therefore the ability of these cytokines to support angiogenesis was tested in the same hind-limb ischemia model used

for VEGF studies. Alginate gels that released VEGF and SDF, VEGF alone, or control gels (See Chapter 2, Figure 2.5 for release profiles) were injected into the hind-limb muscle tissue of C57Bl/6J mice immediately after ischemia was induced. Laser Doppler Perfusion Imaging (LDPI) was used to monitor blood perfusion in the ischemic limb relative to the control limb at one week intervals following surgery. Both VEGF and VEGF+SDF gel treatments performed significantly better than control gels, restoring blood flow to a higher level at 5 weeks (Figure 3.7A). Gels delivering a combination of VEGF and SDF did not improve perfusion recovery better than VEGF-only gels, perhaps because the VEGF-only gels were highly effective in this animal model of ischemia.

OEC and CAC Recruitment for Ischemic Reperfusion

Since both types of endothelial progenitors were found to contribute to angiogenic sprouting *in vitro*, both directly (OECs) and via paracrine signaling (OECs and CACs), the ability of these cells to enhance angiogenesis and restore perfusion was next tested *in vivo* in the mouse hind-limb ischemia model. OECs or CACs were systemically delivered via intracardiac injection into SCID mice one day after mice had undergone hind-limb ischemia surgery. Mice also received a local injection of a control alginate gel or alginate gel containing VEGF and SDF in the muscle surrounding the site of vessel ligation, to additionally assist with progenitor cell accumulation in the nearby tissue. Mice that received only a control alginate gel injection showed poor overall recovery, with the blood flow ratio in the ischemic limb versus the contralateral, non-ischemic limb only reaching 48% four weeks after surgery (Figure 3.7B). At the same time point, there was a trend of increased perfusion for mice which had received VEGF+SDF gels or VEGF+SDF gels with an injection of OECs (55% blood flow ratio), compared to the control, but these differences were not statistically significant. Strikingly, though, transplantation of CACs into mice which had received VEGF+SDF gel injection led to a significantly improved blood flow ratio by four weeks compared to all other conditions. These mice showed perfusion recovery in the ischemic limb that reached 73% of the level in the contralateral, control limb. Blood vessel density in the hind-limbs was quantified by staining tissue sections for CD31, an endothelial cell marker, to confirm that perfusion

differences were due to vessel formation or maintenance. Here, all treatment conditions showed statistically significant differences compared to control gels, and VEGF+SDF gels with a CAC injection also demonstrated significantly higher blood vessel density compared to VEGF+SDF gels alone or gels with an OEC injection (Figure 3.7 C-H). These *in vivo* data show that systemic delivery of CACs leads to improved perfusion recovery and increased blood vessel density, while delivery of OECs does not enhance recovery or capillary density over VEGF+SDF gels alone.

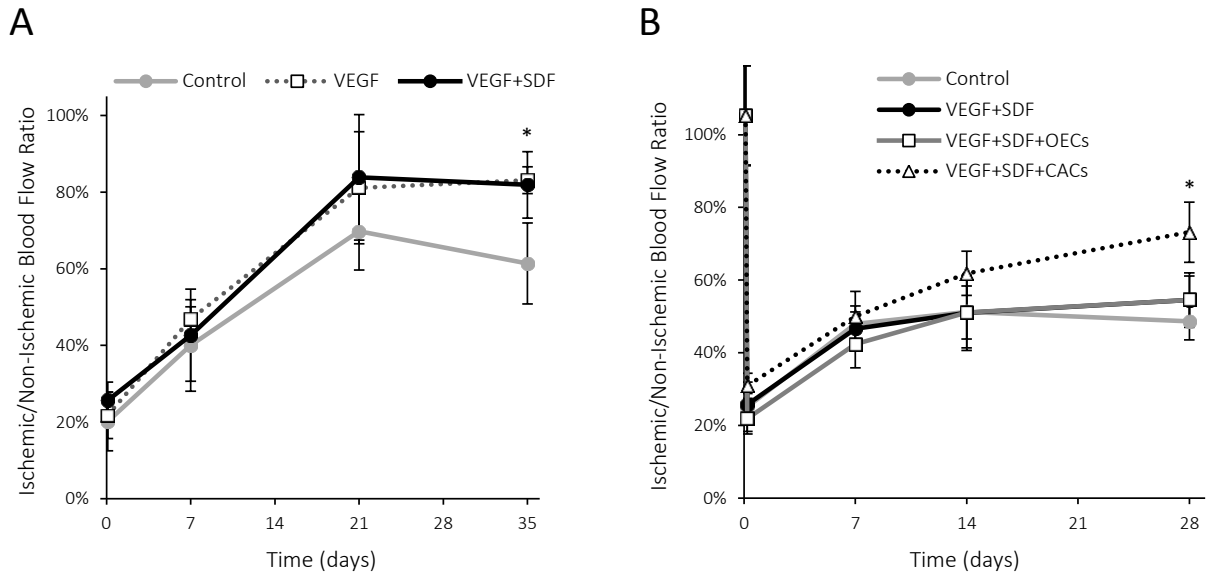

Figure 3.7. Blood vessel perfusion recovery and capillary density after hind-limb ischemia surgery with VEGF and SDF treatment, with and without OEC or CAC delivery. A) C57BL6/J mice were treated with injectable alginate gels loaded with VEGF or VEGF+SDF, or control gels. Perfusion is plotted as the ratio of the mean perfusion in the ischemic limb over the non-ischemic, contralateral limb. Mean ± SD, n = 5. * $p < 0.05$ for VEGF and VEGF+SDF compared to the control. B) Blood perfusion ratio in ischemic hind-limbs of SCID mice after treatment with VEGF+SDF gels and a systemic injection of either OECs or CACs, compared to control alginate gels with no cell delivery. Mean ± SD, n = 7. * $p < 0.05$.

Figure 3.7 (Continued)

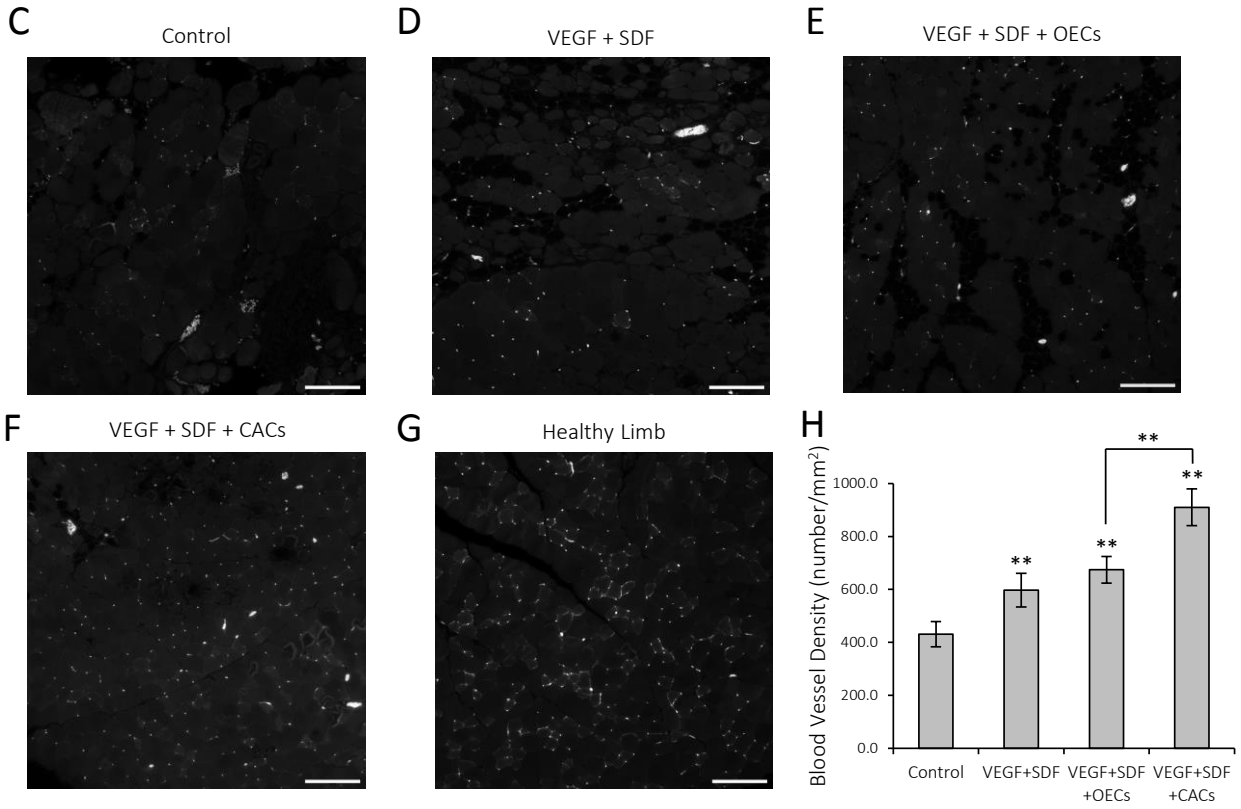

Figure 3.7 (Continued). C-G) Images of hind-limb muscle sections stained with CD31 from control (C), VEGF+SDF gel only (D), VEGF+SDF gel with OEC delivery (E), VEGF+SDF gel with CAC delivery (F) treatment conditions, and a healthy, non-ischemic limb (G). Scale bars are 100µm. H) Quantification of blood vessel density in ischemic hind-limbs 4 weeks after surgery. Mean ± SD, n = 4 mice per condition. ** $p < 0.01$.

3.5 Discussion

The results of these experiments together clarified the roles of OECs and CACs in contributing to sprout formation, and revealed the effects of VEGF and SDF on each cell types' role. Specifically, OECs formed sprouts, while CACs did not, in this 3D model of angiogenesis. In direct comparison to mature endothelial cells, OECs preferentially localized to the tip cell position. The combination of VEGF+SDF yielded more sprouts per bead for OECs, HUVECs, and HMVECs compared to either factor alone or control media. The combination of VEGF+SDF also reduced OEC sprout initiation time, resulted in the most sprout formation relative to the control at 24 hours, and showed better sprout maintenance at 72

hours compared to HUVECs and HMVECs. OECs and CACs both supported sprout formation by HUVECs in a paracrine manner; on a per cell basis, the cytokines from CACs were more potent than those from OECs. Blocking factors secreted by OECs and CACs, including PlGF, IL-8, FGFb, and Leptin, significantly reduced sprouting by HUVECs. Finally, testing the functional contribution of both endothelial progenitor cell types showed that CACs, which accumulated in the ischemic hind-limb with local delivery of VEGF and SDF from an alginate hydrogel, promoted perfusion recovery better than accumulated OECs or gels alone.

Comparisons of endothelial progenitors with mature endothelial cells showed that OECs formed sprouts, similar to HUVECs and HMVECs, while CACs did not in this assay. CACs did not adhere to the beads used in the sprouting assay, and therefore could not form sprouts. Previous studies have used a 2D tube-forming assay to assess angiogenic capabilities, which have indicated that 'early-EPCs' (CACs) can participate in tube formation when co-incubated with HUVECs, but not alone[29,30]. Tube-forming assays also yield false positives, as CD34+ cells can form tubes, even though these are a mixture of cells of hematopoietic lineage, which do not form vessels *in vivo*[19,31,32]. The 3D sprouting assay was also used to directly compare the ability of OECs *vs*. HUVECs or HMVECs to form sprouts by co-seeding both cell types onto beads, and allowing them to compete for tip cell position. OECs were preferentially found in the tip cell location compared to HMVECs, and often also supported sprouts initiated by HMVECs at the stalk. Additionally, the profile of the number of sprouts per bead at 24, 48, and 72 hours resembles that of OECs alone more than HMVECs alone. The ratio of OECs to HMVECs on the beads was counted at the start of the experiment, but this was not quantified each day. Preferential sprout formation by OECs could also be achieved by their higher proliferation rate over HMVECs, but this would also lead to an increasing fraction of OEC sprouts over time, which was not observed. When OECs were directly compared to HUVECs, similar trends were observed, with OECs preferentially localizing to the tip cell position. These experiments demonstrated that OECs have an increased capability to form sprouts, and also function in concert with mature endothelial cells. These results are further in agreement with other

models of vessel network formation, in which evenly distributed OECs in a 3D collagen gel matrix condense to form vessel-like structures which have increased microvessel density compared to networks of HMVECs[33]. Therapeutically, this suggests that if OECs are correctly located at sites of new blood vessel growth, they should exhibit a higher angiogenic potential than the resident endothelial cells, but this *in vivo* result was not shown here.

The combination of VEGF and SDF had a significant effect on sprouting OECs and endothelial cells. First, VEGF and SDF together increased sprouting at 72 hours for OECs, HUVECs and HMVECs compared to VEGF alone, SDF alone or control media. VEGF is known to promote blood vessel formation *in vitro* and *in vivo*, and has been tested in this assay previously[13,14]. SDF on the other hand is claimed to be angiogenic because it supports tube formation in 2D assays, although again, this is not a rigorous assay[16]. Here, SDF alone did not stimulate sprout formation at any time point, while the combination of VEGF and SDF synergistically promoted sprouting. Previous studies have shown that mature endothelial cells exposed to SDF, secrete VEGF, and cells exposed to VEGF secrete SDF as well as up-regulate the expression of CXCR4 (the receptor for SDF), possibly protecting the cells from desensitization[16,34]. These interactions have the potential to create an autocrine positive feedback loop, and may be responsible for strong sprout promotion. The resultant increased sprouting can be accomplished by reducing the sprout initiation time, encouraging more continuous sprout formation, and/or by maintaining sprouts for longer. The combination of VEGF and SDF was shown to reduce the sprout initiation time. At later time points, the significant differences between VEGF+SDF and other conditions could be achieved by either of the other two mechanisms. In the experiments performed here, the initiation time of only the *first* sprout formed was recorded, but the initiation time, total time of sprout maintenance, and retraction time for *all* sprouts between 0-72 hours was not determined. VEGF and SDF were shown to promote OEC migration chemotactically (Chapter 2, Figure 2.4), but this combination could perhaps also increase migration of OECs in a chemokinetic manner. SDF has been shown to induce actin polymerization through a RhoA- ROCK1 dependent pathway, which results in increased migration

in multiple myeloma cells[35]. Here, VEGF and SDF may act synergistically to enhance the overall migratory ability of OECs, which could help promote continuous sprout formation by individual cells, since sprouting is initiated by migration of a cell into the fibrin matrix. Enhancing OEC migration with the combination of VEGF and SDF could then be responsible for the increase in total number of sprouts formed, even if the retraction rate is similar in all conditions. Analysis of the full dynamics would reveal which mechanism is responsible for a higher number of sprouts per bead at later time points. Overall, these experiments suggest that the combination of VEGF and SDF has a strong potential to support new blood vessel formation, both by resident mature endothelial cells and by OECs that have localized to ischemic tissue.

OECs and CACs were also shown to stimulate HUVEC sprout formation by secreting angiogenic factors that act in a paracrine manner. While both progenitor cell types secrete multiple factors, the combination of factors secreted by CACs was more potent than from OECs. Both cell types secreted IL-8, VEGF and FGFb, which are known to be angiogenic[8,36] and was also demonstrated here, while only OECs secrete PlGF and CACs secrete leptin. The addition of blocking antibodies to each of these factors reduced sprouting by HUVECs significantly, demonstrating the importance of each component. Mature endothelial cells also secrete IL-8 and FGFb[12], which likely was responsible for the dramatic decreases in sprouting when each of these factors was blocked. An alternative method to eliminate the contribution of secreted factors from OECs and CACs, while keeping HUVEC signaling intact, would be to use siRNA against IL-8 and FGFb. This would allow the determination of the relative importance of each factor, and may elucidate whether the difference in IL-8 secretion is mainly responsible for the increased potency of CACs compared to OECs. Furthermore, the angiogenesis array assays for many common factors involved in new blood vessel formation, but there are still other factors and combinations that may support angiogenesis and be secreted by progenitors which were not tested here, including SDF, Insulin-like Growth Factor, Epidermal Growth Factor, etc. Of the cytokines investigated, these experiments confirmed

that factors secreted by OECs and CACs support angiogenesis by directly modifying endothelial sprouting potential.

In vivo functional testing of blood perfusion recovery showed that CACs, which were recruited to the ischemic hind-limb and exposed to VEGF+SDF from an alginate hydrogel, performed better than OECs gels alone. First, the baseline recovery for VEGF+SDF gels was established, since this combination of factors showed significantly enhanced sprout formation *in vitro*. In C57BL6/J mice, VEGF+SDF gels out-performed control gels, but not VEGF-only gels, possibly due to the fact that VEGF treatment alone showed pronounced perfusion recovery in this animal model. SDF-only gels were not tested in this model because SDF did not promote sprout formation in the *in vitro* model system, and *in vitro* sprouting assay results often correlate with perfusion recovery performance *in vivo*[10,13,14]. VEGF is produced naturally in response to ischemia[8], therefore it may be possible for the exogenously delivered SDF to interact with the endogenous VEGF to promote enhanced recovery. In SCID mice, the effect of VEGF+SDF gel treatment over the control is markedly reduced, likely due to the severity of the ischemic injury. VEGF+SDF gel treatment resulted in a higher capillary density, but this did not translate to a statistically significant difference in perfusion. This result is not unexpected for SCID mice, as VEGF-only treatments also have not been shown to promote significant perfusion differences, whereas endothelial progenitor cell and growth factor combination treatments are more effective[12].

As modeled in the sprouting assays, CACs secrete factors that act in a paracrine manner to potently promote angiogenesis, which may be the mechanism by which enhanced functional perfusion recovery is achieved. The panel of factors secreted by CACs promoted sprout formation more strongly than those from OECs, and additionally, CACs were shown (in Chapter 2) to accumulate more efficiently than OECs. The combination of secreting more potent angiogenic factors and accumulating in greater number could both explain why CACs demonstrated a significant therapeutic effect compared to OECs. Further, while these factors were shown to directly act on endothelial cells, they may also enhance or alter the recruitment of other cell types to the ischemic limb as well as influence their behavior or the behavior of

other support cells. In Chapter 2, CAC accumulation in *non-ischemic* limbs led to a significant and multiplicative effect on the infiltration of inflammatory cells, including CD11b+ cells (myeloid-lineage), F4/80+ cells (macrophages) and Gr1+cells (likely granulocytes), but this was not tested in *ischemic* limbs. If VEGF+SDF delivery and CAC localization in ischemic limbs alter the presence of inflammatory cell populations (e.g. macrophages, see Chapter 2, Figure 2.6 and 2.9), these cells could also potentially contribute to neovascularization in a paracrine manner or by physically interacting with endothelial cells[37]. Alternatively, it is unknown how long the CACs maintain a presence or stay alive in the ischemic limb, and for how long they secrete significant levels of cytokines. The exact location of CACs is also unclear, but (as shown in Chapter 2) some are likely stuck in capillaries, a reasonable proximity to act on resident endothelial cells. Lastly, it is unknown whether CACs can promote the same level of perfusion recovery if allowed to accumulate due to ischemia alone, without a VEGF+SDF-releasing alginate gel. Overall though, CACs were effective at restoring blood flow to the ischemic limb.

OECs were also shown to preferentially accumulate in ischemic limbs, but their presence was not therapeutically beneficial. OECs demonstrated potential to contribute to blood vessel formation *in vitro* by directly participating in sprouting and by secreting paracrine factors, which were both promising results before moving *in vivo*. Similar to many cell therapies, it is likely that too few OECs were recruited to observe enhanced recovery (Chapter 2, Figure 2.9)[38]; they may also not be in the correct location or microenvironment to participate. These issues can potentially be overcome by using biomaterials for cell delivery. Biomaterial systems have been designed with specific microenvironments that maintain cell viability and promote cell deployment into surrounding tissue[12]. Alginate hydrogels loaded with $VEGF_{121}$ enhanced migration of OECs from the scaffold, which were later found within blood vessels[12,39]. Additionally, tissue engineered networks of blood vessels that have been pre-formed within a biomaterial can anastomose with host vessels to carry blood and perfuse tissue[33,40–42]. Since the combination of VEGF and SDF increased sprout formation significantly in the *in vitro* models tested here, it may also possibly enhance or speed the formation of these *ex vivo* engineered vessel networks. Even though OECs were not

effective *in vivo* with the delivery method employed here, biomaterial-based solutions exist which achieve a therapeutic benefit, supporting the future use of these cells. In summary, the results of these experiments emphasize the enhanced regenerative capacity of endothelial progenitors and validate the use of these cells in therapies for the treatment of ischemia as contrasted to relying on resident endothelial cells alone.

3.6 References

1. Asahara, T. *et al.* Isolation of Putative Progenitor Endothelial Cells for Angiogenesis. *Science.* **275,** 964–966 (1997).

2. Kawamoto, A. & Asahara, T. Role of progenitor endothelial cells in cardiovascular disease and upcoming therapies. *Catheter. Cardiovasc. Interv. Off. J. Soc. Card. Angiogr. Interv.* **70,** 477–484 (2007).

3. Kawamoto, A. & Losordo, D. W. Endothelial progenitor cells for cardiovascular regeneration. *Trends Cardiovasc. Med.* **18,** 33–7 (2008).

4. Losordo, D. W. & Dimmeler, S. Therapeutic angiogenesis and vasculogenesis for ischemic disease: part II: cell-based therapies. *Circulation* **109,** 2692–7 (2004).

5. Fadini, G. P., Losordo, D. & Dimmeler, S. Critical reevaluation of endothelial progenitor cell phenotypes for therapeutic and diagnostic use. *Circ. Res.* **110,** 624–37 (2012).

6. Kalka, C. *et al.* Transplantation of ex vivo expanded endothelial progenitor cells for therapeutic neovascularization. *PNAS* **97,** 3422–7 (2000).

7. Hirschi, K. K., Ingram, D. a & Yoder, M. C. Assessing identity, phenotype, and fate of endothelial progenitor cells. *Arterioscler. Thromb. Vasc. Biol.* **28,** 1584–95 (2008).

8. Carmeliet, P. Mechanisms of angiogenesis and arteriogenesis. *Nat. Med.* **6,** 389–395 (2000).

9. Yuen, W. W. *et al.* Statistical platform to discern spatial and temporal coordination of endothelial sprouting. *Integr. Biol. (Camb).* **4,** 292–300 (2012).

10. Cao, L., Arany, P. R., Wang, Y.-S. & Mooney, D. J. Promoting angiogenesis via manipulation of VEGF responsiveness with notch signaling. *Biomaterials* **30,** 4085–4093 (2009).

11. Brudno, Y., Ennett-Shepard, A. B., Chen, R. R., Aizenberg, M. & Mooney, D. J. Enhancing microvascular formation and vessel maturation through temporal control over multiple pro-angiogenic and pro-maturation factors. *Biomaterials* **34,** 9201–9 (2013).

12. Silva, E. a, Kim, E.-S., Kong, H. J. & Mooney, D. J. Material-based deployment enhances efficacy of endothelial progenitor cells. *PNAS* **105,** 14347–14352 (2008).

13. Chen, R. R. *et al.* Integrated approach to designing growth factor delivery systems. *FASEB J.* **21,** 3896–3903 (2007).

14. Silva, E. A. & Mooney, D. J. Effects of VEGF temporal and spatial presentation on angiogenesis. *Biomaterials* **31,** 1235–41 (2010).

15. Kanda, S., Mochizuki, Y. & Kanetake, H. Stromal cell-derived factor-1alpha induces tube-like structure formation of endothelial cells through phosphoinositide 3-kinase. *J. Biol. Chem.* **278,** 257–262 (2003).

16. Salvucci, O. *et al.* Regulation of endothelial cell branching morphogenesis by endogenous chemokine stromal-derived factor-1. *Blood* **99,** 2703–2711 (2002).

17. Salcedo, R. & Oppenheim, J. J. Role of chemokines in angiogenesis: CXCL12/SDF-1 and CXCR4 interaction, a key regulator of endothelial cell responses. *Microcirculation* **10,** 359–370 (2003).

18. Peled, A. *et al.* The chemokine SDF-1 activates the integrins LFA-1 , VLA-4 , and VLA-5 on immature human CD34+ cells : role in transendothelial / stromal migration and engraftment of NOD / SCID mice. *Blood* **95,** 3289–3296 (2000).

19. Zemani, F. *et al.* Ex vivo priming of endothelial progenitor cells with SDF-1 before transplantation could increase their proangiogenic potential. *Arterioscler. Thromb. Vasc. Biol.* **28,** 644–650 (2008).

20. Yamaguchi, J. *et al.* Stromal cell-derived factor-1 effects on ex vivo expanded endothelial progenitor cell recruitment for ischemic neovascularization. *Circulation* **107,** 1322–1328 (2003).

21. Richardson, T. P., Peters, M. C., Ennett, A. B. & Mooney, D. J. Polymeric system for dual growth factor delivery. **19,** 1029–1034 (2001).

22. Chen, R. R., Silva, E. a, Yuen, W. W. & Mooney, D. J. Spatio-temporal VEGF and PDGF delivery patterns blood vessel formation and maturation. *Pharm. Res.* **24,** 258–264 (2007).

23. Silva, E. A. & Mooney, D. J. Spatiotemporal control of vascular endothelial growth factor delivery from injectable hydrogels enhances angiogenesis. *J. Thromb. Haemost.* **5,** 590–598 (2007).

24. Nehls, V. & Drenckhahn, D. A novel, microcarrier-based in vitro assay for rapid and reliable quantification of three-dimensional cell migration and angiogenesis. *Microvasc. Res.* **50,** 311–322 (1995).

25. Bouhadir, K. H. *et al.* Degradation of partially oxidized alginate and its potential application for tissue engineering. *Biotechnol. Prog.* **17,** 945–950 (2001).

26. Dorshkind, K., Pollack, S. B., Bosma, M. J. & Phillips, R. a. Natural killer (NK) cells are present in mice with severe combined immunodeficiency (scid). *J. Immunol.* **134,** 3798–801 (1985).

27. Chen, R. R. *et al.* Host immune competence and local ischemia affects the functionality of engineered vasculature. *Microcirculation* **14,** 77–88 (2007).

28. Chen, R. R., Silva, E. a, Yuen, W. W. & Mooney, D. J. Spatio-temporal VEGF and PDGF delivery patterns blood vessel formation and maturation. *Pharm. Res.* **24,** 258–264 (2007).

29. Hur, J. *et al.* Characterization of two types of endothelial progenitor cells and their different contributions to neovasculogenesis. *Arterioscler. Thromb. Vasc. Biol.* **24,** 288–93 (2004).

30. Sieveking, D. P., Buckle, A., Celermajer, D. S. & Ng, M. K. C. Strikingly different angiogenic properties of endothelial progenitor cell subpopulations: insights from a novel human angiogenesis assay. *J. Am. Coll. Cardiol.* **51,** 660–8 (2008).

31. Ziegelhoeffer, T. *et al.* Bone marrow-derived cells do not incorporate into the adult growing vasculature. *Circ. Res.* **94,** 230–8 (2004).

32. Case, J. *et al.* Human CD34+AC133+VEGFR-2+ cells are not endothelial progenitor cells but distinct, primitive hematopoietic progenitors. *Exp. Hematol.* **35,** 1109–18 (2007).

33. Melero-Martin, J. M. *et al.* In vivo vasculogenic potential of human blood-derived endothelial progenitor cells. *Blood* **109,** 4761–8 (2007).

34. Salcedo, R. *et al.* Vascular endothelial growth factor and basic fibroblast growth factor induce expression of CXCR4 on human endothelial cells: In vivo neovascularization induced by stromal-derived factor-1alpha. *Am. J. Pathol.* **154,** 1125–1135 (1999).

35. Azab, A. K. *et al.* RhoA and Rac1 GTPases play major and differential roles in stromal cell–derived factor-1–induced cell adhesion and chemotaxis in multiple myeloma. *Blood* **114,** 619–629 (2009).

36. Li, A., Dubey, S., Varney, M. L., Dave, B. J. & Singh, R. K. IL-8 directly enhanced endothelial cell survival, proliferation, and matrix metalloproteinases production and regulated angiogenesis. *J. Immunol.* **170,** 3369–76 (2003).

37. Nucera, S., Biziato, D. & De Palma, M. The interplay between macrophages and angiogenesis in development, tissue injury and regeneration. *Int. J. Dev. Biol.* **55,** 495–503 (2011).

38. Chavakis, E., Urbich, C. & Dimmeler, S. Homing and engraftment of progenitor cells: a prerequisite for cell therapy. *J. Mol. Cell. Cardiol.* **45,** 514–22 (2008).

39. Vacharathit, V., Silva, E. a & Mooney, D. J. Viability and functionality of cells delivered from peptide conjugated scaffolds. *Biomaterials* **32,** 3721–8 (2011).

40. Wu, X. *et al.* Tissue-engineered microvessels on three-dimensional biodegradable scaffolds using human endothelial progenitor cells. *Am. J. Physiol. Heart Circ. Physiol.* **287,** H480–7 (2004).

41. Melero-Martin, J. M. *et al.* Engineering robust and functional vascular networks in vivo with human adult and cord blood-derived progenitor cells. *Circ. Res.* **103,** 194–202 (2008).

42. Kang, K.-T., Allen, P. & Bischoff, J. Bioengineered human vascular networks transplanted into secondary mice reconnect with the host vasculature and re-establish perfusion. *Blood* **118,** 6718–21 (2011).

CHAPTER 4:

Major Conclusions, Implications and Future Directions

4.1 Major Conclusions

Endothelial progenitors have shown therapeutic potential as a treatment for ischemic cardiovascular diseases, but with limited efficacy likely because too few cells reach the tissue of interest[1,2]. A biomaterial system was used here to create a tissue microenvironment capable of enhancing the recruitment of endothelial progenitors and encouraging their contribution to neovascularization. Specifically, SDF and VEGF, two factors that play key roles in modulating progenitor cell trafficking[3], were delivered from alginate hydrogels and were tested for therapeutic efficacy. This biomaterial system was used to investigate the hypothesis that local, sustained delivery of exogenous VEGF and SDF can enhance recruitment of endothelial progenitors to ischemic sites and also promote their contribution to new blood vessel growth. In addition, all studies were performed with both OECs and CACs in order to compare the specific roles and therapeutic potential of these two cell populations.

The first aim of this thesis focused on the mechanism by which cells are recruited to target tissues. *In vitro* assays were used to dissect the influence of VEGF and SDF on both adhesion and migration, two key steps in the homing process. SDF increased adhesion of both OECs and CACs to endothelial cells in static and flow-based assays. CACs were more responsive than OECs to changes in the inflammatory state of endothelial cells and to SDF exposure, likely due to higher β2 expression. In contrast to SDF, VEGF is not implicated in the modulation of adhesion. SDF enhanced migration of CACs, while the combination of VEGF and SDF increased migration of OECs to a greater extent than either factor alone. The ability of VEGF and SDF to enhance adhesion and migration of OECs and CACs *in vitro* suggested that these factors may have a substantial impact on recruitment *in vivo*. VEGF and SDF released from

alginate hydrogels in target tissues significantly increased recruitment of OECs and CACs *in vivo* both in ischemic and non-ischemic muscle tissue. In close agreement with *in vitro* trends, CACs accumulated to a greater extent than OECs. VEGF and SDF delivery exhibited a minimal impact on inflammatory cell infiltration, affecting only macrophages, but not the other cell types tested. Interestingly, systemic injection of CACs led to significant infiltration of inflammatory cells at the gel injection site in non-ischemic mouse hind-limbs. Overall, the work presented in Aim 1 established that VEGF and SDF release from alginate hydrogels constitutes an effective strategy to increase endothelial progenitor recruitment to target tissues, and that CACs are recruited more efficiently than OECs.

The second aim of this thesis concentrated on the roles of OECs and CACs in contributing to new blood vessel growth and the effects of VEGF and SDF on each cell types' role. In a three-dimensional *in vitro* sprouting model, OECs directly participated in sprout formation, while CACs could not. In addition, OECs demonstrated a greater potential to initiate sprouts when placed directly in competition with mature endothelial cells. The combination of VEGF and SDF dramatically increased sprouting by OECs, likely by reducing sprout initiation time and improving sprout maintenance. OECs and CACs enhanced sprout formation by mature endothelial cells through secretion of angiogenic factors that acted in a paracrine manner. On a per cell basis, factors secreted by CACs were more potent than those from OECs. These *in vitro* assays confirmed that OECs and CACs play different roles in contributing to the formation of new blood vessels. Finally, homing of CACs to ischemic limbs containing VEGF and SDF alginate gels improved perfusion recovery better than accumulated OECs or gels alone in an *in vivo* mouse model. The results presented in Aim 2 clearly demonstrated that OECs can take part in angiogenic sprout formation, and this process was significantly enhanced by VEGF and SDF. In contrast, CACs were limited to secreting paracrine factors that encourage sprout formation by endothelial cells. *In vivo*, CACs were more therapeutically effective than OECs in these studies.

The results of the experiments performed in this thesis comprehensively show that local delivery of exogenous VEGF and SDF from an alginate hydrogel enhanced recruitment of endothelial progenitors to

ischemic tissue, which allowed significant contribution to perfusion recovery by CACs. VEGF and SDF promoted sprout formation by OECs *in vitro*, but systemically delivered OECs that accumulated in the ischemic tissue did not improve overall blood perfusion.

4.2 Implications and Future Directions

The results of these studies emphasize the differing roles of OECs and CACs, and suggest that their use therapeutically should differ as well. These findings may also guide the investigation of new methods to enhance recruitment of circulating cells for improving cell therapy outcomes in general, as well as the development of strategies to augment endothelial progenitor contribution to neovascularization.

Circulating Angiogenic Cells

CACs were highly responsive to SDF, as demonstrated by enhanced recruitment *in vivo*, and were therapeutically effective at restoring blood perfusion to ischemic tissue. Together, these results emphasize the clinical potential of using CACs as a traditional, systemically delivered cell therapy in combination with a biomaterial system designed to increase their targeting efficiency. These results also establish SDF as a promising candidate for delivery from a biomaterial system clinically, particularly considering SDF's well-recognized role in cell trafficking[3].

Important questions still remain, related to the precise mechanism by which controlled release of VEGF and SDF enhanced recruitment of CACs to target tissues and led to improved therapeutic recovery as compared to gels alone. Only SDF is implicated in modulating adhesion, and CACs also only showed increased migration towards SDF, while VEGF had no effect. Therefore, it is possible that VEGF may not have an effect on CAC recruitment *in vivo*, but SDF-only and VEGF-only gels would need to be studied to dissect the roles of each individual factor. If SDF-only gels recruit an equal number of CACs as the VEGF+SDF gels, then they may also show similar regenerative capabilities as the combination gels, *if*

recovery is highly dependent on the number of CACs present. Alternatively, the VEGF may be essential for inducing sprouting by endogenous endothelial cells and for creating a pro-angiogenic microenvironment. A further possibility is that the paracrine factors secreted by a small number of CACs are potent enough to exhibit a therapeutic effect, even without SDF to increase their recruitment or VEGF to stimulate endothelial cells.

A major focus of future work should be determining the mechanism by which CACs achieve their therapeutic effect. The results presented in Aim 2 made clear that CACs do not directly participate in blood vessel growth, but they exhibit two behaviors that both may enhance regeneration. CAC localization leads to significant infiltration of various other types of inflammatory cells, which could subsequently contribute to vessel growth[4]. CACs also secrete a panel of potent angiogenic factors that can act on mature endothelial cells to induce sprout formation. Examining the extent to which of these mechanisms is responsible for the improved recovery from ischemia by CACs should be a priority for future studies. First, it should be determined if CACs can modulate the infiltration of inflammatory cells within *ischemic* tissue, since a large number of these cells are inherently recruited after induction of ischemia. If the presence of CACs alters the profile of recruited cells, then those specific cells could be delivered *without CACs* after inducing ischemia to assess whether that cell population exerts a therapeutic effect. Macrophages are one example of possible cells recruited by CACs that may mediate improved healing[4]. This could be tested by delivering macrophages directly to the ischemic hind-limb to determine if the increased presence of these cells improves blood vessel regeneration. Second, the cytokines and growth factors secreted by CACs likely act both on endothelial cells *and* stimulate inflammatory cell recruitment. It is also possible that physical interactions between CACs and other accessory cells are essential for therapeutic efficacy. The paracrine and physical effects of the CACs on both perfusion recovery and inflammatory cell infiltration could be discriminated by comparing CAC delivery to delivery of conditioned media from CACs. Specifically, conditioned media from CACs could be collected, concentrated and then delivered into hind-limb muscle, possibly within an alginate hydrogel to

provide sustained release, in order to determine if these cytokines alone induce infiltration of inflammatory cells (on a short time scale) and/or improve perfusion recovery in an ischemia model (on a long time scale). Results from this set of experiments would clarify how the presence of CACs led to a beneficial therapeutic effect.

Independent of the mechanism by which CACs contribute to regeneration, their therapeutic efficacy could likely be improved by further increasing the number of CACs within ischemic tissue. One method to accomplish this would be to increase the number of CACs in culture that can be re-delivered. The culture methods employed to isolate CACs result in a population of cells with almost non-existent proliferation potential[5]. As CACs are a type of monocyte[6], it may be possible to adapt alternative culture methods that promote proliferation while maintaining the beneficial properties of CACs. It is likely that some period of cell culture is necessary to obtain the CAC population, because injecting freshly isolated CD14+ monocytes does not yield a sufficient therapeutic effect[7]. Further, the field as a whole would significantly benefit from a better understanding of the general biology of CACs (*e.g.* determining their origin, their relationship to and differentiation from myeloid precursors, and standardized cell markers or a genetic profile definition for these cells). This could partially be accomplished through direct comparisons with the better understood behaviors of different monocyte populations (*e.g.* Classical/Inflammatory $CD14^{++}/CD16^{-}$ monocytes, Non-Classical/Resident/Patrolling $CD14^{+}/CD16^{++}$ monocytes, or Intermediate $CD14^{++}/CD16^{+}$ monocytes)[8–11]. (See Appendix F for CD14 and CD16 co-staining of CACs.) Inflammatory monocytes and patrolling monocytes, for example, infiltrate acutely injured ischemic tissue with different temporal profiles. Following myocardial infarction, inflammatory monocytes are first recruited in high numbers in a CCR2-dependent manner after being released from both the bone marrow and spleen[9]. These cells secrete the pro-inflammatory cytokine TNFα. The heart muscle tissue then transitions to being populated by the patrolling monocytes, which are recruited in a CX_3CR1-dependent manner, and exert a pro-angiogenic function by secreting VEGF[9]. Monocytes may also give rise to Macrophages and Dendritic Cells that can participate in tissue repair[12,13]. A better understanding of the

relationship of CACs to these monocyte populations may reveal that only a specific subset of the CAC population exhibits a strong regenerative potential, which could translate to a more efficient therapeutic use of these cells.

A second method to increase the number of CACs in the target tissue could be achieved by further enhancing their recruitment or by delivering the cells directly into the tissue, either by bolus injection or within a biomaterial system. Biomaterials may be especially useful because of the beneficial effects of delivering cells within a protected and controlled environment. The design of a biomaterial system should account for the specific mechanism by which CACs contribute to new vasculature. For example, if paracrine secretion of factors is most important, then the cells should be delivered in a material that easily allows diffusion of these factors to the surrounding environment. On the other hand, if CACs need to be in close proximity or physically interact with sprouting endothelial cells, then the biomaterial should encourage deployment of the cells beyond its boundaries[14]. As discussed above, the mechanism of CAC contribution to new vessel growth is still unknown.

Traditional cell therapies that employ systemic delivery eventually may not be needed if it becomes possible to recruit endogenous CACs directly out of the circulation. For this reason, a thorough understanding of how to enhance targeting and how to selectively recruit subsets of CACs will prove valuable for eventual clinical translation. To this end, a careful, quantitative study of the specific concentrations and kinds of gradients that effectively induce recruitment may be beneficial for designing a more effective material-based therapy. Preliminary studies were initiated using a dual-channel microfluidic device that mimics the vascular and extracellular tissue compartments[15]. This device was capable of presenting SDF from the extracellular compartment to progenitor cells flowing through the vascular compartment (See Appendix C). This device allows investigation of the effects of chemokine exposure on both adhesion and migration of endothelial progenitors, thereby creating a physiologically relevant model of the complete recruitment process. Hopefully, when an ‘endothelial progenitor cell’ (CACs, OECs, or a subset) can be identified from the circulation by surface markers, the information

gathered about effective chemokine gradients using these devices could be employed to recruit cells directly.

Outgrowth Endothelial Cells

In vitro studies demonstrated that OECs exhibit a superior potential to directly contribute to neovascularization compared to mature endothelial cells, but they showed minimal recruitment *in vivo* and an overall insignificant therapeutic effect. OECs were likely not deployed *in vivo* in a manner that permitted a therapeutic benefit, since direct delivery of OECs within alginate hydrogels that were designed to release the cells within the tissue of interest led to enhanced perfusion[14]. These results suggest that OECs are better suited to local delivery methods using biomaterials to control the microenvironment.

OECs have also been shown to form networks of blood vessels in three-dimensional scaffolds, which could be adapted for the treatment of ischemic diseases[16,17]. These *ex vivo* formed networks anastomose with host vessels upon implantation[16,18]. Investigations using these vessel networks are most often focused on tissue engineering applications, where blood flow and oxygen delivery are essential to the formation of any tissue with a diameter greater than ~200μm (based on the diffusion limit of oxygen)[17,19,20]. (See Appendix G for a comparison of OEC and HUVEC network forming potential in a fibrin-PLGA scaffold.) The local deployment of a healthy vascular network could possibly alleviate ischemic damage due to insufficient blood flow by replacing the dysfunctional vessels. For example, preformed networks of vessels made of OECs could be implanted in the muscle tissue in a mouse model of hind-limb ischemia in order to determine the therapeutic potential. The normal recovery process includes angiogenic sprouting by resident endothelial cells to form a capillary network, which then remodels over time to regenerate larger vessels[21]. Implantation of a pre-formed network may allow the healing tissue to effectively skip the sprouting phase and directly go to the remodeling phase. Additionally, incorporating VEGF into these vascular networks may speed the rate at which the implanted vessels anastomose with host vessels. Overall, the recruitment strategies employed in this thesis did not yield beneficial therapeutic outcomes

with OECs, but OECs have a great potential to contribute to new vessel formation if they are delivered within a proper, supporting microenvironment.

The effect of VEGF and SDF on OEC sprouting was very dramatic and likely results from decreased sprout initiation time and better sprout maintenance, but the molecular mechanisms by which these behaviors are achieved remain undefined. It would be interesting to understand the full dynamics (*e.g.* by completing and analyzing 72 hour time lapse experiments) and the molecular mechanisms involved in this process (*e.g*. whether it is caused by maintenance of CXCR4 expression, increased signaling in pathways related to migration, or some other mechanism)[22–26]. Further, the combination of VEGF and SDF may also prove beneficial to speed the formation or maintain the growth of the aforementioned *ex vivo* vessel networks.

Finally, the overall low recruitment efficiency in these studies, although enhanced by VEGF and SDF, was still less than 1%, which is typical for cell therapies. The low number cells reaching target tissues through systemic delivery is an inherent problem and may be an insurmountable challenge to their clinical utility. It is likely that too many cells simply become trapped in capillaries throughout the entire body, especially in highly vascularized tissues such as the lungs and liver. The use of biomaterials for cell delivery currently may be the best strategy for maintaining viability and controlling localization within the tissue of interest, especially since many attractive materials exist and have been validated in pre-clinical and clinical studies[27]. Studying the recruitment and trafficking is valuable though, because incremental improvements could have significant, and possibly multiplicative, therapeutic effects (*e.g.* for each CAC recruited, hundreds of inflammatory cells are recruited (Chapter 2, Figure 2.8) that *may* subsequently enhance healing). It may also be possible that only certain subsets of CACs or OECs are sensitive to recruitment signals, and/or that the culture methods employed to isolate these cells alter their ability to respond compared to the circulating cell types that give rise to either CACs or OECs. Again, if these cell types eventually can be identified based on specific surface marker expression, then they could be directly recruited from the circulation without the need for an isolation procedure.

In summary, OECs and CACs both demonstrated the capacity to contribute to new blood vessel formation, and should be investigated further to determine the best method to deploy these cells in order to yield the greatest therapeutic benefit.

4.3 References

1. Möbius-Winkler, S., Höllriegel, R., Schuler, G. & Adams, V. Endothelial progenitor cells: implications for cardiovascular disease. *Cytom. Part A J. Int. Soc. Anal. Cytol.* **75,** 25–37 (2009).

2. Raval, Z. & Losordo, D. W. Cell therapy of peripheral arterial disease: from experimental findings to clinical trials. *Circ. Res.* **112,** 1288–302 (2013).

3. Caiado, F. & Dias, S. Endothelial progenitor cells and integrins: adhesive needs. *Fibrogenesis Tissue Repair* **5,** 4 (2012).

4. Nucera, S., Biziato, D. & De Palma, M. The interplay between macrophages and angiogenesis in development, tissue injury and regeneration. *Int. J. Dev. Biol.* **55,** 495–503 (2011).

5. Yoder, M. C. *et al.* Redefining endothelial progenitor cells via clonal analysis and hematopoietic stem/progenitor cell principals. *Blood* **109,** 1801–1809 (2007).

6. Rehman, J. Peripheral Blood "Endothelial Progenitor Cells" Are Derived From Monocyte/Macrophages and Secrete Angiogenic Growth Factors. *Circulation* **107,** 1164–1169 (2003).

7. Urbich, C. *et al.* Relevance of monocytic features for neovascularization capacity of circulating endothelial progenitor cells. *Circulation* **108,** 2511–6 (2003).

8. Auffray, C. *et al.* Monitoring of blood vessels and tissues by a population of monocytes with patrolling behavior. *Science (80-.).* **317,** 666–70 (2007).

9. Nahrendorf, M. *et al.* The healing myocardium sequentially mobilizes two monocyte subsets with divergent and complementary functions. *J. Exp. Med.* **204,** 3037–47 (2007).

10. Favre, J., Terborg, N. & Horrevoets, A. J. G. The diverse identity of angiogenic monocytes. *Eur. J. Clin. Invest.* **43,** 100–7 (2013).

11. Fernandez Pujol, B. *et al.* Endothelial-like cells derived from human CD14 positive monocytes. *Differentiation.* **65,** 287–300 (2000).

12. Ziegler-Heitbrock, L. The CD14+ CD16+ blood monocytes: their role in infection and inflammation. *J. Leukoc. Biol.* **81,** 584–92 (2007).

13. Shi, C. & Pamer, E. G. Monocyte recruitment during infection and inflammation. *Nat. Rev. Immunol.* **11,** 762–74 (2011).

14. Silva, E. a, Kim, E.-S., Kong, H. J. & Mooney, D. J. Material-based deployment enhances efficacy of endothelial progenitor cells. *PNAS* **105,** 14347–14352 (2008).

15. Huh, D. *et al.* Reconstituting organ-level lung functions on a chip. *Science (80-.).* **328,** 1662–1668 (2010).

16. Melero-Martin, J. M. *et al.* In vivo vasculogenic potential of human blood-derived endothelial progenitor cells. *Blood* **109,** 4761–8 (2007).

17. Phelps, E. a, Landázuri, N., Thulé, P. M., Taylor, W. R. & García, A. J. Bioartificial matrices for therapeutic vascularization. *Proc. Natl. Acad. Sci. U. S. A.* **107,** 3323–8 (2010).

18. Kang, K.-T., Allen, P. & Bischoff, J. Bioengineered human vascular networks transplanted into secondary mice reconnect with the host vasculature and re-establish perfusion. *Blood* **118,** 6718–21 (2011).

19. Bae, H. *et al.* Building vascular networks. *Sci. Transl. Med.* **4,** 160ps23 (2012).

20. Nugent, H. M. & Edelman, E. R. Tissue engineering therapy for cardiovascular disease. *Circ. Res.* **92,** 1068–78 (2003).

21. Carmeliet, P. Mechanisms of angiogenesis and arteriogenesis. *Nat. Med.* **6,** 389–395 (2000).

22. Salcedo, R. *et al.* Vascular endothelial growth factor and basic fibroblast growth factor induce expression of CXCR4 on human endothelial cells: In vivo neovascularization induced by stromal-derived factor-1alpha. *Am. J. Pathol.* **154,** 1125–1135 (1999).

23. Salvucci, O. *et al.* Regulation of endothelial cell branching morphogenesis by endogenous chemokine stromal-derived factor-1. *Blood* **99,** 2703–2711 (2002).

24. Salcedo, R. & Oppenheim, J. J. Role of chemokines in angiogenesis: CXCL12/SDF-1 and CXCR4 interaction, a key regulator of endothelial cell responses. *Microcirculation* **10,** 359–370 (2003).

25. Shireman, P. K. The chemokine system in arteriogenesis and hind limb ischemia. *J. Vasc. Surg.* **45,** A48–56 (2007).

26. Azab, A. K. *et al.* RhoA and Rac1 GTPases play major and differential roles in stromal cell–derived factor-1–induced cell adhesion and chemotaxis in multiple myeloma. *Blood* **114,** 619–629 (2009).

27. Huebsch, N. & Mooney, D. J. Inspiration and application in the evolution of biomaterials. *Nature* **462,** 426–32 (2009).

APPENDIX A:

Chapter 2 Supplemental Figures and Tables

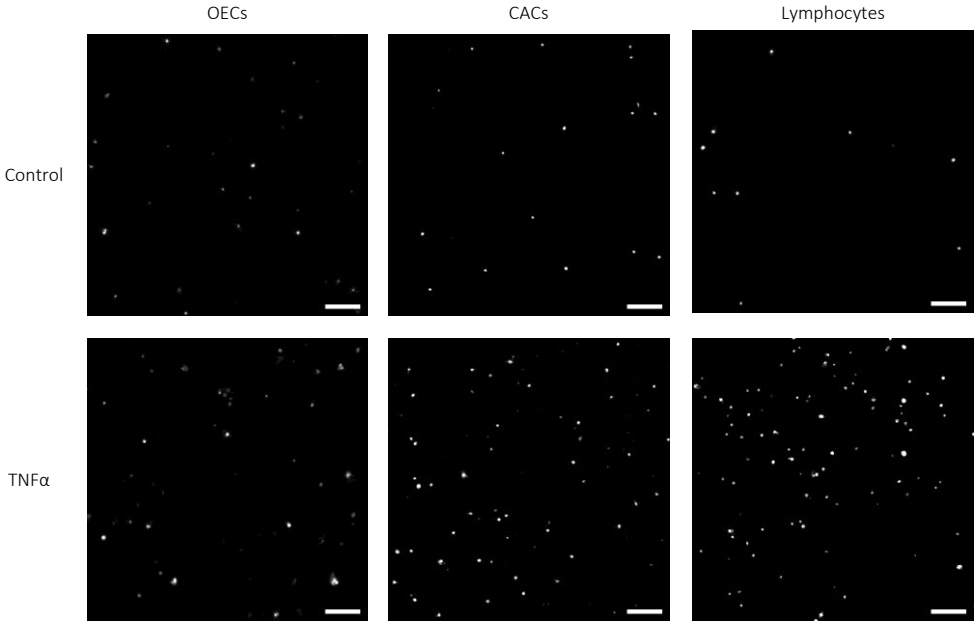

Supplemental Figure 2.1. Photomicrographs of OECs, CACs and Lymphocytes adhered to HMVECs. Low magnification images were used to quantify cell number adhered per area. Scale bars are 200µm.

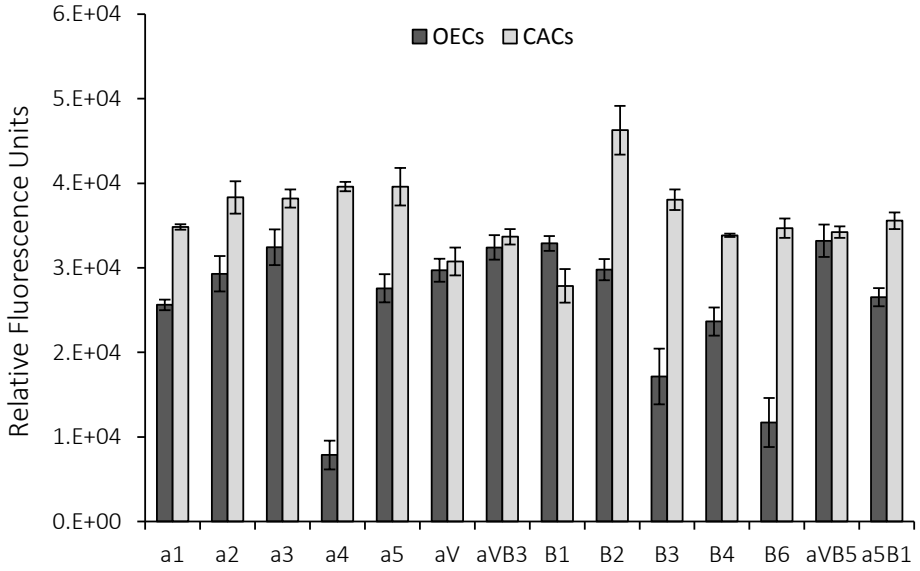

Supplemental Figure 2.2. Relative integrin expression of OECs and CACs. An antibody adhesion-based array was used to assess integrin expression. Data are scaled to negative controls and presented as Mean ± SEM from three separate experiments.

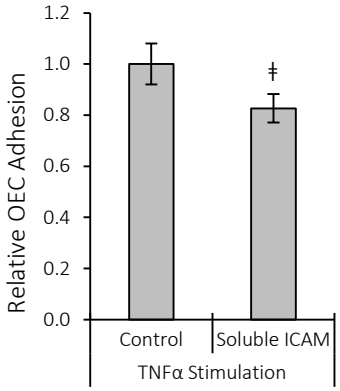

Supplemental Figure 2.3. OEC adhesion to HMVECs with recombinant human soluble ICAM protein added. Soluble ICAM reduces adhesion to an equivalent level as the addition of a β2 antibody. Mean ± SEM.

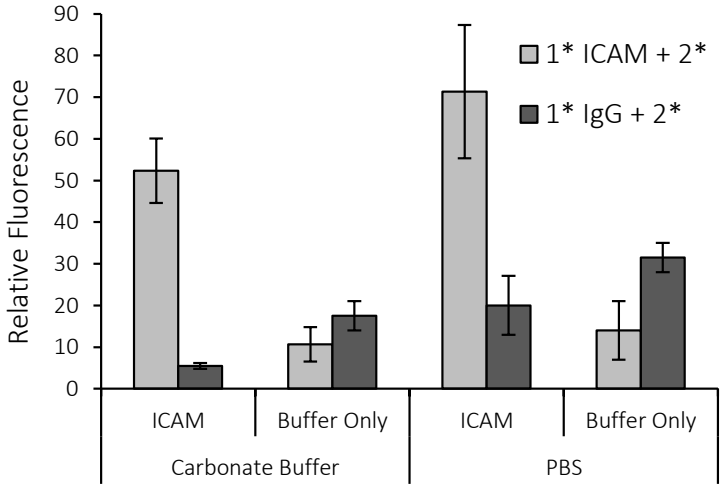

Supplemental Figure 2.4. ICAM surface coating method verification. ICAM was coated on the surface in Carbonate Buffer (pH=9.5) or PBS (pH=7.4) overnight at 4^{o}C. A primary ICAM antibody (or IgG control) was used to detect ICAM on the surface, with an Alexa-fluor 488 secondary antibody used to generate signal. Mean ± SD.

A

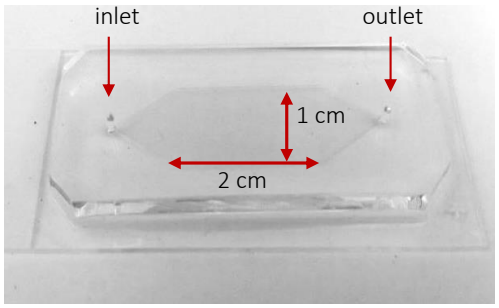

B

Experimental Parameters	
Channel Height (h)	80µm
Flow Rate (Q)	10 µl/min
Average Flow Velocity	~200 µm/sec
Shear Stress ($T = 6\mu Q / h^2 w$)	~0.1 dyn/cm^2

C

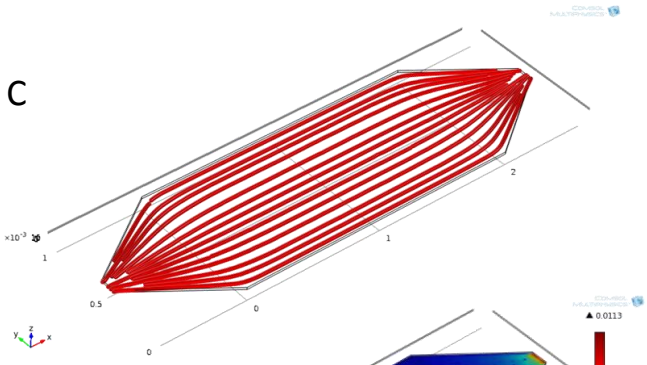

D

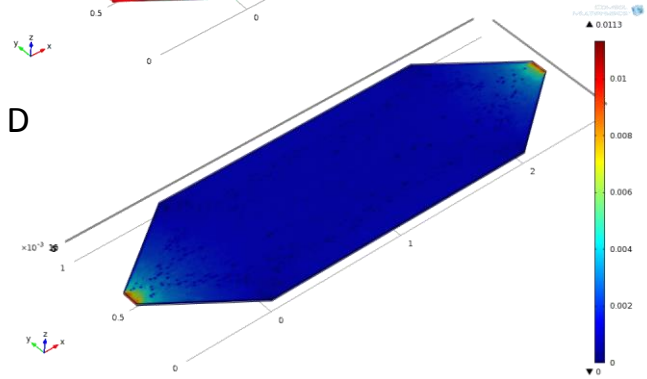

E

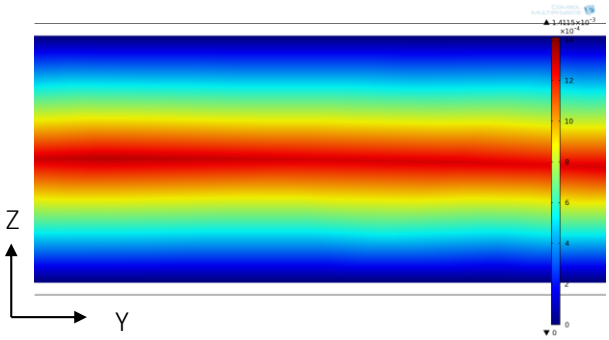

Supplemental Figure 2.5. Parallel flow channel design and characterization. A) Photo of PDMS flow channel mounted on a glass slide. B) Table of experimental parameters. C-E) A COMSOL model was generated to verify channel design and flow properties, including streamlines (C), velocity profile in the XY plane (D), and parabolic velocity profile in ZY plane (flow is in X-direction, E). Units in D and E legends are m/sec.

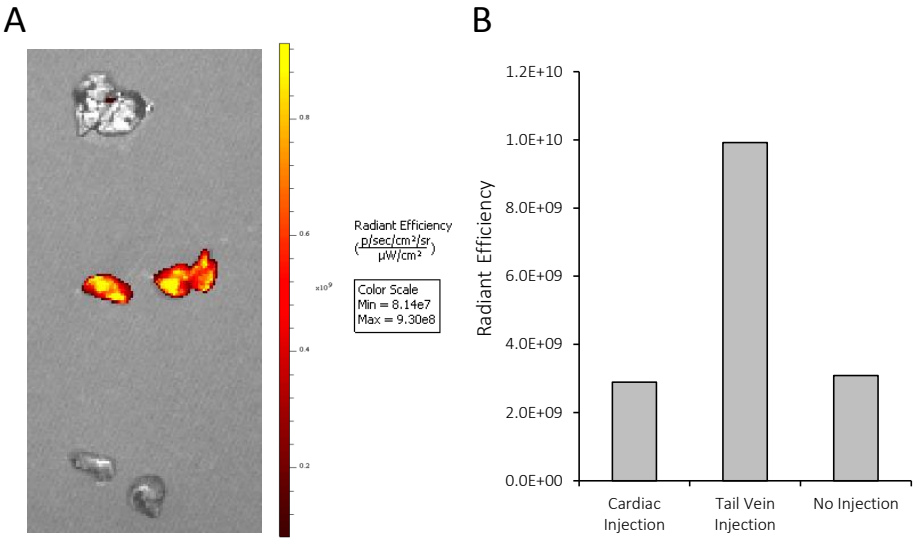

Supplemental Figure 2.6. Accumulation of fluorescent OECs in the lungs for different routes of systemic administration. A) IVIS image of lungs after cardiac injection (top), tail vein injection (middle), or no injection (bottom) of DiD-labeled OECs. B) Quantification of fluorescence shown in (A).

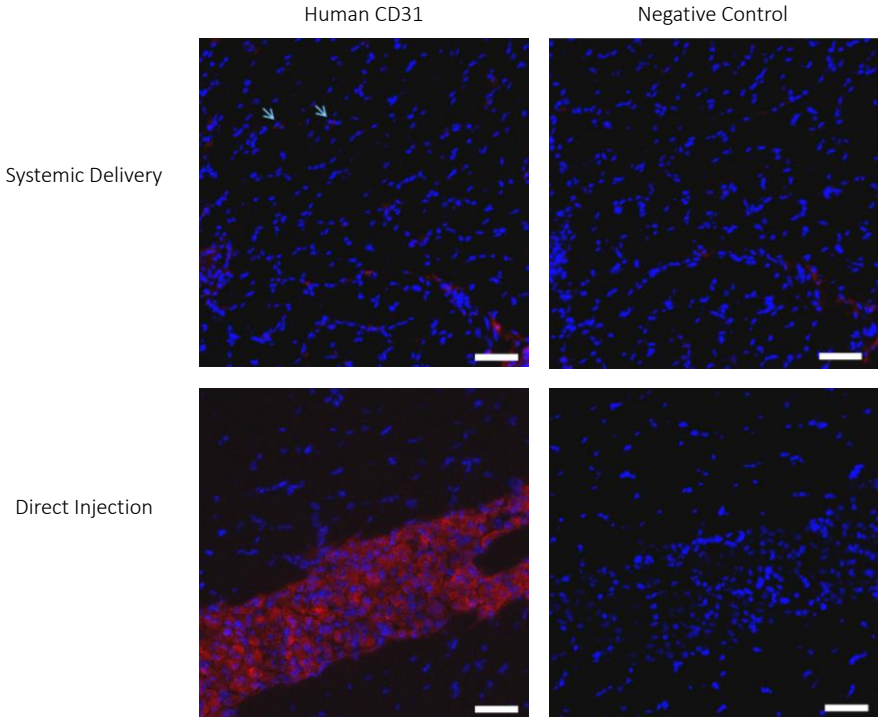

Supplemental Figure 2.7. Detection of OECs by immunohistochemistry on mouse muscle sections. A-B) Muscle sections were stained for OECs after systemic delivery via a cardiac injection into mice which had undergone ischemia surgery (A, arrows indicate identified OECs), or after direct injection of OECs into the hind-limb muscle tissue (B). A primary Human CD31 antibody was used for OEC detection, with an Alexa-fluor 647 fluorescent secondary used for visualization. Negative controls were with secondary antibody only. Scale bars are 50µm.

Supplemental Table 2.1. 3-way ANOVA table for main effect analysis of Ischemia, Cell type, and VEGF+SDF treatment.

Tests of Between-Subjects Effects

	Source	Type III Sum of Squares	Degrees of Freedom	Mean Square	F Statistic	Significance (P)
	Corrected Model	3.159E-5[a]	3	1.053E-05	4.220	.012
	Intercept	.000	1	.000	61.527	.000
Factor	Ischemia	7.041E-06	1	7.041E-06	2.822	.102
	Cell Type ‡	1.432E-05	1	1.432E-05	5.737	.022
	Treatment (VEGF+SDF or Control) ‡	1.023E-05	1	1.023E-05	4.101	.050
	Error	8.984E-05	36	2.495E-06		
	Total	.000	40			
	Corrected Total	.000	39			
	F statistic for df(numerator)=1 and df(denomemator) = 39; α = 0.05				4.091	

a. R Squared = .260 (Adjusted R Squared = .199)
‡ Statistically Significant for α = 0.05

APPENDIX B:

Chapter 3 Supplemental Figures

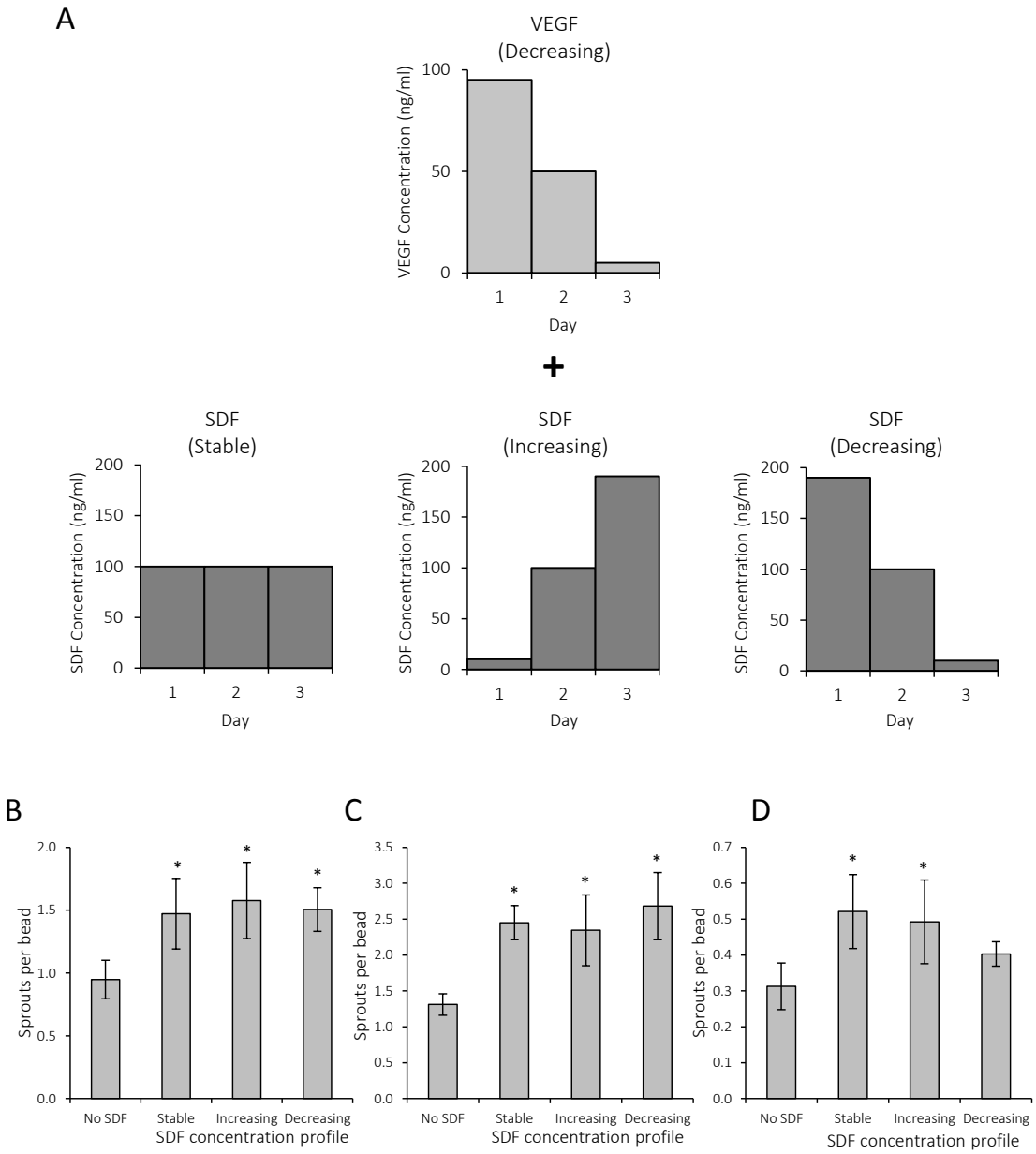

Supplemental Figure 3.1. Effect of temporal presentation of SDF in combination with a decreasing VEGF profile. A) Schematic of VEGF and SDF concentrations applied to create stable, increasing or decreasing profiles. B-D) Quantification of the number of sprouts per bead formed by OECs (B), HUVECs (C), and HMVECs (D) at 72 hours. Mean ± SD, n=4. * $p < 0.05$.

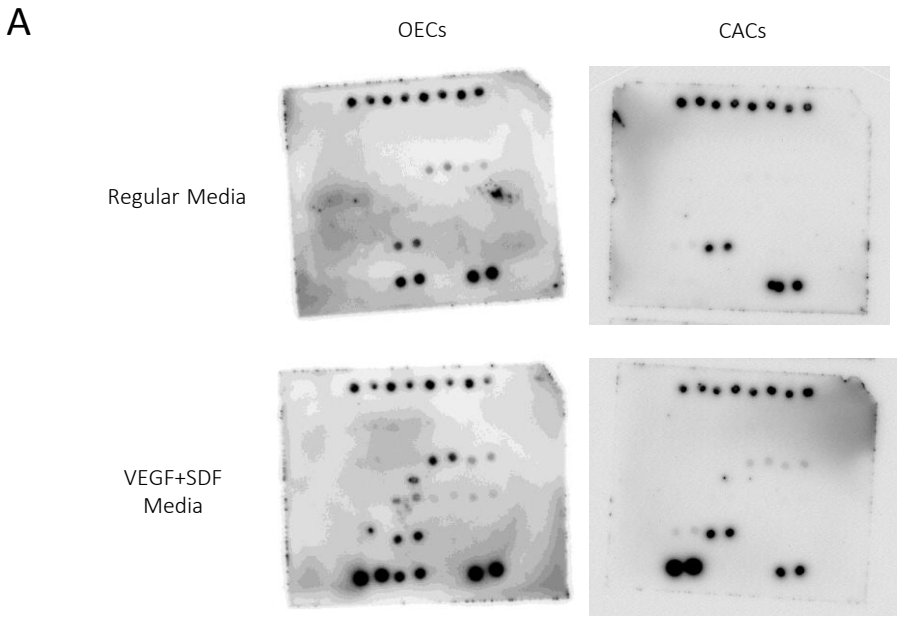

	1	2	3	4	5	6	7	8
A	POS	POS	POS	POS	POS	POS	POS	POS
B	Ang	Ang	IL-1α	IL-1α	FGFα	FGFα	IFNγ	IFNγ
C	G-CSF	G-CSF	IL-1β	IL-1β	FGFβ	FGFβ	IL-12	IL-12
D	HGF	HGF	IL-6	IL-6	TNFα	TNFα	IP-10	IP-10
E	Leptin	Leptin	IL-8	IL-8	TGFα	TGFα	TIMP-1	TIMP-1
F	VEGF	VEGF	PlGF	PlGF	NEG	NEG	TIMP-2	TIMP-2

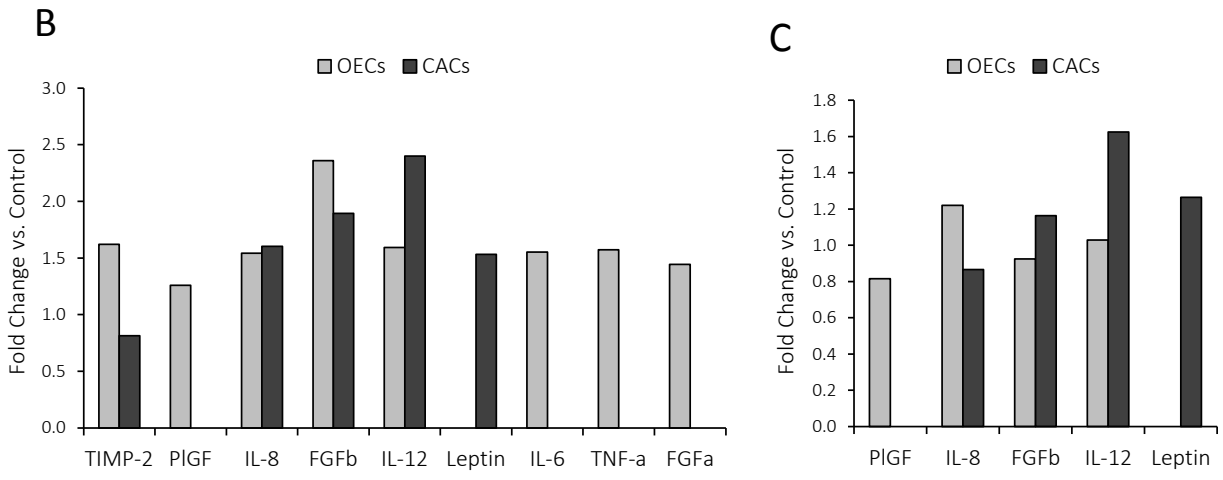

Supplemental Figure 3.2. Changes in secretion of factors from OECs and CACs with VEGF+SDF exposure. A) Chemiluminescent images of array membranes used for analysis of secreted factors from OECs and CACs with cytokine location map shown below. B) Relative change in secretion of factors when VEGF+SDF is applied to OECs or CACs, as measured by the angiogenesis array shown in A. C) Relative change in secretion of factors when VEGF+SDF is applied to OECs or CACs, as measured by ELISA.

APPENDIX C:

Dual Compartment Microfluidic Device for Studying Endothelial Progenitor Adhesion and Migration

Purpose of Studies

The objective was to develop a microfluidic device that could be used to quantitatively study endothelial progenitor recruitment in a model system that mimicked relevant physiological characteristics[1]. Specifically, the device had two channels, representing a vascular compartment and an extracellular compartment; these were separated by a membrane on which endothelial cells were grown. The device was used to test the effect of SDF presentation from the extracellular compartment on the adhesion and migration of endothelial progenitors flowing through the vascular compartment. Because the flow in a microfluidic device is laminar, diffusion limits molecular transport from one compartment to the other, in addition to the barrier function imposed by the porous membrane and endothelial monolayer[2]. A diffusion-based flow regime was quantitatively modeled, and transport of SDF through the endothelial layer was then experimentally measured. This model could then be adapted to understand the concentrations and types of gradients that are necessary to induce endothelial progenitor adhesion to mature endothelial cells as well as migration through the monolayer.

Experimental Setup

Two channel microfluidic devices were fabricated as shown in Figure C1. Endothelial cells were grown on top of the porous membrane separating the two channels. SDF was then added to the media and flowed through the bottom channel and was re-collected after exiting the top and bottom channels so that the concentration could be measured. Outgrowth Endothelial Cells (OECs) were flowed through the top channel (vascular compartment) as SDF was presented from the bottom channel (extracellular

compartment) to test for increased adhesion to endothelial cells and to determine if SDF enhances migration through the monolayer. Last, a diffusion-based flow model of the microfluidic device was developed in COMSOL, and was used to predict the shape of the gradient formed by the experimentally-measured SDF concentration.

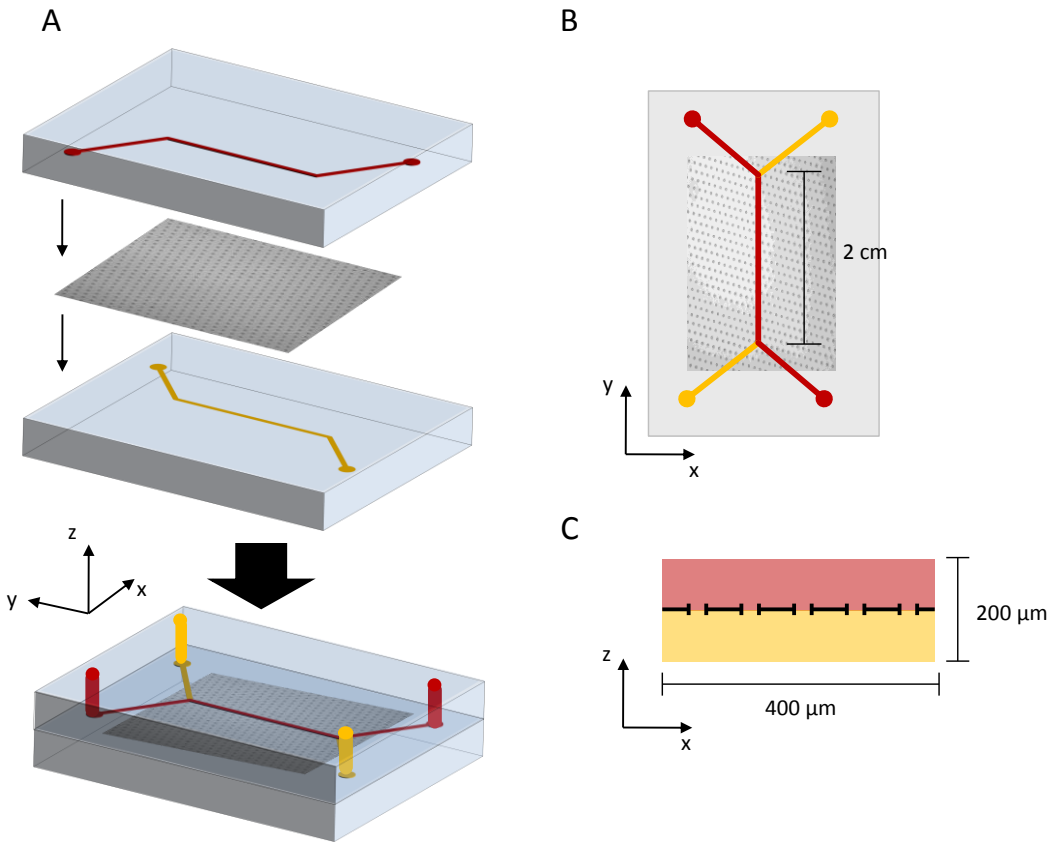

Figure C1. Fabrication of dual-compartment microfluidic device. A) Two PDMS channels separated by a 10µm thick spin-coated PDMS membrane with 10µm pores. Channels and membrane were permanently bonded together with following plasma treatment. B) Top view of device. C) View down the channels. Device design and fabrication was adapted from [1].

Results

Endothelial cells (HMVECs) were cultured on top of the membrane until confluent monolayers formed (Figure C2). Monolayer formation was verified prior to beginning SDF diffusion testing.

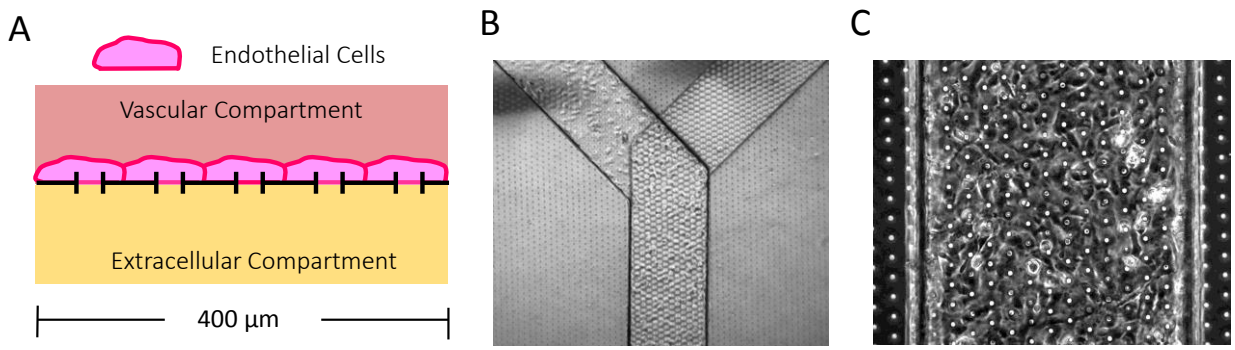

Figure C2. Microfluidic device with endothelial cell monolayers. A) Schematic of endothelial cells growing on the membrane. B) Low resolution image of endothelial cells in the top channel only. C) Confluent layer of endothelial cells.

COMSOL was used to create a quantitative model of the gradients of SDF produced by diffusion as it flows through the channel (Figure C3). No membrane was incorporated in this model. When SDF was allowed to diffuse across an endothelial monolayer, 9% of the total SDF delivered was transported into the vascular channel. The model predicted that diffusion would allow 27% of the total SDF delivered to cross into the opposite channel (Figure C3). The presence of the membrane and endothelial cells reduced the total SDF crossing the barrier by 1/3. The model was then used to predict the shape of the gradient when only 9% of the total SDF is transported to the opposite channel by diffusion alone (Figure C3).

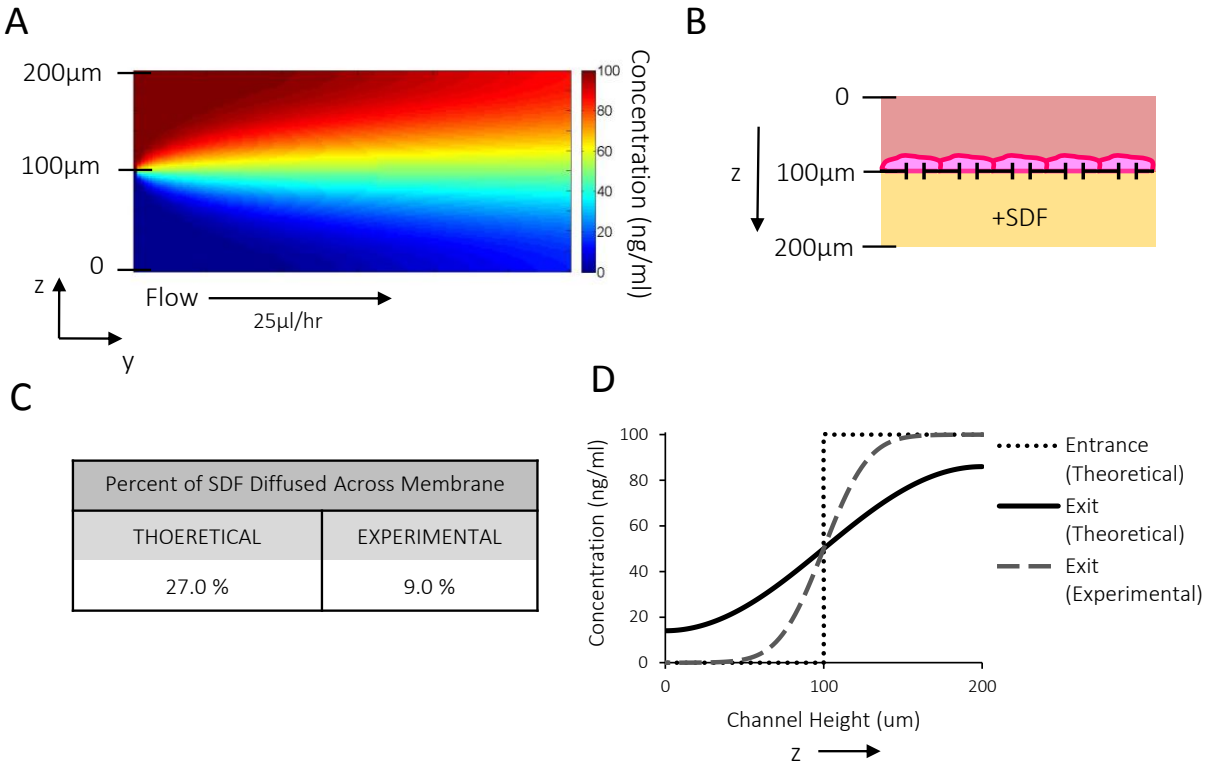

Figure C3. Changes in the concentration gradient of SDF down the length of the 2cm channel. A) Theoretical model of SDF concentration in the channel as media flows at 25µl/hr. Model is based on diffusion only. B) Schematic of experimental set up for measuring SDF transport from the extracellular compartment (bottom) to the vascular compartment (top). Note channel height labels are altered to match the model. C) Amount of SDF diffused into the vascular compartment of the total delivered. Theoretical amount is calculated from the COMSOL model, and experimental was measured using an ELISA. D) Concentration gradients of SDF at the entrance and exit of the microfluidic device. The experimental concentration gradient is determined using the model based on 9% of the total SDF crossing into the vascular compartment.

OECs were flowed through the vascular compartment as SDF was presented from the extracellular compartment. Videos were captured of this process to monitor OEC adhesion to the endothelial cells (data not shown). OECs adhered to endothelial cells were kept in culture for 24 hours following their administration (Figure C4).

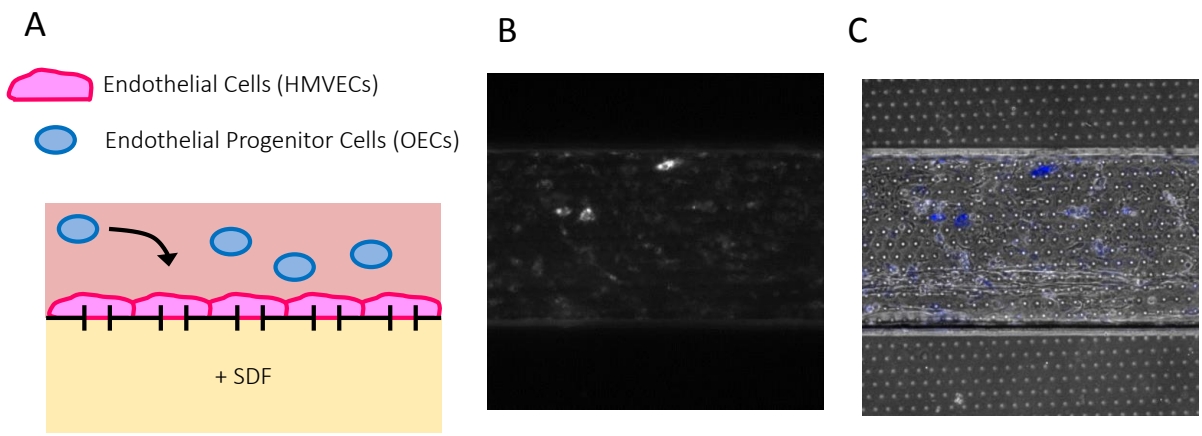

Figure C4. OEC adhesion to endothelial cells in the microfluidic device. A) Schematic of adhesion assay setup. SDF was presented from the bottom channel to OECs flowing through the top channel. B) Fluorescently-labeled OECs that remained adhered to the endothelial cells 24 hours after delivery. C) Overlay of phase contrast image of endothelial cells on the membrane and a fluorescent image of adhered OECs. Channel width is 400µm.

Summary of Outcomes and Possible Future Studies

A two-compartment microfluidic device was capable of presenting SDF from the extracellular compartment to endothelial progenitors flowing through the vascular compartment. The device also permitted adhesion of OECs and the possibility to observe their migration through the endothelial monolayer.

These studies were completed prior to collecting any of the data that is included in Chapters 2 or 3 of this thesis, and the mechanisms of adhesion by OECs and CACs were not yet understood. There are many possible future experiments that could be completed to develop a quantitative understanding of OEC and CAC responses to SDF exposure. First, a thorough characterization of the transport of SDF across the endothelial monolayer should be completed with multiple concentrations of SDF used. A permeability coefficient for this process could additionally be calculated[3]. This would allow the development of a more relevant model of the gradients of SDF that are formed in the device, and how the gradient likely changes between the entrance and exit of the device. With this understanding, adhesion assays could then be completed with this device. For example, if the density of adhesion events changes down the length of the

channel, this could indicate a preferential adhesion when exposed to the specific SDF gradient presented in that region. Migration events could also be spatially monitored, and locations of enhanced migration could be used as an indicator of gradients that may be effective for inducing recruitment. If cells demonstrate selectivity for specific gradients, this information could be translated to the development of a therapy for enhancing endothelial progenitor recruitment.

Acknowledgements

Dongeun (Dan) Huh was absolutely instrumental in the gathering these results. Dan and Mohammed Khan both taught me the fabrication methods used to construct these devices and the cell culture methods. Hyun Jung Kim generously donated his time for answering questions about specific experimental setups and endothelial permeability.

References

1. Huh, D. *et al.* Reconstituting organ-level lung functions on a chip. *Science* **328,** 1662–1668 (2010).

2. Beebe, D. J., Mensing, G. a & Walker, G. M. Physics and applications of microfluidics in biology. *Annu. Rev. Biomed. Eng.* **4,** 261–286 (2002).

3. Gao, J., Hugger, E. D., Beck-Westermeyer, M. S. & Borchardt, R. T. Estimating intestinal mucosal permeation of compounds using Caco-2 cell monolayers. *Curr. Protoc. Pharmacol.* **Chapter 7,** Unit 7.2 (2001).

APPENDIX D:

Systems to Study Cell Migration in Response to Chemotactic Gradients

Purpose of Studies

Endothelial progenitor migration is one of the key steps in the cell recruitment process. A better understanding of the types and magnitude of gradients of chemotactic factors that enhance cell migration could translate to improved recruitment-inducing biomaterials. Here two *in vitro* systems were employed to study endothelial progenitor migration in response to well-controlled gradients of SDF and in a 3D model replicating the extracellular matrix environment.

Experimental Setup

A PDMS-based, gradient-generating microfluidic device was used to monitor OEC migration in two dimensions. A gradient of SDF was introduced and OEC migration was monitored over time using time-lapse microscopy. Second, OECs and CACs were seeded into a 3D collagen matrix in the corner position of an L-shaped, PDMS mold. Collagen containing SDF or VEGF was placed in one arm of the mold, and collagen without growth factor was placed in the other arm as a control. Migration of cells through the matrix was monitored over time using time-lapse microscopy.

Results

OEC were seeded into 2D gradient-generating microfluidic device and migration was tracked over time (Figure D1). Fluorescently labeled cells could be tracked to determine migration direction and velocity (data not shown). The theoretical concentration gradient in this device follows the non-linear equation

$$C = C_0 * x^{4.2}$$

where C_0 is the initial chemokine concentration and x is the position across the channel[1].

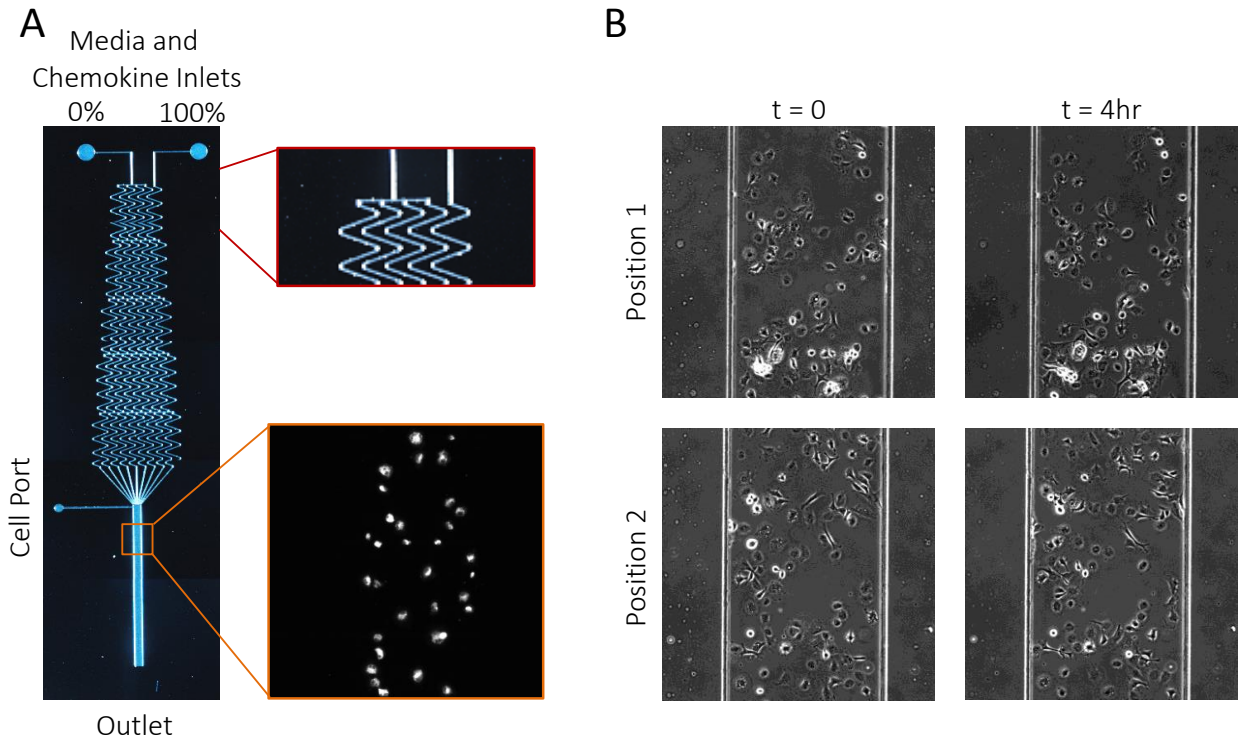

Figure D1. Experimental setup and OEC monitoring in 2D migration microfluidic devices. A) Image of microfluidic device (left), with non-linear gradient-generating design highlighted (top right), and fluorescently-labeled OECs seeded in the device. B) Example images of two positions used for cell tracking in a time-lapse experiment at the start (t=0) and end (t=4hr) of the experiment. The channel is 300µm wide. Device design was adapted from [1].

OECs and CACs were additionally seeded in a collagen matrix into L-shaped PDMS mold to monitor migration in 3D over 4 hours (Figure D2).

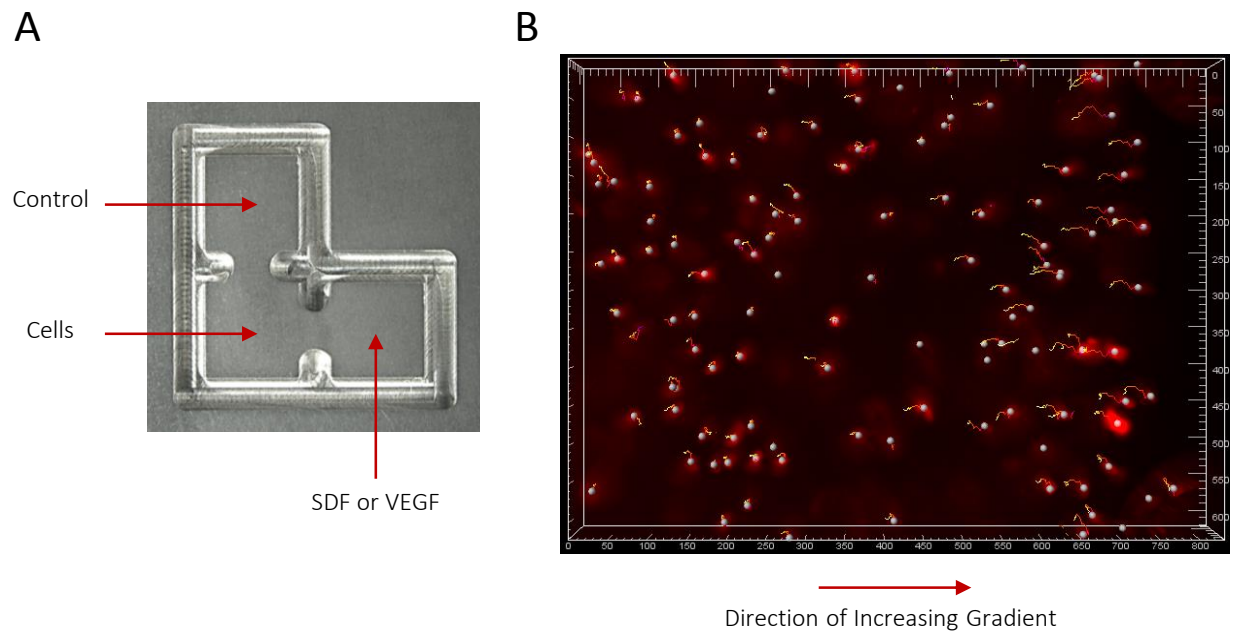

Figure D2. Three-dimentional device used to track endothelial progenitor migration in response to chemokines. A) Image of mold used to fabricate PDMS device, with cell and chemokine placement indicated. Each square chamber is 3mm x 3mm. B) Example tracking of OECs toward a VEGF concentration source over 4 hours. End positions are indicated by spots. Device design was adapted from [3,4].

Summary of Outcomes and Possible Future Studies

Feasibility of tracking OEC migration in 2D and both OEC and CAC migration in a 3D collagen matrix toward a chemokine source was demonstrated in these studies. A full quantitation of migration kinetics for OECs and CACs towards VEGF and SDF has not yet been completed in these devices. Both systems permit measurement of cell migration and calculation of representative population migration variables (*e.g.* directional preference or speed and velocity)[1–4]. The more physiologically relevant 3D system could further be adapted for testing the effects of chemokines released from a biomaterial on migration by placing the material in the source chamber[4].

These types of devices could be used to gain a quantitative understanding of the types of gradients (*e.g.* linear or non-linear) and the magnitude of the concentration gradients for different chemotactic factors that effectively enhance cell migration[5]. This information could then be translated into improved biomaterial designs for increasing endothelial progenitor recruitment.

Acknowledgements

Dr. Bobak Mosadegh demonstrated the 2D PDMS assembly and procedures for testing cell migration in the device. Dr. Prakriti Tayalia demonstrated the procedures for using the 3D device and instructed me on the analysis methods for cell tracking.

References

1. Wang, S.-J., Saadi, W., Lin, F., Minh-Canh Nguyen, C. & Li Jeon, N. Differential effects of EGF gradient profiles on MDA-MB-231 breast cancer cell chemotaxis. *Exp. Cell Res.* **300,** 180–9 (2004).

2. Walker, G. M. *et al.* Effects of flow and diffusion on chemotaxis studies in a microfabricated gradient generator. *Lab Chip* **5,** 611–618 (2005).

3. Tayalia, P., Mendonca, C. R., Baldacchini, T., Mooney, D. J. & Mazur, E. 3D Cell-Migration Studies using Two-Photon Engineered Polymer Scaffolds. *Adv. Mater.* **20,** 4494–4498 (2008).

4. Tayalia, P., Mazur, E. & Mooney, D. J. Controlled architectural and chemotactic studies of 3D cell migration. *Biomaterials* **32,** 2634–2641 (2011).

5. Beebe, D. J., Mensing, G. a & Walker, G. M. Physics and applications of microfluidics in biology. *Annu. Rev. Biomed. Eng.* **4,** 261–286 (2002).

APPENDIX E:

Recruitment of Bone Marrow Cells to SDF-releasing PLG Scaffolds

Purpose of Studies

Endothelial progenitor cells originate in the bone marrow and their mobilization into the circulation from the bone marrow is controlled by gradients of SDF[1–5]. The hypothesis of this experiment is that local release of SDF from a PLG scaffold creates a gradient capable of recruiting circulating bone marrow cells.

Experimental Setup

PLG scaffolds loaded with SDF or control scaffolds were created by the gas foaming method, followed by leaching to dissolve incorporated salt crystals and induce pore formation. These scaffolds were implanted into the hind-limbs of mice. Bone marrow cells were then isolated from GFP mice and introduced into the circulation of the mice with the scaffold implants by intraocular injection. Six days after GFP-bone marrow injection, scaffolds were collected and analyzed for the presence of GFP+ cells by flow cytometry. (See Figure E1 for experimental timeline.)

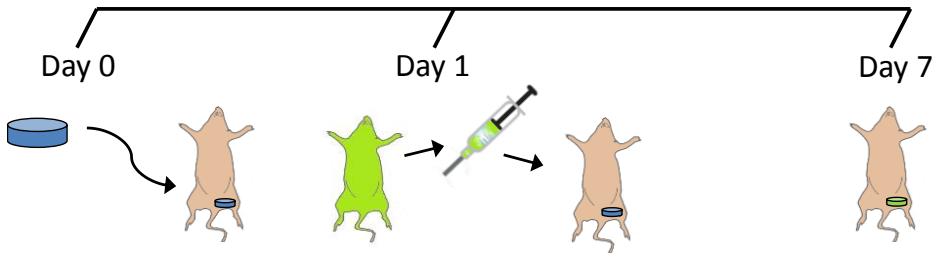

Figure E1. Experimental timeline for GFP bone marrow cell recruitment to PLG scaffolds. Scaffolds were implanted on Day 0, followed by GFP bone marrow cell isolation and delivery to mice with scaffolds on day 1. Scaffolds were then collected and analyzed on day 7.

Results

PLG scaffolds were created that steadily released SDF over time (Figure E2). A large portion of bone marrow cells were found to express CXCR4, the receptor for SDF (Figure E3). Scaffolds containing SDF recruited more GFP+ cells than blank scaffolds (Figure E3).

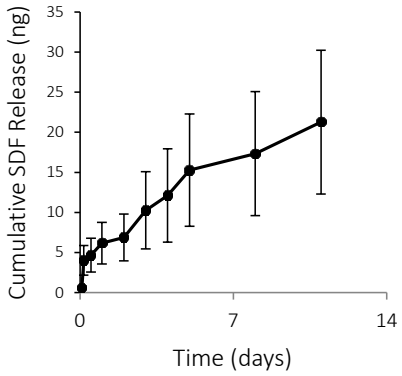

Figure E2. Cumulative release of SDF from porous PLG scaffolds. n=3.

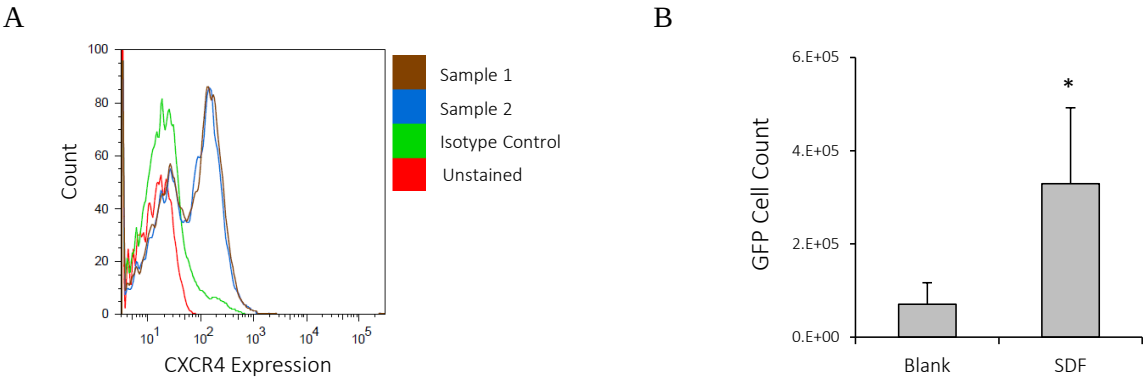

Figure E3. Bone marrow cell expression of CXCR4 and recruitment to SDF scaffolds. A) CXCR4 Expression. B) Number of GFP cells collected from PLG scaffolds on day 7. n=4.

Summary of Outcomes

SDF-loaded PLG scaffolds demonstrated the ability to enhance the recruitment of bone marrow cells, which express CXCR4. This result implies that scaffolds releasing SDF may also be able to recruit endothelial progenitor cells, since they also express CXCR4.

References

1. Lin, Y., Weisdorf, D. J., Solovey, a & Hebbel, R. P. Origins of circulating endothelial cells and endothelial outgrowth from blood. *J. Clin. Invest.* **105,** 71–7 (2000).

2. Lévesque, J.-P., Hendy, J., Takamatsu, Y., Simmons, P. J. & Bendall, L. J. Disruption of the CXCR4/CXCL12 chemotactic interaction during hematopoietic stem cell mobilization induced by GCSF or cyclophosphamide. *J. Clin. Invest.* **111,** 187–196 (2003).

3. Petit, I. *et al.* G-CSF induces stem cell mobilization by decreasing bone marrow SDF-1 and up-regulating CXCR4. *Nat. Immunol.* **3,** 687–694 (2002).

4. Hattori, K. *et al.* Plasma elevation of stromal cell-derived factor-1 induces mobilization of mature and immature hematopoietic progenitor and stem cells. *Blood* **97,** 3354–3360 (2001).

5. Jin, D. K. *et al.* Cytokine-mediated deployment of SDF-1 induces revascularization through recruitment of CXCR4+ hemangiocytes. *Nat. Med.* **12,** 557–567 (2006).

APPENDIX F:

Expanded Flow Cytometry Characterization of Circulating Angiogenic Cells

Purpose of Studies

The objective of this experiment was to further characterize CACs with surface markers used to identify sub-populations of monocytes. These monocyte sub-populations include Classical/Inflammatory $CD14^{++}/CD16^{-}$ monocytes, Non-Classical/Resident/Patrolling $CD14^{+}/CD16^{++}$ monocytes, and Intermediate $CD14^{++}/CD16^{+}$ monocytes[1–4]. Integrin expression was also characterized.

Experimental Setup

CACs were isolated as usual and then were stained for the expression of CD45, CD14, CD16, β2, αL, and αM.

Results

CACs stained positive for CD45, CD14, β2, αL, and αM. Approximately 20% of the CACs were positive for CD16. β2, αL, and αM staining confirms the expected high levels of expression for these integrins.

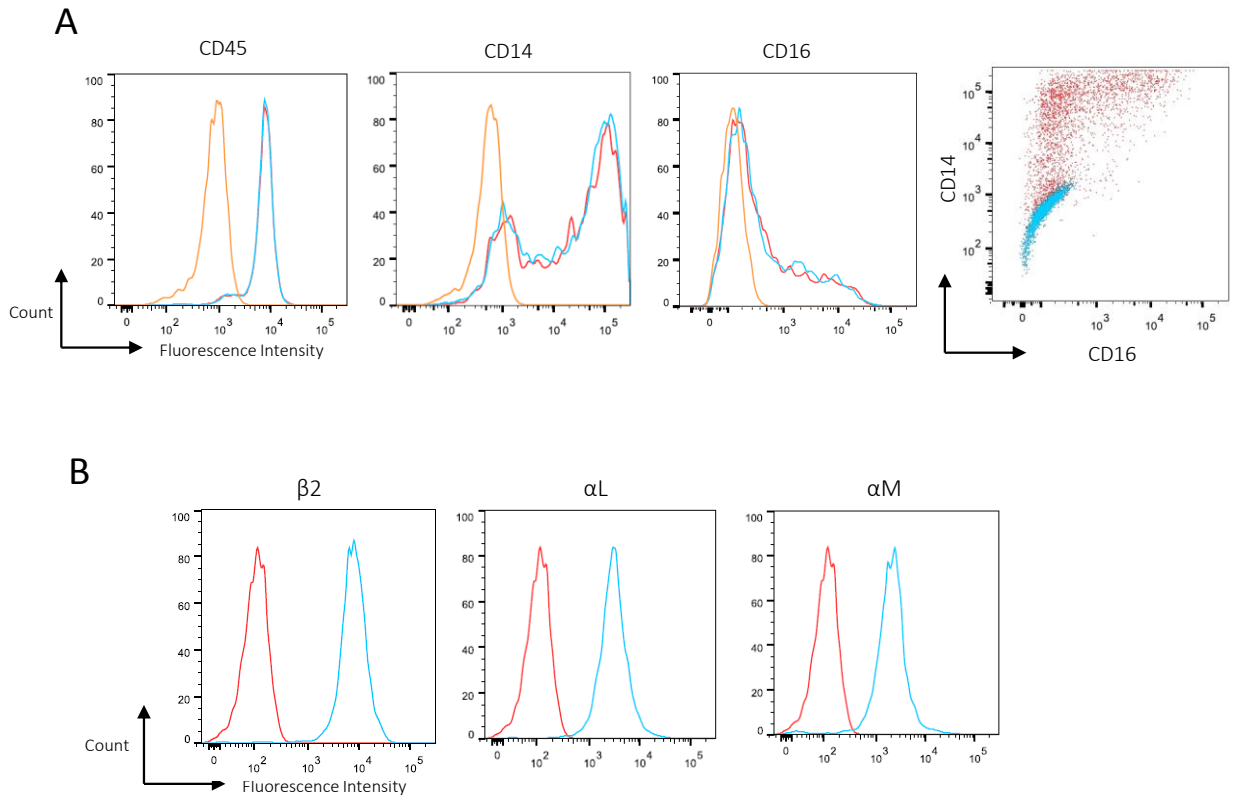

Figure F1. Flow cytometry characterization of CACs. A) Expression of hematopoietic marker CD45, monocyte marker CD14, and CD16. The combination of CD14 and CD16 is used to identify sub-populations of monocytes. B) Histograms of β2, αL, and αM integrin expression.

Summary of Outcomes

CACs that were co-stained with CD14 and CD16 show that all CD16+ cells also express a high level of CD14. In relation to the better understood sub-populations of monocytes, approximately 80% of CACs exhibit the Classical/ Inflammatory ($CD14^{++}/CD16^{-}$) phenotype, while 20% show a similar phenotype to the Intermediate monocyte population ($CD14^{++}/CD16^{+}$). These results are suggestive of a heterogenous population of CACs, which may have implications for their behavior and recruitment capabilities *in vivo*.

References

1. Favre, J., Terborg, N. & Horrevoets, A. J. G. The diverse identity of angiogenic monocytes. *Eur. J. Clin. Invest.* **43,** 100–7 (2013).

2. Auffray, C. *et al.* Monitoring of blood vessels and tissues by a population of monocytes with patrolling behavior. *Science (80-.).* **317,** 666–70 (2007).

3. Nahrendorf, M. *et al.* The healing myocardium sequentially mobilizes two monocyte subsets with divergent and complementary functions. *J. Exp. Med.* **204,** 3037–47 (2007).

4. Fernandez Pujol, B. *et al.* Endothelial-like cells derived from human CD14 positive monocytes. *Differentiation.* **65,** 287–300 (2000).

APPENDIX G:

Comparison of OEC vs. HUVEC network formation in fibrin-PLGA scaffolds

Purpose of Studies

When OECs and HUVECs or HMVECs were placed in direct competition in sprouting assays, OECs demonstrated a higher potential to initiate sprouts. OECs and mature endothelial cells are both capable of forming networks of blood vessels in three-dimensional matrices, which anastomose with host vessels upon implantation[1–3]. Combination fibrin-PLGA scaffolds were used here as another method to compare the neovascularization potential of OECs and HUVECs.

Experimental Setup

OECs or HUVECs were seeded with fibroblasts into fibrin-PLGA scaffolds, and were placed in culture in EGM-2 media (Lonza #CC-3162) for 5 and 8 days. At these time points, scaffolds were fixed and stained for CD31, and then were imaged with a confocal microscope.

Results

Both OECs and HUVECs condensed into vessel-like networks. Qualitative differences in network formation were not overly dramatic on day 5 or 8 (Figure G1), but OECs appear to form a more connected network on day 5, and may possibly form a more branched network on day 8. More rigorous quantitative analysis is necessary to make strong conclusions about these differences though. (Methods for quantitative image analysis were still in development at the time these studies were completed.)

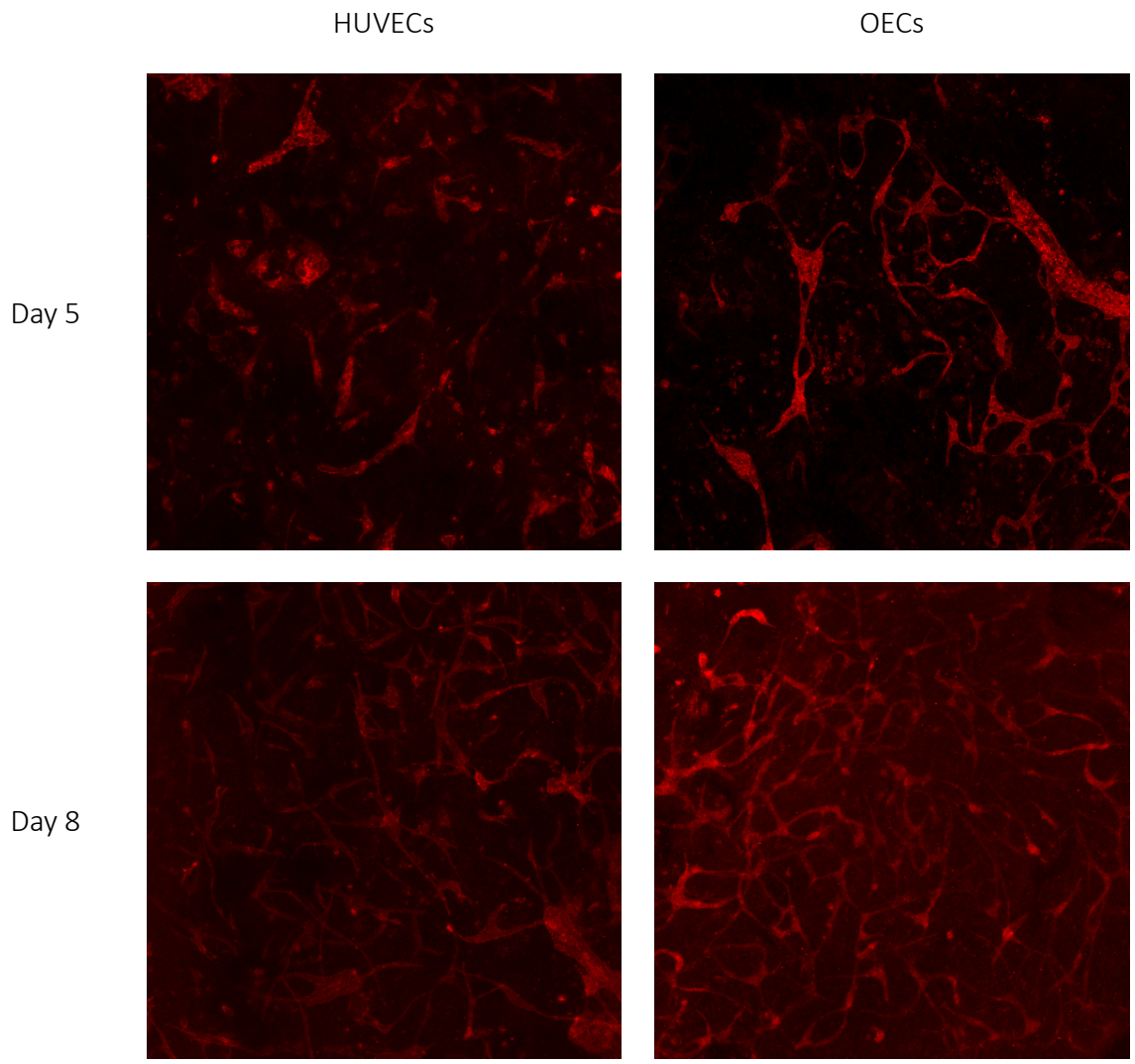

Figure G1. Fluorescent images of vessel-like network formation by OECs and HUVECs on days 5 and 8.

Summary of Outcomes

The network forming potential of OECs and HUVECs were compared in these studies. Images suggest OECs may condense to form networks in an accelerated manner compared to HUVECs, but this was not strongly apparent by qualitative analysis alone. Further studies and quantitative analysis using this system may confirm that OECs exhibit enhanced network forming capabilities, similar to the enhanced sprouting potential demonstrated in three-dimensional angiogenesis assays.

Acknowledgements

PLGA scaffold sponges were provided by the laboratory of Dr. Shulamit Levenberg at Technion Institute of Technology in Israel. Experiments were completed in collaboration with Yaron Blinder.

References

1. Wu, X. *et al.* Tissue-engineered microvessels on three-dimensional biodegradable scaffolds using human endothelial progenitor cells. *Am. J. Physiol. Heart Circ. Physiol.* **287,** H480–7 (2004).

2. Melero-Martin, J. M. *et al.* In vivo vasculogenic potential of human blood-derived endothelial progenitor cells. *Blood* **109,** 4761–8 (2007).

3. Lesman, A. *et al.* Engineering vessel-like networks within multicellular fibrin-based constructs. *Biomaterials* **32,** 7856–69 (2011).

APPENDIX H:

Auto-fluorescence Characterization of Ischemic Hind-limbs Imaged with the In Vivo Imaging System (IVIS)

Purpose of Studies

Use of the IVIS machine is a fast and quantitative way to measure localization of particles or cells. In my studies, the IVIS machine was used to characterize endothelial progenitor cell recruitment to ischemic hind-limbs, until control experiments revealed that the ischemic limbs are highly auto-fluorescent. The IVIS machine was not sensitive enough to discriminate ischemia due to auto-fluorescence from cell accumulation. The data presented here characterizes the auto-fluorescence across the entire range of excitation and emission wavelengths available on the IVIS.

Experimental Setup

Bare ischemic and non-ischemic hind-limbs were imaged using the IVIS at various time points following surgery. Auto-fluorescence of the hind-limb tissue region was then quantified.

Results

Ischemia leads to significantly high levels of auto-fluorescence in bare hind-limbs across many wavelengths. No differences are detected when the skin remains on the mouse (data not shown). Longer wavelengths of light tend to show less background fluorescence in the non-ischemic limbs, and also a lower ratio of the fluorescence in the ischemic limb to the non-ischemic limb (Figure H1).

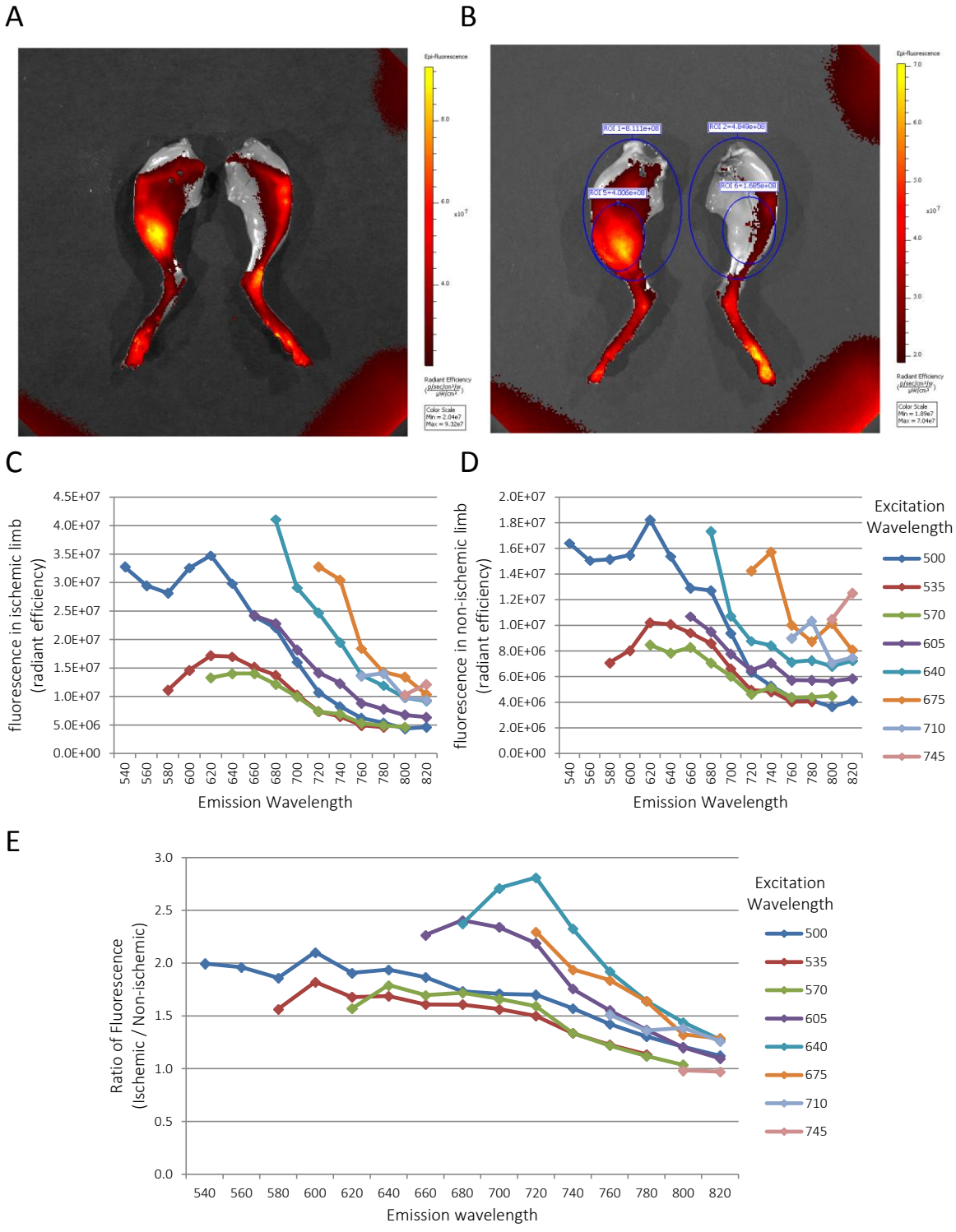

Figure H1. Auto-fluorescence characterization in ischemic hind-limbs on day 3 following surgery. A-B) Example images of auto-fluorescence in the ischemic hind-limb (left side) compared to the non-ischemic limbs (right side), shown both without (A) and with (B) ROI's used for quantification. C-D) Auto-fluorescence measurements, in units of Radiant Efficiency, in the ischemic limb (C) and non-ischemic limb (D). E) Ratio of radiant efficiency measurements (ischemic / non-ischemic).

Auto-fluorescence of the ischemic limb persisted for nearly two weeks after surgery at the excitation wavelength of 640nm and the emission wavelength of 680nm (Figure H2).

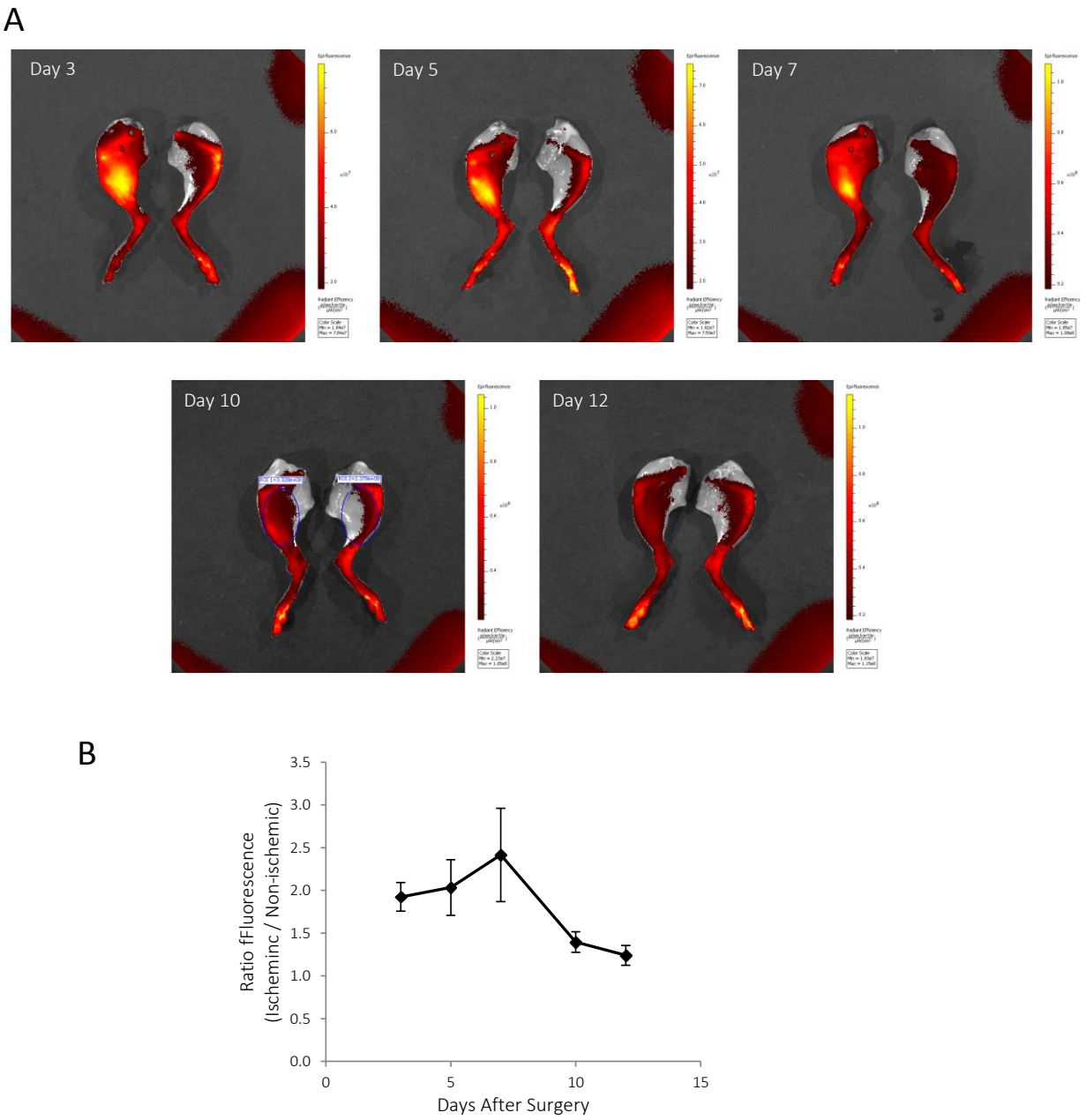

Figure H2. Persistence of increased auto-fluorescence following ischemia surgery at excitation and emission wavelengths of 640nm and 680nm, respectively. A) Representative images of hind-limbs exhibiting increased auto-fluorescence at multiple time points following surgery. b) Quantification of the auto-fluorescence over time, shown as the ratio of the radiant efficiency in the ischemic to the non-ischemic limb.

A better method for detecting cell localization is to use luciferase-expressing cells. Ischemia surgery did not cause auto-luminescence in the ischemic limb.

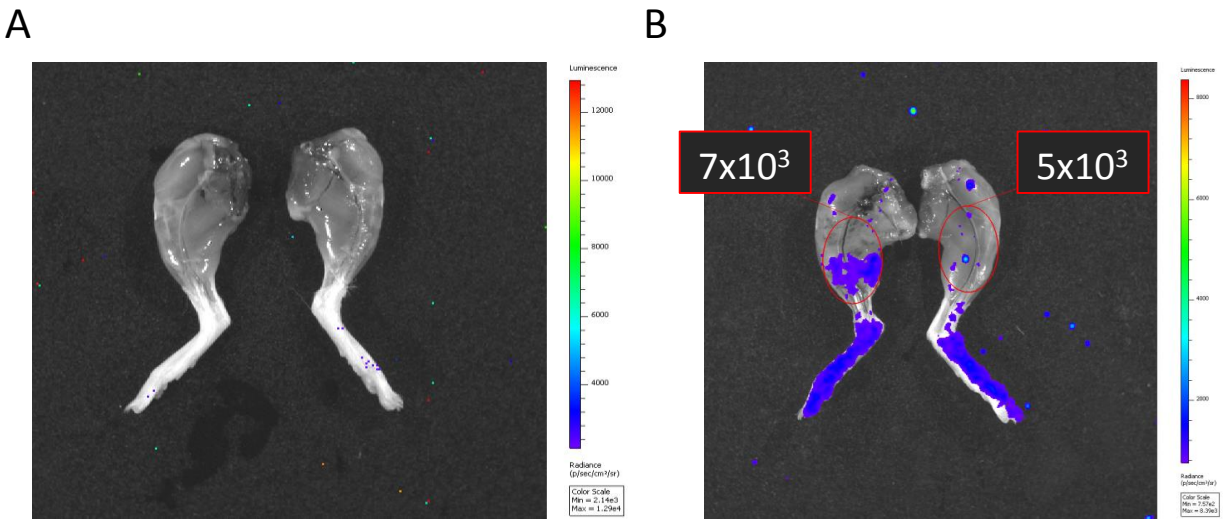

Figure H3. Luminescent images taken with the IVIS 3 days following surgery. A) Luminescence without injection of luciferase-expressing OEC (negative control) on day 3 after ischemia surgery. B) Luminescent image of hind-limbs from a mouse which underwent ischemia surgery and received an intra-cardiac injection of luciferase-expressing OECs. OECs localize to the ischemic hind-limb (left side) more than in the non-ischemic hind-limb (right side).

Summary of Outcomes

The data presented here is meant to be informative and useful for future users of the IVIS in conjunction with ischemia surgery. These data highly suggest that the best method to detect localization of cells within the ischemic hind-limb is by using luciferase-expressing cells, since auto-fluorescence is present across nearly all available wavelengths, and persists for up to two weeks. The IVIS may still be useful for detection of very bright particles, especially because particles are often detectable without the removal of the skin.

APPENDIX I:

Protocol for Adhesion of OECs/CACs to Endothelial Cells

Materials

Human Collagen IV – BD #354245
12mm diameter glass slides – VWR #100500-834
TNFα – Peprotech #300-01A
Octadecyle Rhodamine – Life Technologies #O-246
Endothelial Growth Media (EGM-2MV – Lonza #CC3202 or EGM-2 – Lonza #CC3162)
ProLong Gold Anti-fade Reagent with Dapi – Life Technologies #P36935

Procedure

Preparation

1) Place individual glass slides in wells of 24 well plate (n=6 per condition)
2) Place well plate containing slides in Plasma Generator with lid open; Turn on plasma for 1 min
3) Remove plate and immediately transfer to biosafety cabinet and coat with COL IV for 1 hr at room temp or overnight at 4^{o}C
    a. Dilute COL IV to5µg/ml in 10mM acetic acid
4) Rinse slides 2X with excess PBS
5) Place 0.5ml endothelial growth media (EGM-2MV for HMVECs or EGM-2 for HUVECs) into each well
6) Seed HMVECs or HUVECs by gently dropping 100µl of cell suspension onto center of glass slide
7) Change media every other day until HMVECs have formed a 95% confluent monolayer of cells on the glass slides prior to starting experiment
8) Apply activation molecule (TNFα) to wells ~8 hrs prior to start of experiment (overnight)
9) Apply Octadecyl Rhodamine to OECs/CACs in culture overnight

Perform Experiment

1) Change media in wells to EBM-2 + 5% FBS (0.5ml/well); for some wells, add 500ng/ml SDF for 1 hour prior to applying cells for surface presentation
2) Trypsinize and prepare a single cell suspension of OECs/CACs (50,000 cells/well in 100µl)
3) Change wells with SDF to EBM-2 + 5% FBS; for SDF presentation during adhesion, change media to 125ng/ml SDF (0.4ml/well) immediately before applying cells (gets diluted to final concentration of 100ng/ml with cell addition)
4) Gently drop 100µl of cell suspension onto center of glass slide; place in incubator for 1 hour
5) To stop experiment, lift slide from well and dip in PBS while holding with tweezers, move around slightly
6) Place slide in 20% Methanol in PBS for 5 min
7) Mount on glass slide with Dapi-Prolong Gold
8) Leave at room temp over night, cover with foil to protect from light
9) Place in fridge in slide box the next day until ready to image
10) Take 6 images per glass slide at 5X magnification; count fluorescent cells adhered for quantification

APPENDIX J:

Protocol for ICAM Adhesion Assay

Materials & Buffers

Recombinant Human Soluble ICAM (rhsICAM) – eBioscience #BMS313
β2 Antibody – CalBiochem #217660
Recombinant Human SDF – R&D #350-NS
TrypLE Select (without phenol red) – Life Technologies #12563029
CyquantGR dye – Life Technologies #C7026

Adhesion Buffer
0.1%w/v BSA, 25mM HEPES in HBSS

Lysis Buffer
3mM Na_2HPO_4, 0.8mM NaH_2PO_4, 0.1M NaCl, 0.25%v/v Triton-100 in ddH2O

Procedure

Plate preparation

1) Place a non-TC 48 well plate in Plasma Generator. Turn on plasma for 1 min.
2) Immediately coat the plate with 5μg/ml rhsICAM, 80μl/well in a biosafety cabinet.
3) For negative control apply 80μl of 1% BSA in PBS to each well.
4) Parafilm wrap plate and place at 4^oC overnight

Perform Experiment

5) Aspirate ICAM and apply 200μl of 1%BSA in PBS for 1 hr at room temp
6) Rinse OECs/CACs in PBS, then remove using 5mM EDTA in PBS for ~15 min (must tap hard or pipette up and down to remove cells)
7) Centrifuge for 5 min at 1200 rpm.
8) Resuspend in Adhesion Buffer; Count.
    a. Want a minimum of 100K cells/well; 100μl/well
9) Divide cells into tubes for β2 block or SDF stimulation
    a. β2 block : 0.5μg/sample for 5-10 min prior to applying cells to well
    b. SDF : 300ng/ml immediately prior to applying cells to well (dilute by 3X when added to well for 100ng/ml final concentration)
10) Apply cells to wells
    a. Aspirate BSA block
    b. Apply 200μl Adhesion Buffer to each well
    c. Dilute cells so that 100μl of cells are applied to each well
    d. Add cells to one or two wells (never rinse) – positive controls (100%)
11) Place plate in incubator for 30 min

    a. After 30 min observe plate under microscope – visually check for adhered vs. unadhered cells

12) ***Thaw Cyquant GR dye***
13) Swirl plate and tilt to remove un-adhered cells
14) Rinse with 0.5ml PBS in each well (pipette to top side of well with plate tilted and let run down); do this 3X; BE GENTLE
15) Add 300µl of TrypLE Select and let incubate at 37^{o}C for 5 min
16) Observe cell detachment under the microscope
17) Pipette cells up and down to help with removal
18) Add 100µl of Lysis Buffer with Cyquant Dye to each well
    a. 100µl Lysis Buffer/well
    b. Add 4µl of CyquantGR Dye per 300µl of lysis buffer
19) Let sit at room temp for 15 min, cover plate with foil
20) Check fluorescence under microscope – green filter; check for lysis
21) Pipette up and down in each well to mix
22) Take 2x 150µl from each well and place into 2 wells of a 96-well black bottom plate
23) Read fluorescence on plate reader at ex:485nm, em: 528nm

APPENDIX K:

Protocol for Adhesion Assay in PDMS-based Wide Flow Channel

Materials

PDMS (Sylgard ® 184 Silicone Elastomer Kit)
Human Collagen IV – BD #354245
Recombinant Human SDF – R&D #350-NS
TrypLE Select (without phenol red) – Life Technologies #12563029
Endothelial Growth Media (EGM-2MV – Lonza #CC3202 or EGM-2 – Lonza #CC3162)
EBM-2 – Lonza # CC3156
ProLong Gold Anti-fade Reagent with Dapi – Life Technologies #P36935

Other materials for fabricating devices (tubing, "Y" branch connectors, blunt end needles, metal connectors) are common microfluidics laboratory supplies.

Procedure

Device Preparation

1. Prepare tubing and UV sterilize (Figure K1).
2. Cut out PDMS wide channel from mold. Cut to fit on a microscope slide. Punch 1.5mm holes at channel ends. Remove dust with tape.
3. Place PDMS channel and clean microscope slide into plasma generator. Turn on for ~1 min. Once vacuum has re-pressurized, remove PDMS and slide and bond together. Be careful not to touch middle of channel so as not to bond this region. Place components in a petri dish. (Figure K2)
4. Quickly move to a biosafety cabinet and pipette ~100µl of COL IV (5µg/ml diluted in 10mM acetic acid) into the channel, filling the device.
5. Store for 3 hours at room temperature or wrap petri dish with parafilm and store overnight at $4^{o}C$.
6. Place a few ml of media in a petri dish and put in incubator ($37^{o}C$, 5% CO_2) for 30 min.
7. Fill sterile tubing with warm, CO_2-adjusted media, using a 1ml slip tip syringe. Make sure there are no bubbles.
8. Place metal component into PDMS hole at end of device, being careful not to introduce bubbles.
9. Place short tube in opposite end of device. Push excess media through channel, thoroughly rinsing COL IV solution. Clamp closed with binder clips and place in incubator (3-24 hours). Return excess media to incubator as well.

Cell Culture in Device

1. Use a nearly-confluent T75 of HMVECs to fill ~4 devices.
2. Trypsinize as usual and resuspend in 1ml of media from petri dish in incubator.
3. Place 22G needle on 1ml slip tip syringe and draw up cell solution into syringe, maintaining a small air bubble next to the plunger and being careful to keep syringe pointed down. Make sure there are no bubbles in the solution (besides the one at the plunger).

4. Verify there are no bubbles in the device or tubing. Adjust binder clips for cell seeding.
5. Push a small amount of cell solution to end of needle. Insert needle into the short tube at the channel exit, and pinch around the needle. Introduce approximately 150-200µl of cell solution through the device, or until the solution exiting the "Y" branch is slightly cloudy.
6. Pinch off tube with binder clips, verify seeding using the microscope, and place device in incubator for 3-6 hours to allow cells to attach.
7. Place 10ml of media per device into a T25, and place upright in incubator to allow temperature and CO_2 to equilibrate.
8. Hook up inlet tubing to a 10 ml syringe with plunger removed and place upright in a tube rack. Fill syringe with equilibrated media. Fill tubing with media, making sure there are no bubbles.
9. Remove short tube at the outlet and insert long tube attached to a 10 or 20ml syringe.
10. Place device in incubator and hook up the syringe at the outlet to the syringe pump. Flow media at 10µl/min. Adjust binder clips for proper cell culture.
11. Allow endothelial cells to grow until a confluent monolayer is formed. Make sure to replenish media. DO NOT LET DEVICE RUN DRY.

Preparation of OECs/ CACs

1. Use TrypLE Select to remove cells from surface, centrifuge and resuspend in 5-10ml PBS. Centrifuge and resuspend again.
2. Stain OECs/CACs with 1µM CFSE according to manufacturer's protocol. This takes approximately 45 min total. Plan accordingly to coordinate with device preparation so cells do not sit in suspension for long prior to starting experiment.
3. Perform the final resuspension in EBM-2 + 5% FBS to a concentration of 5M cells/ml. Divide into tubes as necessary for ±SDF exposure during adhesion.

Adhesion Assay

1. Prepare EBM-2 + 5% FBS and place in T25 in incubator to allow temperature and CO_2 to equilibrate. Use this for all remaining steps. Return flask to incubator when not in use.
2. Change media source-syringes to the 3 ml size. Fill with ~1ml EBM-2 + 5% FBS. Let media run over cells in device to rinse away normal growth media. Clamp off tubing and place devices in incubator for ~1 hour.
3. For the SDF-surface presentation condition, remove excess rinse media from 3 ml syringe and add ~300µl of EBM-2 + 5% FBS supplemented with 500ng/ml SDF. Let this media run over the cells, clamp with binder clips, and place in incubator for 1 hour.
4. Rinse SDF-surface presentation device with fresh EBM-2 + 5% FBS.
5. Remove excess media from source syringe.
6. Draw up OEC/CAC cell suspension into 1ml slip tip syringe with a 22G needle attached using the same methods as for endothelial cell seeding. For SDF-during adhesion conditions, add 100ng/ml SDF to the cell suspension before drawing into syringe.
7. With path into the device clamped off, insert the needle into the short end of the tube off of the "Y" branch. Fill upstream tubing with 200µl of cell solution (1M cells). Some solution will likely back-fill the syringe. Clamp off the short tube after filling with cells.

8. Hook up device outlet syringes to the syringe pump. Adjust binder clips so that cell may flow through the device. Start flow over the device (10µl/min).
9. After ~18 min, add 200µl of EBM-2 + 5% FBS to the source syringe. Repeat after another ~18 min.
10. Clamp off device, remove from incubator and verify under the microscope that OECs/CACs in the device are adhered and not still floating/flowing through the device.
11. Carefully remove tubing from device and very slowly pipette a dilute solution of PBS containing dapi through the channel. Cover top of device with a cover slip.
12. Image device immediately. Take pictures in as many locations as possible (where the endothelial monolayer confluence is verified).

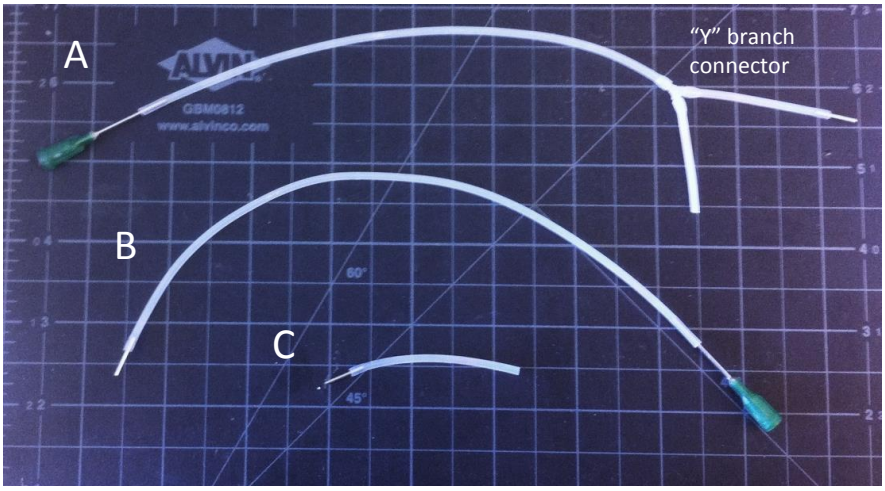

Figure K1. Tubing components necessary for cell culture in the flow device.
A) Inlet tubing. B) Outlet tubing. C) Cell-seeding short tubing.

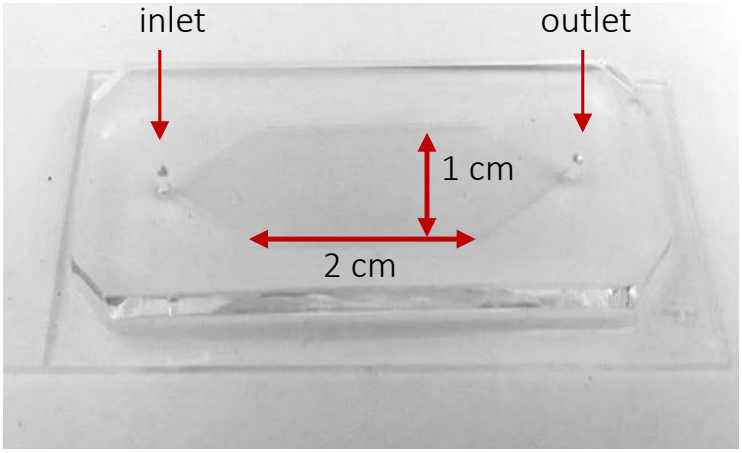

Figure K2. PDMS channel bonded to a glass slide.

APPENDIX L:

Protocol for Muscle Cell Isolation and Staining for Flow Cytometry

Materials & Buffers

Collagenase II – Life Technologies #17101-015
Dispase II – Roche #04942078001
Normal Goat Serum – VWR # 100180-976
CD11b Antibody – eBioscience #25-0112
F4/80 Antibody – eBiosceince #12-4801
Gr1 Antibody – eBioscience #11-5931

FACS Buffer
0.1% BSA in PBS (or BD #554657)

Procedure

Muscle cell collection and digestion

1) Prepare Collagenase II solution (250U/ml) in DMEM
    a. Will need 4ml/sample total
2) Pipette 2 ml of Collagenase solution into a 15ml tube for each muscle sample
3) Record weight of each tube
4) Collect muscles of interest from mouse legs
    a. Using scissors, cut up each muscle into as small of pieces as possible
    b. Wipe down scissors with isopropanol of ethanol between chopping each muscle (to prevent mixing of cells)
5) Place muscle chunks into 2ml of Collagenase solution; make sure all pieces are in solution (i.e. none stuck to the sides of the tube)
6) Weigh tubes again to determine mass of muscle collected
7) Place tubes on shaker at 37^{o}C for 1.5hr
8) Using a short glass Pasteur pipet, pipet up and down gently until muscle solution is smooth (no brown chunks); do this in 15ml tube and change Pasteur pipette between every sample
9) Add 3-5 ml PBS to each tube
10) Centrifuge at 500g for 5 min (re-spin if muscle has not pelleted well)
11) Remove supernatant
12) Resuspend in Collagenase II / Dispase / media solution
    a. Prepare 6U/ml dispase in DMEM (1ml/sample)
    b. Add 1 ml of 6U/ml dispase (resuspend using 1 ml pipettor)
    c. Add 2 ml of 250U/ml Collagenase II (prepared earlier)
    d. Add 3 ml media DMEM
13) Place tubes on shaker at 37^{o}C for 1hr
14) Vortex each tube for 1 minute on max speed to release the cells

15) Pass cell suspensions through 40µm filters into 50 ml tubes using 10ml pipettes to push solution through the filter
16) Add 5ml PBS to each 50ml tube through the filter to rinse cell suspension through
17) Centrifuge at 500g for 5 min; Remove supernatant
18) Resuspend each tube into 200µl RBC lysis buffer
    a. Let sit for 5 min at RT; swirl a few times to mix cell suspension
19) Add 800µl PBS
20) Transfer cell suspension into 2ml brown tubes
    a. Optional: add a small volume of pfa to fix the cells (~100ul of 4% pfa is sufficient)
    b. Place tubes in fridge if not going to run flow/stain cells immediately

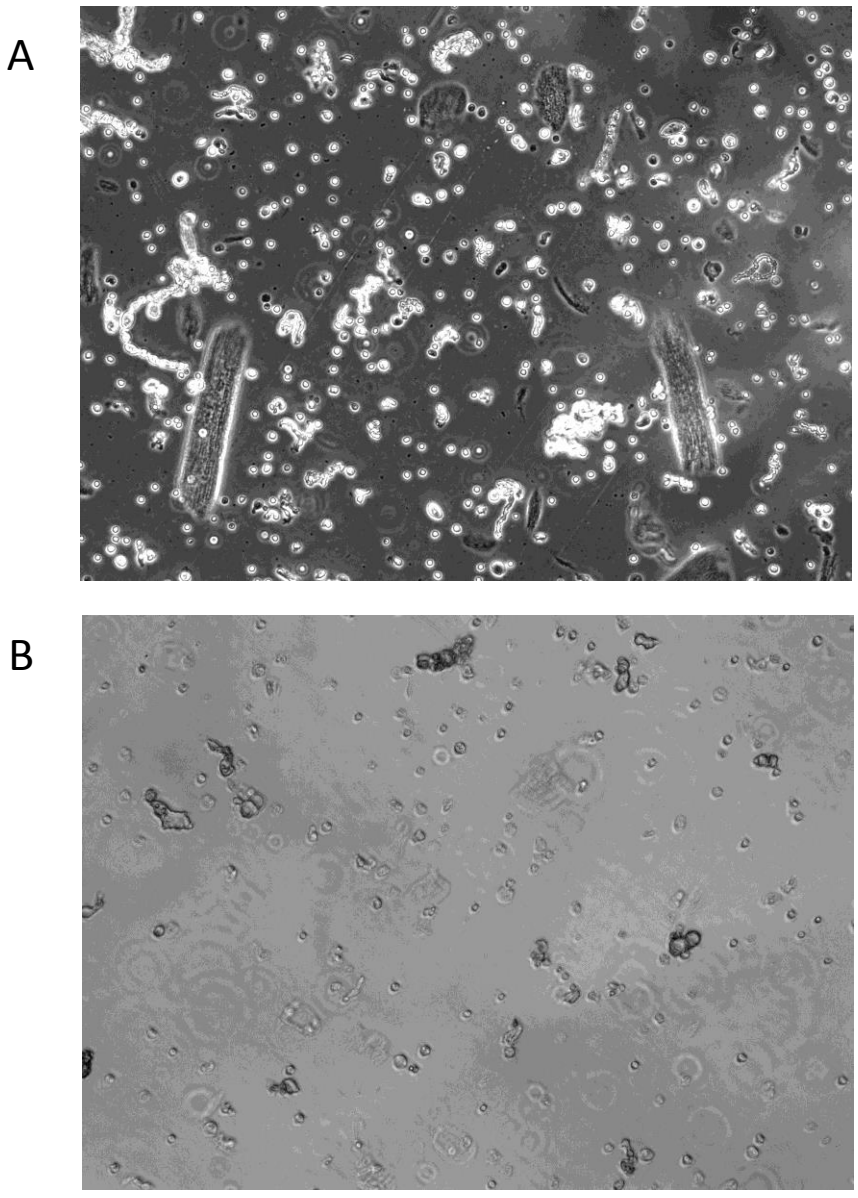

Figure L1. Example images of cell suspension after completing the muscle digestion procedure. A) Phase contrast image. B) Bright field image.

Flow Cytometry Staining

1) Centrifuge cells at 600g for 5 min
2) After centrifuging in brown tubes, dump out supernatant
3) Resuspend in FACS Buffer
    a. 600µl for ischemic limb
    b. 400µl for non-ischemic limb
4) Pipette ~80-100µl per sample into wells of round bottom plate compatible with HTS system on flow cytometer
5) Add 20µl blocking buffer to each tube/well; let sit 15 min at RT
    a. Blocking buffer: 10%NGS + 1% BSA in PBS
6) Add primary antibody to each tube/well (5µl/sample; 0.25µg/sample); place tubes on ice for 45 min, protect from light (Check antibody concentration to calculate volume of each antibody needed)
7) Add 0.75ml FACS Buffer to each tube; centrifuge at 600g for 5 min, 4^{o}C; Repeat twice
    a. Add 100ul if using round bottom plates, then centrifuge as above
    b. After centrifuging, dump supernatant into the sink by turning plate over quickly
    c. Resuspend each well in 200ul (use multi-channel pipettor; no mixing necessary until final resuspension)
8) For 1^{o} AB with fluorophore, after final spin, resuspend into 250µl FACS Buffer per well and place on ice protected from light until time to run samples
9) Add 1µl hoescht or DAPI to each tube immediately before running samples